

Supporting Information

5,5'-Bistriazoles as axially chiral, multidentate ligands: Synthesis, configurational stability and catalytic application of their scandium(III) complexes

Pablo Etayo,*^a Eduardo C. Escudero-Adán,^{a,b} and Miquel A. Pericàs*^{a,c}

^a *Institute of Chemical Research of Catalonia (ICIQ), The Barcelona Institute of Science and Technology (BIST), Avgda. Països Catalans 16, E-43007 Tarragona, Spain. E-mail: petayo@iciq.es, mapericas@iciq.es; Fax: +34 977920244*

^b *X-Ray Diffraction Unit*

^c *Department de Química Inorgànica i Orgànica, Universitat de Barcelona, 08028 Barcelona, Spain*

Table of Contents

(A) General considerations	SI-2
(B) Solid-state structural characterization of 5,5'-bistriazoles 4	SI-3
(C) Mechanistic insights on the formation of 5,5'-bistriazoles 4	SI-5
(D) Single-crystal X-ray structure determinations	SI-8
(E) Synthesis and characterization of monotriazoles and 5,5'-bistriazoles	SI-11
(F) Determination of rotational energy barriers and half-life times	SI-24
(G) Comparative FC outcomes with monotriazole 3a vs. 5,5'-bistriazole 4a	SI-31
(H) Screening of conditions for the FC reaction of N-unsubstituted isatin 7b	SI-32
(I) Rationalization of the FC reaction catalyzed by 4a·Sc(OTf)₃	SI-33
(J) Synthesis and characterization of FC reaction products	SI-34
(K) NMR spectra of all compounds	SI-55

(A) General considerations

All reactions were conducted in anhydrous solvents using chemicals as purchased from commercial sources, unless otherwise stated. Catalytic applications of triazole-based ligands were all run under argon atmosphere by using standard Schlenk-type techniques. Glassware was dried under vacuum and heated with a hot air gun before use. All anhydrous solvents were dried by using a Solvent Purification System (SPS), with the caveat of dried ethanol which was purchased from Merck[®] (SeccoSolv[®] quality solvent).

All reactions were monitored by thin layer chromatography (TLC). TLC analyses were performed on precoated aluminium sheets equipped with UV fluorescence indicator F254 by using TLC Silica gel 60 F₂₅₄ plates from Merck[®]. Compounds were visualized using UV light (254 nm) and ethanolic phosphomolybdic acid (PMA) stain solution followed by heating with a hot air gun. Flash column chromatography was performed on a Teledyne Isco CombiFlash[®] system equipped with multiple UV detector by using empty cartridges refilled with silica gel 60 (230–400 mesh) or commercial dry-packed silica gel cartridges.

NMR spectra were recorded in CDCl₃ unless otherwise cited, using a 400 MHz or 500 MHz Bruker spectrometer. ¹H NMR and ¹³C{¹H} NMR chemical shifts are quoted in ppm relative to residual solvent peaks, whereas ¹⁹F{¹H} NMR chemical shifts are quoted in ppm relative to BF₃·OEt₂ in CDCl₃. High resolution mass spectra (HRMS) were recorded by using an ESI ionization method in positive mode, unless otherwise indicated. Specific optical rotations ([α]) were measured under ambient temperature at the sodium D line (589 nm) in cells with 1 or 10 cm path length by using a Jasco P-1030 polarimeter, with concentrations given in g/100 mL. Infrared spectroscopy (IR) was recorded on neat samples by using attenuated total reflectance (ATR) technique in a Bruker Tensor 27 FT-IR spectrometer, with wavenumbers (ν_{max} values) expressed in cm⁻¹ and given for the absorption bands of the main functional groups. Melting points (mp) were measured in open capillaries on a Büchi B-540 instrument and are uncorrected. Enantiomeric excess (ee) values were determined by analytical HPLC on using chiral stationary phases. Resolutions and separations of atropisomeric 5,5'-bistriazoles were accomplished by means of semi-preparative HPLC on a suitable chiral stationary phase. HPLC analyses were performed on an Agilent 1200 Series chromatograph equipped with a diode array UV detector (DAD).

(B) Solid-state structural characterization of 5,5'-bistriazoles **4**

The C_2 -symmetric structure of the 5,5'-bistriazole **4a** was firstly characterized in solution by means of NMR and HRMS analyses (*vide infra*). Notoriously, the ^1H NMR spectrum of **4a** displays two couples of geminally coupled doublets (two independent AB systems) corresponding to diastereotopic methylene protons of the aminomethyl and benzyl substituents ($^2J_{\text{H-H}} = 13.6$ and 15.1 Hz, respectively). Gratifyingly, the structure of **4a** could be further unambiguously established by single-crystal X-ray diffraction (SCXRD) analysis. The solid-state structure of **4a** showed a non-planar bistriazole core, likely indicative of axial chirality resulting from restricted rotation around the C5–C5' bond. As expected, the two putative enantiomeric atropisomers of **4a** [(R_a)-**4a** and (S_a)-**4a**] were found within the unit cell of **4a**. Noteworthy, **4a** adopts two distinct conformations in the solid state (a and b; Fig. SI-1) featuring slightly different dihedral angles across the C5–C5' chiral axis. As shown in Fig. SI-1, the two triazole rings of **4a** were perpendicular each other in both solid-state conformations (a and b). Accordingly, those triazole rings were titled with dihedral angle values $\psi = 93.26^\circ$ and 104.48° for conformations a and b, respectively.¹

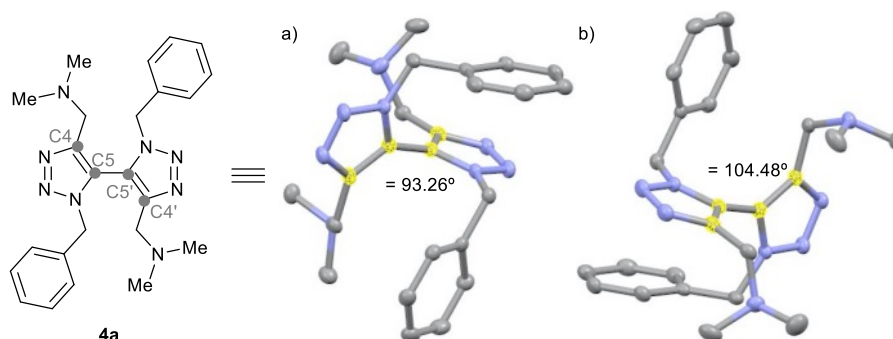


Fig. SI-1 Crystal structure of 5,5'-bistriazole **4a** (ORTEP plots showing thermal ellipsoids at 50% probability; all hydrogen atoms have been omitted for clarity). a) Conformation of **4a** displaying a dihedral angle $\psi = 93.26^\circ$; b) Conformation of **4a** displaying a dihedral angle $\psi = 104.48^\circ$.

Interestingly, we also succeeded in obtaining the crystal structure of a diammonium salt of **4a** by growing suitable single crystals for XRD from the diammonium bistriflate **4a**·2HOTf, derived from **4a** after selective protonation of the two tertiary amino groups by trifluoromethanesulfonic acid (TfOH). Contrariwise to the free diamine **4a**,

¹ Dihedral angles (ψ) defined as the torsion angles measured between the four atoms C4–C5–C5'–C4' and given as absolute values matching to the corresponding negative or positive values found for the enantiomeric atropisomers of each conformation.

4a·2HOTf adopts a single conformation in the solid state displaying a dihedral angle $\psi = 95.11^\circ$ across the rotatable C5–C5' bond (Fig. SI-2).¹ This different behavior in the solid state shows how dihedral angle values can be easily modified by choosing the neutral diamine form or the doubly protonated diammonium form of a given 4,4'-aminomethyl-substituted 5,5'-bistriazole. Moreover, the crystal structure of **4a**·2HOTf showed very close hydrogen bond contacts between each protonated *N,N*-dimethylamino group and each trifluoromethanesulfonate anion [$d(\text{N–H}\cdots\text{O}) = 1.94$ and 2.33 \AA].

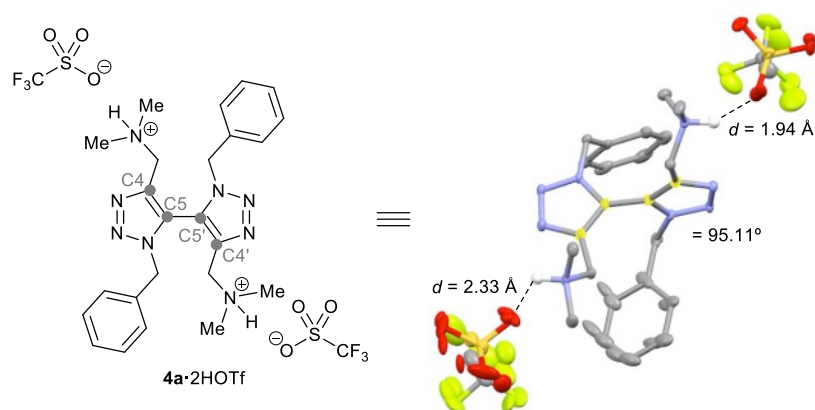


Fig. SI-2 Crystal structure of 5,5'-bistriazole **4a**·2HOTf (ORTEP plot showing thermal ellipsoids at 50% probability; all hydrogen atoms attached to carbons have been omitted for clarity). Single conformation of **4a**·2HOTf displaying a dihedral angle $\psi = 95.11^\circ$ and showing close hydrogen bond $\text{Me}_2\text{N}^+\text{–H}\cdots\text{O}^-\text{–S(=O)}_2\text{CF}_3$ contacts. The two trifluoromethanesulfonate counterions and one of the benzyl fragments are disordered into two distinct positions.

Furthermore, the structure of bistriazole dihydrochloride **4b**·2HCl was also unambiguously assured from SCXRD analysis. In contrast to the diammonium salt **4a**·2HOTf and as found for the free diamine **4a**, the dihydrochloride **4b**·2HCl adopts two distinct and partially overlapped conformations in the solid state featured by slightly different dihedral angles across the rotatable C5–C5' bond. As shown in Fig. SI-3, the two triazole rings of **4b**·2HCl were perpendicular to each other in both partially overlapped solid-state conformations displaying very similar dihedral angle values ($\psi = 100.85^\circ$ and 102.13°).¹ Additionally, the crystal structure of the dihydrochloride salt **4b**·2HCl showed very close hydrogen bond contacts between each protonated *N*-methylamino group and each chloride anion [$d(\text{N–H}\cdots\text{Cl}) = 2.16, 2.25$ and 2.34 \AA].

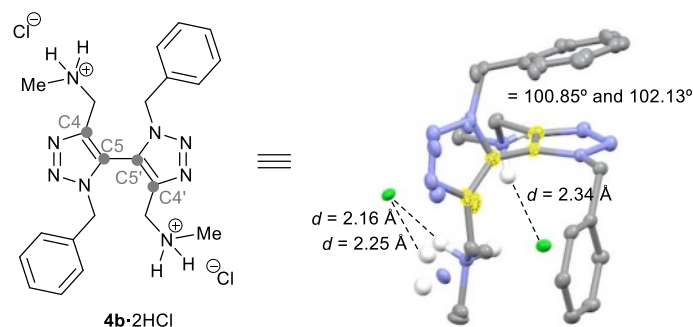


Fig. SI-3 Crystal structure of 5,5'-bistriazole **4b**·2HCl (ORTEP plot showing thermal ellipsoids at 50% probability; all hydrogen atoms attached to carbons have been omitted for clarity). Two distinct and partially overlapped conformations of **4b**·2HCl displaying dihedral angles $\psi = 100.85^\circ$ and 102.13° and showing close hydrogen bond $\text{Me}(\text{H})\text{N}^+ - \text{H} \cdots \text{Cl}^-$ contacts.

(C) Mechanistic insights on the formation of 5,5'-bistriazoles **4**

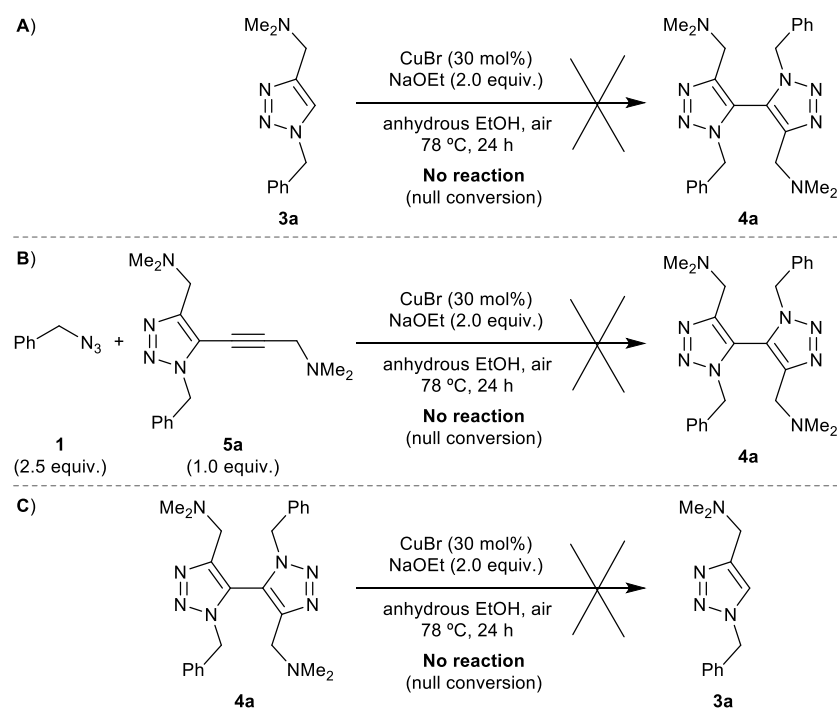
During the last decade, the mechanistic understanding of CuAAC reactions has progressed considerably.² Concerning the closely related tandem CuAAC–oxidative coupling processes giving rise to 4,4'-disubstituted 5,5'-bistriazoles, there have been some mechanistic proposals,³ but none of them seems to be consistent with the behavior observed for propargylamine **2a**.

Of mechanistic relevance, the formation of the 1,3-diyne dimer **6a** as the oxidative homocoupling product of the terminal alkyne **2a** has never been observed during our work (see Table 2); thus, we can exclude the intermediacy of diyne **6a** in the formation of bistriazole **4a**. In addition to that, we have also confirmed that monotriazole **3a** is unreactive under the conditions used for the preparation of **4a** from **1** and **2a** (Scheme SI-1A). Similarly, when 5-alkynyltriazole **5a** was treated with excess benzyl azide (**1**) under the usual reaction conditions, no conversion was observed (Scheme SI-1B). These results seem to rule out the possible involvement of compounds **3a** and **5a** as reaction intermediates leading to **4a**, in turn suggesting that the $[3+2]$ cycloaddition process

² For reviews on the mechanism of CuAAC, see: (a) B. R. Buckley and H. Heaney, *Top. Heterocycl. Chem.*, 2012, **28**, 1–30; (b) R. Berg and B. F. Straub, *Beilstein J. Org. Chem.*, 2013, **9**, 2715–2750; (c) L. Zhu, C. J. Brassard, X. Zhang, P. M. Guha and R. J. Clark, *Chem. Rec.*, 2016, **16**, 1501–1517.

³ (a) J. González, V. M. Pérez, D. O. Jiménez, G. Lopez-Valdez, D. Corona and E. Cuevas-Yañez, *Tetrahedron Lett.*, 2011, **52**, 3514–3517; (b) Z.-J. Zheng, F. Ye, L.-S. Zheng, K.-F. Yang, G.-Q. Lai and L.-W. Xu, *Chem. – Eur. J.*, 2012, **18**, 14094–14099; (c) L. Li, X. Fan, Y. Zhang, A. Zhu and G. Zhang, *Tetrahedron*, 2013, **69**, 9939–9946; (d) D. Goyard, A. S. Chajistamatiou, A. I. Sotiropoulou, E. D. Chrysina, J.-P. Praly and S. Vidal, *Chem. – Eur. J.*, 2014, **20**, 5423–5432; (e) C. J. Brassard, X. Zhang, C. R. Brewer, P. Liu, R. J. Clark and L. Zhu, *J. Org. Chem.*, 2016, **81**, 12091–12105.

should occur before the oxidative dimerization step. Furthermore, we also subjected bistriazole **4a** to the same reaction conditions, and found that **4a** remained completely unconverted after 24 h (Scheme SI-1C). This lack of reactivity of **4a** ensured that the bistriazole formation is not a reversible process, in sharp contrast to what was previously reported for the 5,5'-bistriazole derived from benzyl azide and phenylacetylene.^{3a}



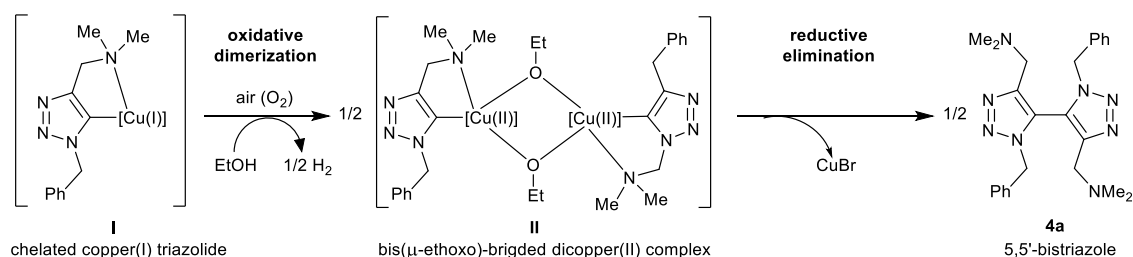
Scheme SI-1 Control experiments.

Taking all the previous observations into account, we propose (Scheme SI-2) the intermediacy of a bis(μ -alkoxo)dicopper(II) intermediate (**II**) as the precursor in the dimerization step leading to **4a**. When propargylamines are involved in the CuAAC reaction, the usual copper(I) triazolid intermediate **I**,⁴ will be stabilized through chelation by the electron-rich *N,N*-dimethylamino group.⁵ Favored by the aerobic conditions (air atmosphere), intermediate **I** could suffer from an oxidative dimerization

⁴ (a) C. Nolte, P. Mayer and B. F. Straub, *Angew. Chem., Int. Ed.*, 2007, **46**, 2101–2103; (b) B. T. Worrell, J. A. Malik and V. V. Fokin, *Science*, 2007, **340**, 457–460; (c) J. Winn, A. Pinczewski and S. M. Goldup, *J. Am. Chem. Soc.*, 2013, **135**, 13318–13321; (d) C. Iacobucci, S. Reale, J.-F. Gal and F. De Angelis, *Angew. Chem., Int. Ed.*, 2015, **54**, 3065–3068.

⁵ For metal chelates of 4-aminomethyl-1,2,3-triazole ligands, see: (a) A. Maisonia, P. Serafin, M. Traïkia, E. Debiton, V. Théry, D. J. Aitken, P. Lemoine, B. Viossat and A. Gautier, *Eur. J. Inorg. Chem.*, 2008, 298–395; (b) A. Chevy, M.-L. Teyssot, A. Maisonia, P. Lemoine, B. Viossat, M. Traïkia, D. J. Aitken, G. Alves, L. Morel, L. Nauton and A. Gautier, *Eur. J. Inorg. Chem.*, 2010, 3513–3519; (c) S. Fernández, J. Giglio, A. M. Rey and H. Cerecetto, *Bioorg. Med. Chem.*, 2012, **20**, 4040–4048; (d) D. Mendoza-Espinosa, G. E. Negrón-Silva, D. Ángeles-Beltrán, A. Álvarez-Hernández, O. R. Suárez-Castillo and R. Santillán, *Dalton Trans.*, 2014, **43**, 7069–7077.

process through oxidative coupling of two σ -bonded copper(I) triazolides, with EtOH acting as a bridging ligand in intermediate **II**. A closely related transformation, proceeding also in EtOH under air, has previously been reported for another chelating bidentate ligand,⁶ and a number of bis(μ -alkoxo)dicopper(II) complexes are known in the literature.⁷ The conversion of **I** into **II** could benefit from the high solubility of dioxygen gas in EtOH at 0 °C,⁸ thus making unnecessary the use of an external oxidant for the dimerization to take place. In the last step in the mechanistic pathway, intermediate **II** could readily undergo reductive elimination affording 5,5'-bistriazole **4a** and regenerating the catalyst (CuBr) of the CuAAC reaction.



Scheme SI-2 Tentatively proposed dinuclear stepwise mechanism for the formation of 5,5'-bistriazole **4a**.

The proposed two-step formation of bistriazole **4a** from intermediate **I** formally resembles the Cu(II)-catalyzed aromatic Glaser–Hay reaction, in particular the oxidative dimerization of nitrogen-containing aromatic heterocycles including 1-*n*-butyl-1,3,4-triazole.⁹ In addition, a closely related Cu(I)/Cu(II) stepwise dinuclear mechanism has been recently proposed to mediate the oxidative homocoupling of terminal alkynes.¹⁰

⁶ A. Jakob, C. C. Joubert, T. Rüffer, J. C. Swarts and H. Lang, *Inorg. Chim. Acta*, 2014, **411**, 48–55.

⁷ See, for instance, ref. 6 and: (a) H. E. LeMay, D. J. Hodgson, P. Pruettiangkura and L. J. Theriot, *J. Chem. Soc., Dalton Trans.*, 1979, 781–785; (b) M. Drillon, A. Grand and P. Rey, *Inorg. Chem.*, 1990, **29**, 771–774; (c) G. A. van Albada, I. Mutikainen, I. Riggio, U. Turpeinen and J. Reedijk, *Polyhedron*, 2002, **21**, 141–146; (d) A. Bencini, A. Dei, C. Sangregorio, F. Totti and M. G. F. Vaz, *Inorg. Chem.*, 2003, **42**, 8065–8071.

⁸ R. Battino, T. R. Rettich and T. Tominaga, *J. Phys. Chem. Ref. Data.*, 1983, **12**, 163–178.

⁹ (a) H.-Q. Do and O. Daugulis, *J. Am. Chem. Soc.*, 2009, **131**, 17052–17053; (b) A. E. King, L. M. Huffinan, A. Casitas, M. Costas, X. Ribas and S. S. Stahl, *J. Am. Chem. Soc.*, 2010, **132**, 12068–12073.

¹⁰ X. Qi, R. Bai, L. Zhu, R. Jin, A. Lei and Y. Lan, *J. Org. Chem.*, 2016, **81**, 1654–1660.

(D) Single-crystal X-ray structure determinations

D1 X-Ray Data: Single crystals of compounds **4a**, **4b·2HCl**, **9fa**, **9eb**, **9cc** and **10dc** suitable for X-ray diffraction analysis were grown by slow evaporation of a solution thereof in dichloromethane (**4a**), chloroform (**4b·2HCl**), *ca.* 1:1 toluene/cyclohexane (**9fa**), *ca.* 1:1 acetonitrile/cyclohexane (**9eb**) or ethyl acetate (**9cc** and **10dc**) at room temperature. Single crystals of compounds **4a·2HOTf**, **9aa**, **9ib** and **9dh** suitable for X-ray diffraction analysis were grown by slow diffusion of cyclohexane into a solution thereof in ethanol (**4a·2HOTf**) or acetonitrile (**9aa**, **9ib** and **9dh**) at room temperature. The measured crystals were prepared under inert conditions immersed in perfluoropolyether as protecting oil for manipulation.

D2 Data collection: Crystal structure determinations of **4a**, **9aa** and **9eb** were carried out using a Bruker APEX DUO diffractometer with APEX DUO Kappa 4-axis goniometer equipped with an APEX II 4K CCD area detector, a Microfocus Source E025 IuS using Mo_K α radiation, a Quazar MX Multilayer Optics monochromator and an Oxford Cryosystems low temperature device Cryostream 700 plus (T = –173 °C). Crystal structure determinations of **4a·2HOTf**, **4b·2HCl**, **9fa**, **9ib**, **9cc**, **9dh** and **10dc** were carried out using a Rigaku MicroMax-007HF diffractometer with 1/4chi goniometer equipped with a PILATUS 200K detector, a Microfocus rotating anode X-ray tube using Mo_K α radiation, a Confocal Max Flux optic monochromator and an Oxford Cryosystems low temperature device Cryostream 700 plus (T = –173 or –183 °C). Full-sphere data collection was used with ω and ϕ scans. Programs used in the Bruker system: data collection with APEX-2,¹¹ data reduction with Bruker Saint,¹² and absorption correction with SADABS.¹³ Programs used in the Rigaku system: data collection, data reduction, and absorption correction with CrysAlisPro.¹⁴

¹¹ APEX II versions v1.0-22, v2009.1-0 and v2009.1-02, Bruker AXS Inc., Madison, Wisconsin, USA, 2007.

¹² SAINT versions V.2.10, V/.60A and V7.60A, Bruker AXS Inc., Madison, Wisconsin, USA, 2003/2007.

¹³ SADABS, V.2.10, V2008 and V2008/1, Bruker AXS Inc., Madison, Wisconsin, USA, 2003/2001, see: R. H. Blessing, *Acta Crystallogr., Sect. A*, 1995, **51**, 33–38.

¹⁴ CrysAlisPro version 1.171.38.37f, Rigaku Oxford Diffraction, 2015.

D3 Structure Solution and Refinement: Crystal structure solution was achieved using direct methods as implemented in SHELXTL¹⁵ and visualized using the program XP. Missing atoms were subsequently located from difference Fourier synthesis and added to the atom list. Least-squares refinement on F² using all measured intensities was carried out using the program SHELXTL. All non-hydrogen atoms were refined including anisotropic displacement parameters.

D4 Crystal data for 4a (CCDC 1523647): C₂₄H₃₀N₈, Mr = 430.56; triclinic; space group *P*-1, *a* = 9.4167(6) Å, *b* = 14.0835(8) Å, *c* = 17.8245(10) Å, α = 80.071(2)°, β = 89.817(2)°, γ = 79.781(2)°, *V* = 2290.6(2) Å³, *Z* = 4, ρ_{cal} = 1.248 mg/m³, μ = 0.079 mm⁻¹, 60581 reflections were collected of which 12447 are unique (*R*_{int} = 0.0261), 9472 *F*_o > 4sig(*F*_o), 585 refined parameters, *R*₁ [*I* > 2sigma(*I*)] = 0.0444, *wR*₂ [*I* > 2sigma(*I*)] = 0.1212, Goodness of fit on *F*² = 1.030, maximum residual electron density 0.393 (−0.251) e·Å⁻³.

D5 Crystal data for 4a·2HOTf (CCDC 1523649): C₂₆H₃₂F₆N₈O₆S₂, Mr = 730.71; monoclinic; space group *C*2/*c*, *a* = 30.0913(6) Å, *b* = 10.71870(10) Å, *c* = 23.0764(5) Å, β = 116.049(2)°, *V* = 6687.0(2) Å³, *Z* = 8, ρ_{cal} = 1.452 mg/m³, μ = 0.245 mm⁻¹, 60304 reflections were collected of which 9562 are unique (*R*_{int} = 0.0300), 8087 *F*_o > 4sig(*F*_o), 717 refined parameters, *R*₁ [*I* > 2sigma(*I*)] = 0.0379, *wR*₂ [*I* > 2sigma(*I*)] = 0.1017, Goodness of fit on *F*² = 1.057, maximum residual electron density 0.464 (−0.344) e·Å⁻³.

D6 Crystal data for 4b·2HCl (CCDC 1523648): C₂₂H₂₈Cl₂N₈, Mr = 475.42; triclinic; space group *P*-1, *a* = 10.14276(19) Å, *b* = 10.2202(3) Å, *c* = 11.6711(2) Å, α = 79.961(2)°, β = 89.7958(15)°, γ = 87.646(2)°, *V* = 1190.30(5) Å³, *Z* = 2, ρ_{cal} = 1.326 mg/m³, μ = 0.300 mm⁻¹, 22164 reflections were collected of which 6123 are unique (*R*_{int} = 0.0261), 5471 *F*_o > 4sig(*F*_o), 418 refined parameters, *R*₁ [*I* > 2sigma(*I*)] = 0.0396, *wR*₂ [*I* > 2sigma(*I*)] = 0.1096, Goodness of fit on *F*² = 1.055, maximum residual electron density 1.095 (−0.326) e·Å⁻³.

¹⁵ SHELXTL, versions V6.12 and 6.14, see: G. M. Sheldrick, *Acta Crystallogr., Sect. A*, 2008, **64**, 112–122.

D7 Crystal data for 9aa (CCDC 1523654): $C_{18}H_{16}N_2O_2$, $M_r = 292.33$; monoclinic; space group $C2/c$, $a = 15.7795(13) \text{ \AA}$, $b = 8.7261(8) \text{ \AA}$, $c = 21.0431(19) \text{ \AA}$, $\beta = 101.069(3)^\circ$, $V = 2843.6(4) \text{ \AA}^3$, $Z = 8$, $\rho_{cal} = 1.366 \text{ mg/m}^3$, $\mu = 0.090 \text{ mm}^{-1}$, 3911 reflections were collected of which 3911 are unique ($R_{int} = ?$), 3089 $F_o > 4\text{sig}(F_o)$, 204 refined parameters, $R_1 [I > 2\text{sigma}(I)] = 0.0537$, $wR_2 [I > 2\text{sigma}(I)] = 0.1419$, Goodness of fit on $F^2 = 1.047$, maximum residual electron density $0.298 (-0.293) \text{ e} \cdot \text{\AA}^{-3}$.

D8 Crystal data for 9fa (CCDC 1523653): $C_{20}H_{18}N_2O_2$, $M_r = 318.36$; triclinic; space group $P-1$, $a = 11.5272(7) \text{ \AA}$, $b = 12.3657(7) \text{ \AA}$, $c = 12.7398(8) \text{ \AA}$, $\alpha = 100.159(2)^\circ$, $\beta = 112.561(2)^\circ$, $\gamma = 92.319(2)^\circ$, $V = 1638.97(17) \text{ \AA}^3$, $Z = 4$, $\rho_{cal} = 1.290 \text{ mg/m}^3$, $\mu = 0.084 \text{ mm}^{-1}$, 20988 reflections were collected of which 8081 are unique ($R_{int} = 0.0284$), 6260 $F_o > 4\text{sig}(F_o)$, 474 refined parameters, $R_1 [I > 2\text{sigma}(I)] = 0.0473$, $wR_2 [I > 2\text{sigma}(I)] = 0.1161$, Goodness of fit on $F^2 = 1.042$, maximum residual electron density $0.382 (-0.291) \text{ e} \cdot \text{\AA}^{-3}$.

D9 Crystal data for 9eb (CCDC 1523650): $C_{24}H_{17}F_3N_2O_2$, $M_r = 422.39$; monoclinic; space group Pn , $a = 9.8771(10) \text{ \AA}$, $b = 10.6875(10) \text{ \AA}$, $c = 36.521(4) \text{ \AA}$, $\beta = 96.428(3)^\circ$, $V = 3831.0(6) \text{ \AA}^3$, $Z = 8$, $\rho_{cal} = 1.465 \text{ mg/m}^3$, $\mu = 0.114 \text{ mm}^{-1}$, 49007 reflections were collected of which 18987 are unique ($R_{int} = 0.0592$), 16966 $F_o > 4\text{sig}(F_o)$, 1121 refined parameters, $R_1 [I > 2\text{sigma}(I)] = 0.0935$, $wR_2 [I > 2\text{sigma}(I)] = 0.2610$, Goodness of fit on $F^2 = 1.074$, maximum residual electron density $1.430 (-0.714) \text{ e} \cdot \text{\AA}^{-3}$.

D10 Crystal data for 9ib (CCDC 1523655): $C_{19}H_{15}Cl_1N_2O_2$, $M_r = 338.78$; monoclinic; space group $P2(1)/c$, $a = 10.3350(3) \text{ \AA}$, $b = 31.4198(10) \text{ \AA}$, $c = 9.5959(3) \text{ \AA}$, $\beta = 90.414(2)^\circ$, $V = 3115.93(17) \text{ \AA}^3$, $Z = 8$, $\rho_{cal} = 1.444 \text{ mg/m}^3$, $\mu = 0.259 \text{ mm}^{-1}$, 83805 reflections were collected of which 8303 are unique ($R_{int} = 0.0520$), 7207 $F_o > 4\text{sig}(F_o)$, 438 refined parameters, $R_1 [I > 2\text{sigma}(I)] = 0.0513$, $wR_2 [I > 2\text{sigma}(I)] = 0.1102$, Goodness of fit on $F^2 = 1.059$, maximum residual electron density $0.426 (-0.306) \text{ e} \cdot \text{\AA}^{-3}$.

D11 Crystal data for 9cc (CCDC 1523651): $C_{29}H_{22}N_2O_2$, $M_r = 430.48$; orthorhombic; space group $Pbca$, $a = 19.4045(5) \text{ \AA}$, $b = 7.14236(16) \text{ \AA}$, $c = 30.4827(7) \text{ \AA}$, $V = 4224.72(17) \text{ \AA}^3$, $Z = 8$, $\rho_{cal} = 1.354 \text{ mg/m}^3$, $\mu = 0.085 \text{ mm}^{-1}$, 47181 reflections were collected of which 7267 are unique ($R_{int} = 0.0313$), 6103 $F_o > 4\text{sig}(F_o)$, 299 refined

parameters, $R1 [I > 2\sigma(I)] = 0.0437$, $wR2 [I > 2\sigma(I)] = 0.1161$, Goodness of fit on $F^2 = 1.050$, maximum residual electron density $0.529 (-0.210) \text{ e} \cdot \text{\AA}^{-3}$.

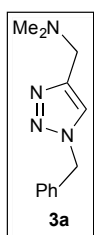
D12 Crystal data for 9dh (CCDC 1525528): $\text{C}_{25}\text{H}_{23}\text{Cl}_1\text{N}_2\text{O}_3\text{S}_1$ [$\text{C}_{23}\text{H}_{17}\text{Cl}_1\text{N}_2\text{O}_2 + \text{CH}_3\text{S}(=\text{O})\text{CH}_3$], $M_r = 466.96$; monoclinic; space group $P2(1)/n$, $a = 9.1959(2) \text{ \AA}$, $b = 11.7982(3) \text{ \AA}$, $c = 21.0279(6) \text{ \AA}$, $\beta = 100.290(3)^\circ$, $V = 2244.73(10) \text{ \AA}^3$, $Z = 4$, $\rho_{\text{cal}} = 1.382 \text{ mg/m}^3$, $\mu = 0.294 \text{ mm}^{-1}$, 24947 reflections were collected of which 7452 are unique ($R_{\text{int}} = 0.0294$), 6278 $F_o > 4\sigma(F_o)$, 292 refined parameters, $R1 [I > 2\sigma(I)] = 0.0395$, $wR2 [I > 2\sigma(I)] = 0.0991$, Goodness of fit on $F^2 = 1.020$, maximum residual electron density $0.604 (-0.273) \text{ e} \cdot \text{\AA}^{-3}$.

D13 Crystal data for 10dc (CCDC 1523652): $\text{C}_{48}\text{H}_{41}\text{N}_3\text{O}_{2.5}$ [$\text{C}_{45}\text{H}_{35}\text{N}_3\text{O} + 0.75 \cdot \text{CH}_3\text{CO}_2\text{CH}_2\text{CH}_3$], $M_r = 699.84$; triclinic; space group $P-1$, $a = 11.9737(2) \text{ \AA}$, $b = 15.3840(3) \text{ \AA}$, $c = 21.9422(4) \text{ \AA}$, $\alpha = 70.396(2)^\circ$, $\beta = 80.7940(10)^\circ$, $\gamma = 74.7630(10)^\circ$, $V = 3662.21(12) \text{ \AA}^3$, $Z = 4$, $\rho_{\text{cal}} = 1.269 \text{ mg/m}^3$, $\mu = 0.078 \text{ mm}^{-1}$, 67913 reflections were collected of which 20091 are unique ($R_{\text{int}} = 0.0358$), 15576 $F_o > 4\sigma(F_o)$, 1051 refined parameters, $R1 [I > 2\sigma(I)] = 0.0465$, $wR2 [I > 2\sigma(I)] = 0.1206$, Goodness of fit on $F^2 = 1.026$, maximum residual electron density $0.367 (-0.270) \text{ e} \cdot \text{\AA}^{-3}$.

(E) Synthesis and characterization of monotriazoles and 5,5'-bistriazoles

The following compounds are all commercially available chemicals which were used as received from the chemical supplier cited in parentheses: sodium ethoxide (Sigma-Aldrich[®]), sodium isopropoxide (Alfa Aesar[®]), copper(I) bromide (Sigma-Aldrich[®]), 2,2,2-trifluoroethanol (TFE; Fluka[®]), anhydrous 2-propanol (Sigma-Aldrich[®]), benzyl azide, 94% purity (**1**; Alfa Aesar[®]), *N,N*-dimethylpropargylamine (**2a**; Sigma-Aldrich[®]), *N*-methylpropargylamine (**2b**; Sigma-Aldrich[®]) and *N*-Boc-propargylamine (**2c**; Alfa Aesar[®]).

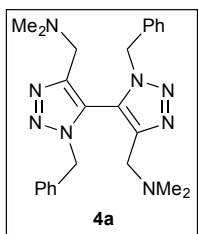
E1 Synthesis of monotriazole **3a** (see Table 2, entry 6)



1-(1-Benzyl-1*H*-1,2,3-triazol-4-yl)-*N,N*-dimethylmethanamine (**3a**)

A solution of NaOEt (82 mg, 1.20 mmol) in TFE (5.6 mL) was prepared inside a 50 mL round bottom flask containing a suitable stirring bar. Benzyl azide, 94% purity (**1**; 80 μ L, 0.60 mmol), *N,N*-dimethylpropargylamine (**2a**; 71 μ L, 0.66 mmol) and CuBr (8.6 mg, 0.060 mmol) were subsequently added over the previous solution at rt. The reaction mixture was stirred at rt overnight under dry air atmosphere by connecting the reaction flask to a glass tube refilled with anhydrous CaCl₂. After 24 h at rt the reaction mixture was concentrated under reduced pressure. The resulting residue was dissolved in DCM (20 mL) and washed with aq. sat. NH₄Cl solution (3 x 20 mL). The organic layer was dried over anhydrous MgSO₄, filtered and concentrated under reduced pressure to render the crude product as a yellowish oil. ¹H NMR analysis of the crude reaction mixture allowed determining full conversion and 100:0:0 molar ratio between monotriazole **3a**, 5,5'-bistriazole **4a** and 5-alkynyltriazole **5a**, respectively, *i.e.*, total product selectivity in favor of **3a**. Purification by silica gel column chromatography (CombiFlash[®] system, 4 g SiO₂ cartridge, 1st eluent: EtOAc, 2nd eluent: 10:90 EtOAc/EtOH, 3rd eluent: 30:70 EtOAc/EtOH) furnished 112 mg of monotriazole **3a** (87% isolated yield) as a pure compound. Physical and spectroscopic data obtained for this known compound were in perfect agreement with the data reported in the literature.¹⁶ ¹H and ¹³C NMR spectra of **3a** are provided in section K.

E2 Synthesis of 5,5'-bistriazole **4a** (see Table 2, entry 12 and Scheme 3a)



1,1'-(3,3'-Dibenzyl-3H,3'H-[4,4'-bi(1,2,3-triazole)]-5,5'-

diyl)bis(N,N-dimethylmethanamine) (4a**)**

A solution of NaOEt (327 mg, 4.81 mmol) in anhydrous EtOH (11.0 mL) was prepared inside a 50 mL round bottom flask containing a suitable stirring bar. Benzyl azide, 94% purity (**1**; 0.80 mL, 6.01 mmol), *N,N*-dimethylpropargylamine (**2a**; 0.26 mL, 2.41 mmol) and CuBr (34 mg, 0.24 mmol) were subsequently added over the previous solution at rt. The reaction mixture was cooled down to 0 °C and stirred at such temperature overnight under dry air atmosphere by connecting the reaction flask to a glass tube refilled with anhydrous CaCl₂. After 24 h at 0 °C the reaction mixture was

¹⁶ E. Ozkal, P. Llanes, F. Bravo, A. Ferrali and M. A. Pericàs, *Adv. Synth. Catal.*, 2014, **356**, 857–869.

concentrated under reduced pressure. The resulting residue was dissolved in DCM (40 mL) and washed with aq. sat. NH_4Cl solution (3 x 40 mL). The organic layer was dried over anhydrous MgSO_4 , filtered and concentrated under reduced pressure to render the crude product as a yellowish oil. ^1H NMR analysis of the crude reaction mixture allowed determining full conversion and 16:83:1 molar ratio between monotriazole **3a**, 5,5'-bistriazole **4a** and 5-alkynyltriazole **5a**, respectively, and 16:84 **3a/4a** ratio, respectively. Purification by silica gel column chromatography (CombiFlash[®] system, 24 g SiO_2 cartridge, 1st eluent: EtOAc, 2nd eluent: 10:90 EtOH/EtOAc, 3rd eluent: 30:70 EtOH/EtOAc) furnished 306 mg of desired 5,5'-bistriazole **4a** (59% isolated yield) and 58 mg of unwanted monotriazole **3a** (11% isolated yield), with both products isolated separately as pure compounds.

Characterization data for **4a**: Crystalline white-yellowish solid; TLC R_f = 0.56 (1:1 EtOAc/EtOH); mp = 103.1–105.3 °C; IR absorption (neat) ν_{max} 3032 ($\text{C}_{\text{sp}2}\text{-H}$), 1619 ($\text{C}=\text{C}$), 1586 ($\text{C}_{\text{Ar}}=\text{C}_{\text{Ar}}$), 1495 ($\text{N}=\text{N}$), 1216, 1042, 1027 and 1013 (C-N); ^1H NMR (500 MHz, CDCl_3) δ 2.13 (s, 12H, 2NMe_2), 2.76 (d, 2H, J = 13.6, 2CHHNMe_2), 3.09 (d, 2H, J = 13.6, 2CHHNMe_2), 4.62 (d, 2H, J = 15.1, 2CHHPh), 5.07 (d, 2H, J = 15.1, 2CHHPh), 6.87–6.96 (m, 4H, H_{Ar}), 7.24–7.35 (m, 6H, H_{Ar}); $^{13}\text{C}\{^1\text{H}\}$ NMR (125 MHz, CDCl_3) δ 45.3 (NMe_2), 52.3 (CH_2Ph), 53.2 (CH_2NMe_2), 122.2 ($\text{Me}_2\text{NCH}_2\text{C}=\text{C}$), 128.1 (CH_{Ar}), 128.7 (CH_{Ar}), 129.0 (CH_{Ar}), 134.3 (C_{Ar}), 147.5 ($\text{Me}_2\text{NCH}_2\text{C}=\text{C}$); HRMS (ESI^+): m/z $[\text{M}+\text{H}]^+$ calcd for $\text{C}_{24}\text{H}_{31}\text{N}_8$ 431.2666, found 431.2670. The crystal structure of **4a** is shown in Fig. SI-1 and crystal data for **4a** are herein given as section D4.

E3 Resolution of *rac*-**4a** by semi-preparative chiral HPLC (see Scheme 4)

Analytical chiral HPLC conditions for *rac*-**4a** (broad peaks): Daicel Chiralpak[®] IA (25 cm x 0.46 cm x 5 μm), 80:15:5 *n*-hexane/2-propanol/ethanol, 1.0 mL/min, 254 nm, $t_R(\mathbf{4a-1})$ = 9.9 min, $t_R(\mathbf{4a-2})$ = 12.8 min (Fig. SI-4).

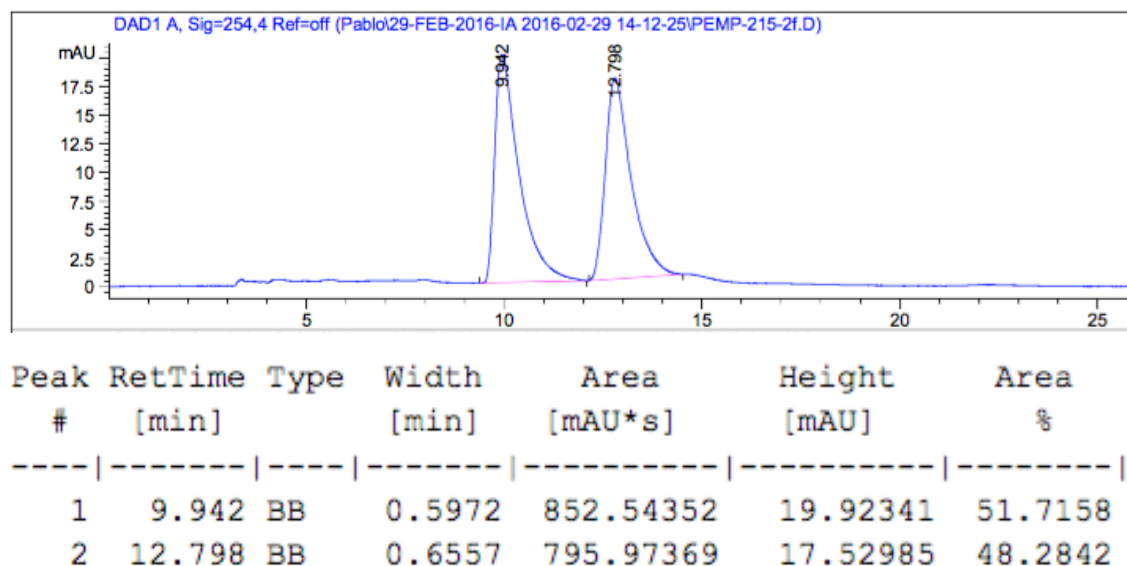


Fig. SI-4 Analytical chiral HPLC analysis of *rac*-4a.

Semi-preparative chiral HPLC conditions for *rac*-4a (sharp peaks): Daicel Chiralpak[®] IA (25 cm x 0.46 cm x 5 μ m), 85:15:0.1 *n*-hexane/2-propanol/diethylamine, 1.0 mL/min, 254 nm, t_R (4a-1) = 8.4 min, t_R (4a-2) = 10.2 min (Fig. SI-5). Loading studies led to injection volumes up to 100 μ L at 10 mg/mL sample concentration.

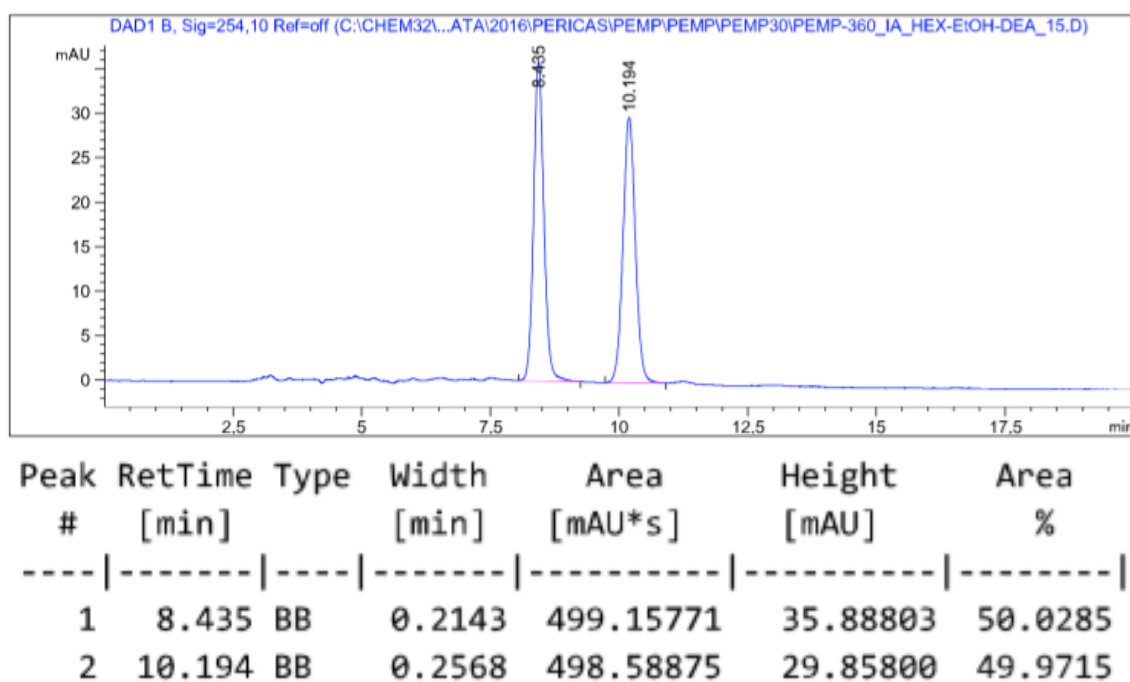
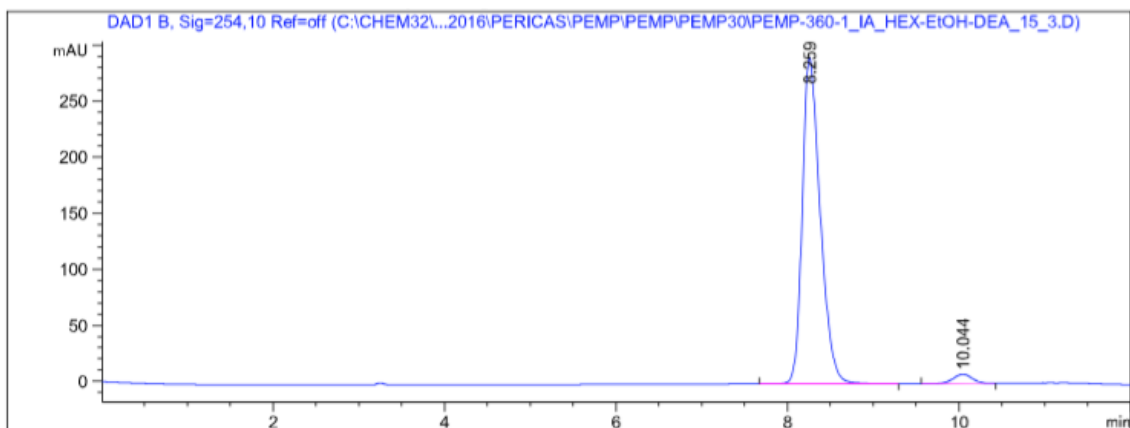
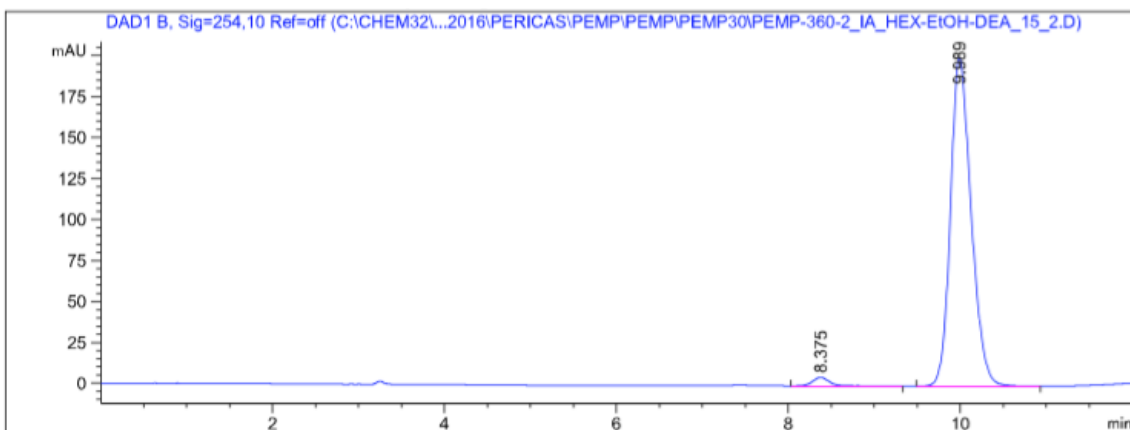


Fig. SI-5 Semi-preparative chiral HPLC analysis of *rac*-4a.



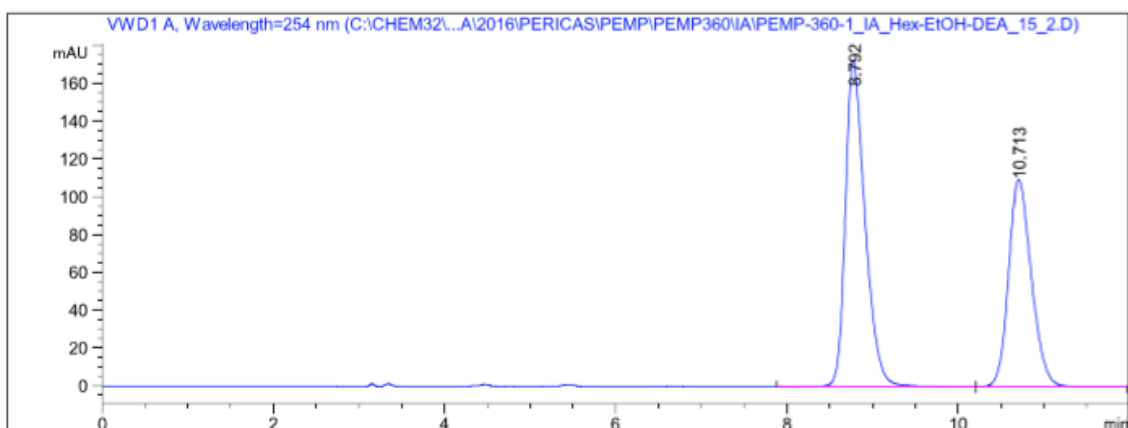
Peak #	RetTime [min]	Type	Width [min]	Area [mAU*s]	Height [mAU]	Area %
1	8.259	BB	0.2219	4240.68652	291.21866	96.9705
2	10.044	BB	0.2409	132.48695	8.44878	3.0295

Fig. SI-6 Enantiomeric purity analysis of the 1st eluting enantiomer **4a-1** after 10 min (94% ee).



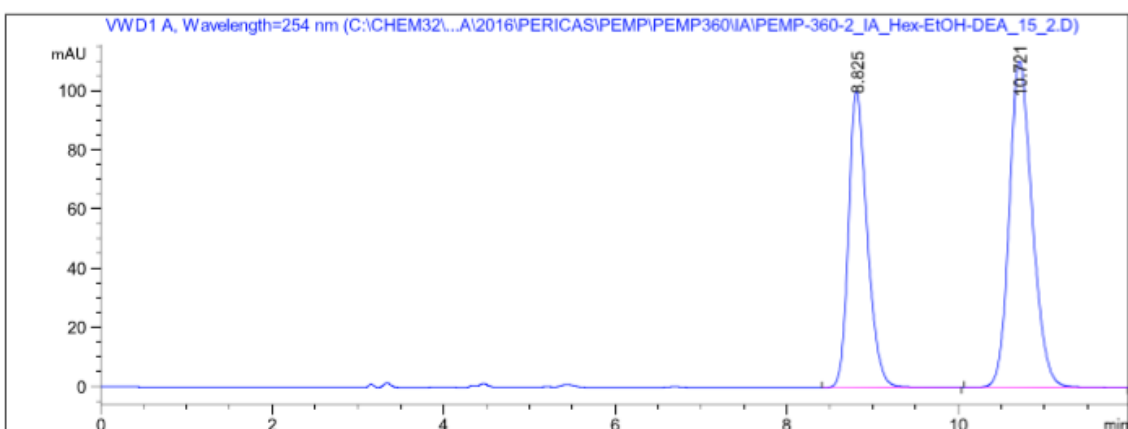
Peak #	RetTime [min]	Type	Width [min]	Area [mAU*s]	Height [mAU]	Area %
1	8.375	BB	0.2093	71.80376	5.19414	2.0957
2	9.989	BB	0.2552	3354.39844	200.46420	97.9043

Fig. SI-7 Enantiomeric purity analysis of the 2nd eluting enantiomer **4a-2** after 10 min (–96% ee).



Peak #	RetTime [min]	Type	Width [min]	Area [mAU*s]	Height [mAU]	Area %
1	8.792	BB	0.2704	2753.57007	160.24147	57.8977
2	10.713	BBA	0.3109	2002.35413	107.31847	42.1023

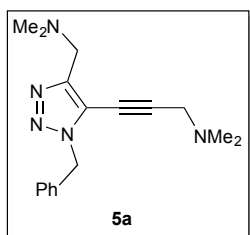
Fig. SI-8 Enantiomeric purity analysis of the 1st eluting enantiomer **4a-1** after 24 h (16% ee).



Peak #	RetTime [min]	Type	Width [min]	Area [mAU*s]	Height [mAU]	Area %
1	8.825	BB	0.2511	1517.89893	97.71999	42.7956
2	10.721	BBA	0.3202	2028.95447	104.28867	57.2044

Fig. SI-9 Enantiomeric purity analysis of the 2nd eluting enantiomer **4a-2** after 24 h (–14% ee).

E4 Synthesis of 5-alkynyltriazole **5a** (see Table 2, entry 14)



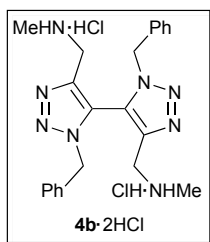
3-(1-Benzyl-4-((dimethylamino)methyl)-1H-1,2,3-triazol-5-yl)-N,N-dimethylprop-2-yn-1-amine (5a**)**

A solution of NaOPr (197 mg, 2.41 mmol) in anhydrous *i*PrOH (5.6 mL) was prepared inside a 50 mL round bottom flask containing a suitable stirring bar. Benzyl azide, 94% purity (**1**; 0.40 mL, 3.01 mmol), *N,N*-dimethylpropargylamine (**2a**; 0.13 mL, 1.20 mmol) and CuBr (17 mg, 0.12 mmol) were subsequently added over the previous solution at rt. The reaction mixture was cooled down to 0 °C and stirred at such temperature overnight under dry air atmosphere by connecting the reaction flask to a glass tube refilled with anhydrous CaCl₂. After 24 h at 0 °C the reaction mixture was concentrated under reduced pressure. The resulting residue was dissolved in DCM (20 mL) and washed with aq. sat. NH₄Cl solution (3 x 20 mL). The organic layer was dried over anhydrous MgSO₄, filtered and concentrated under reduced pressure to render the crude product as a yellowish oil. ¹H NMR analysis of the crude reaction mixture allowed determining full conversion and 10:38:52 molar ratio between monotriazole **3a**, 5,5'-bistriazole **4a** and 5-alkynyltriazole **5a**, respectively, and 20:80 **3a/4a** ratio, respectively. Purification by silica gel column chromatography (CombiFlash[®] system, 12 g SiO₂ cartridge, 1st eluent: EtOAc, 2nd eluent: 10:90 EtOH/EtOAc, 3rd eluent: 30:70 EtOH/EtOAc) furnished 46 mg of 5,5'-bistriazole **4a** (18% isolated yield) and 47 mg of 5-alkynyltriazole **5a** (26% isolated yield), with both products isolated separately as pure compounds.

Characterization data for **5a**: Brownish oil; TLC *R_f* = 0.11 (1:1 EtOAc/EtOH); IR absorption (neat) ν_{max} 3064 and 3032 (C_{sp2}-H), 1604 (C=C), 1586 (C_{Ar}=C_{Ar}), 1497 (N=N), 1259, 1206, 1124 and 1029 (C-N); ¹H NMR (500 MHz, CDCl₃) δ 2.29 (s, 6H, NMe₂), 2.30 (s, 6H, NMe₂), 3.54 (s, 2H, CH₂NMe₂), 3.62 (s, 2H, CH₂NMe₂), 5.57 (s, 2H, CH₂Ph), 7.07–7.55 (m, 5H, H_{Ar}); ¹³C{¹H} NMR (125 MHz, CDCl₃) δ 44.1 (C≡CCH₂NMe₂), 45.1 (C=CCH₂NMe₂), 48.6 (C≡CCH₂NMe₂), 52.7 (CH₂Ph), 53.2 (C=CCH₂NMe₂), 70.6 (C≡CCH₂NMe₂), 97.9 (C≡CCH₂NMe₂), 120.5 (C=CCH₂NMe₂),

127.7 (CH_{Ar}), 128.3 (CH_{Ar}), 128.8 (CH_{Ar}), 134.8 (C_{Ar}), 146.9 (C=CCH₂NMe₂); HRMS (ESI⁺): *m/z* [M+H]⁺ calcd for C₁₇H₂₄N₅ 298.2026, found 298.2020.

E5 Synthesis of 5,5'-bistriazole **4b**·2HCl (see Scheme 3b)



1,1'-(3,3'-Dibenzyl-3H,3'H-[4,4'-bi(1,2,3-triazole)]-5,5'-

diyl)bis(N-methylmethanamine) dihydrochloride (4b**·2HCl)**

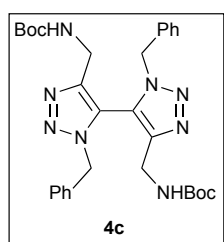
A solution of NaOEt (82 mg, 1.20 mmol) in anhydrous EtOH (5.6 mL) was prepared inside a 50 mL round bottom flask containing a suitable stirring bar. Benzyl azide, 94% purity (**1**; 0.20 mL, 1.50 mmol), *N*-methylpropargylamine (**2b**; 53 μL, 0.60 mmol) and CuBr (8.6 mg, 0.060 mmol) were subsequently added over the previous solution at rt. The reaction mixture was cooled down to 0 °C and stirred at such temperature overnight under dry air atmosphere by connecting the reaction flask to a glass tube refilled with anhydrous CaCl₂. After 24 h at 0 °C the reaction mixture was concentrated under reduced pressure. The resulting residue was dissolved in DCM (20 mL) and washed with aq. sat. NH₄Cl solution (3 x 20 mL). The organic layer was dried over anhydrous MgSO₄, filtered and concentrated under reduced pressure to render the crude product as a yellowish oil. ¹H NMR analysis of the crude reaction mixture allowed determining full conversion and 20:80 molar ratio between monotriazole **3b** and 5,5'-bistriazole **4b**·2HCl, respectively, without detecting the corresponding 5-alkynyltriazole product (**5b**). Purification by silica gel column chromatography (CombiFlash[®] system, 4 g SiO₂ cartridge, 1st eluent: EtOAc, 2nd eluent: 10:90 EtOH/EtOAc, 3rd eluent: 30:70 EtOH/EtOAc) furnished 63 mg of a mixture containing the desired 5,5'-bistriazole **4b**·2HCl (40% yield) along with the unwanted monotriazole **3b**¹⁷ (5% yield) in 17:83 **3b**/**4b**·2HCl molar ratio, respectively.

Characterization data for the very major product **4b**·2HCl (from a 17:83 **3b**/**4b**·2HCl mixture): Crystalline white-yellowish solid; TLC *R_f* = 0.10 (1:1 EtOAc/EtOH); IR absorption (neat) *ν*_{max} 3368 (H–N⁺–H), 3032 (C_{sp2}–H), 1619 (C=C), 1571 (C_{Ar}=C_{Ar}), 1496 (N=N), 1218, 1121, 1074 and 1028 (C–N); ¹H NMR (500 MHz, CDCl₃) δ 2.34 (s,

¹⁷ Known compound. For a full characterization, see: O. Di Pietro, N. Alencar, G. Esteban, E. Viayna, N. Szalaj, J. Vázquez, J. Juárez-Jiménez, I. Sola, B. Pérez, M. Solé, M. Unzeta, D. Muñoz-Torrero and F. J. Luque, *Bioorg. Med. Chem.*, 2016, **24**, 4835–4854.

6H, $2\text{NH}_2^+-\text{Me}$), 3.02 (d, 2H, $J = 13.7$, $2\text{CHHNH}_2^+-\text{Me}$), 3.41 (d, 2H, $J = 13.7$, $2\text{CHHNH}_2^+-\text{Me}$), 3.87 (bs, 4H, $2\text{NH}_2^+-\text{Me}$), 4.61 (d, 2H, $J = 15.6$, 2CHHPh), 5.15 (d, 2H, $J = 15.6$, 2CHHPh), 6.87–6.99 (m, 4H, H_{Ar}), 7.24–7.35 (m, 6H, H_{Ar}); $^{13}\text{C}\{^1\text{H}\}$ NMR (125 MHz, CDCl_3) δ 34.9 (NH_2^+-Me), 44.0 ($\text{CH}_2\text{NH}_2^+-\text{Me}$), 52.9 (CH_2Ph), 121.2 ($\text{C}=\text{CCH}_2\text{NH}_2^+-\text{Me}$), 128.0 (CH_{Ar}), 129.1 (CH_{Ar}), 129.2 (CH_{Ar}), 133.7 (C_{Ar}), 147.0 ($\text{C}=\text{CCH}_2\text{NH}_2^+-\text{Me}$); HRMS (ESI $^+$): m/z $[\text{M}+\text{H}]^+$ calcd for $\text{C}_{22}\text{H}_{27}\text{N}_8$ 403.2353, found 403.2351. The crystal structure of **4b**·2HCl is shown in Fig. SI-3 and crystal data for **4b**·2HCl are herein given as section D6.

E6 Synthesis of 5,5'-bistriazole **4c** (see Scheme 3c)

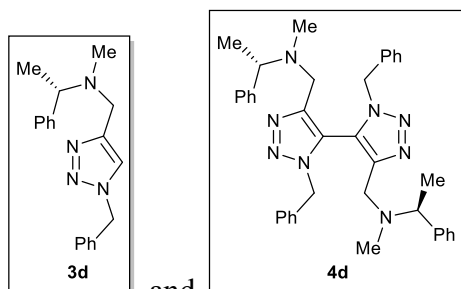


Di-*tert*-butyl ((3,3'-dibenzyl-3*H*,3'*H*-[4,4'-bi(1,2,3-triazole)]-5,5'-diyl)bis(methylene))dicarbamate (**4c**)

A solution of NaOEt (82 mg, 1.20 mmol) in anhydrous EtOH (5.6 mL) was prepared inside a 50 mL round bottom flask containing a suitable stirring bar. Benzyl azide, 94% purity (**1**; 0.20 mL, 1.50 mmol), *N*-Boc-propargylamine (**2c**; 93 mg, 0.60 mmol) and CuBr (8.6 mg, 0.060 mmol) were subsequently added over the previous solution at rt. The reaction mixture was cooled down to 0 °C and stirred at such temperature overnight under dry air atmosphere by connecting the reaction flask to a glass tube refilled with anhydrous CaCl_2 . After 24 h at 0 °C the reaction mixture was concentrated under reduced pressure. The resulting residue was dissolved in DCM (20 mL) and washed with aq. sat. NH_4Cl solution (3 x 20 mL). The organic layer was dried over anhydrous MgSO_4 , filtered and concentrated under reduced pressure to render the crude product as a yellowish oil. ^1H NMR analysis of the crude reaction mixture allowed determining full conversion and 62:35:3 molar ratio between monotriazole **3c**, 5,5'-bistriazole **4c** and 5-alkynyltriazole **5c**, respectively, and 64:36 **3c/4c** ratio, respectively. Purification by silica gel column chromatography (CombiFlash $^{\text{®}}$ system, 4 g SiO_2 cartridge, 1st eluent: cyclohexane, 2nd eluent: 10:90 EtOAc/cyclohexane, 3rd eluent: 30:70 EtOAc/cyclohexane, 4th eluent: 50:50 EtOAc/cyclohexane) furnished 58 mg of a mixture containing the desired 5,5'-bistriazole **4c** (20% yield) along with the unwanted

monotriazole **3b**¹⁸ (14% yield) in 58:42 **3c/4c** molar ratio, respectively. Owing to the low ratio of desired 5,5'-bistriazole **4c**, this product could not be fully characterized although ¹H and ¹³C NMR spectra are provided for the isolated 58:42 **3c/4c** mixture of products (see section K).

E7 Synthesis of chiral monotriazole **3d** and 5,5'-bistriazole **4d** (see Scheme 6)



(*S*)-*N*-((1-Benzyl-1*H*-1,2,3-triazol-4-yl)methyl)-*N*-methyl-1-phenylethan-1-amine (**3d**) and (1*S*,1'*S*)-*N,N'*-((3,3'-dibenzyl-3*H*,3'*H*-[4,4'-bi(1,2,3-triazole)]-5,5'-diyl)bis(methylene))bis(*N*-methyl-1-phenylethan-1-amine) (**4d**)

A solution of (*S*)-*N*-methyl-*N*-propargyl-1-phenylethylamine¹⁹ (**2d**; 400 mg, 2.31 mmol), NaOEt (314 mg, 4.62 mmol) and CuBr (33 mg, 0.23 mmol) in anhydrous EtOH (11.0 mL) was prepared inside a 50 mL round bottom flask containing a suitable stirring bar. Benzyl azide, 94% purity (**1**; 0.77 mL, 5.77 mmol) was subsequently added over the previous solution at rt. The reaction mixture was cooled down to 0 °C and stirred at such temperature overnight under dry air atmosphere by connecting the reaction flask to a glass tube refilled with anhydrous CaCl₂. After 24 h at 0 °C the reaction mixture was concentrated under reduced pressure. The resulting residue was dissolved in DCM (40 mL) and washed with aq. sat. NH₄Cl solution (3 x 40 mL). The organic layer was dried over anhydrous MgSO₄, filtered and concentrated under reduced pressure to render the crude product as a yellowish solid. ¹H NMR analysis of the crude reaction mixture allowed determining full conversion and 96:4 molar ratio between monotriazole **3e** and 5,5'-bistriazole **4e**, respectively, without detecting the corresponding chiral 5-alkynyltriazole product (**5d**). Purification by silica gel column chromatography (CombiFlash[®] system, 24 g SiO₂ cartridge, 1st eluent: cyclohexane, 2nd eluent: 30:70 EtOAc/cyclohexane, 3rd eluent: 50:50 EtOAc/cyclohexane) furnished 496 mg of chiral

¹⁸ Known compound. For a full characterization, see: C. Shao, X. Wang, Q. Zhang, S. Luo, J. Zhao and Y. Hu, *J. Org. Chem.*, 2011, **76**, 6832–6836.

¹⁹ Prepared in enantiopure form from commercially available (*S*)-*N*-methyl-1-phenylethylamine (Sigma-Aldrich[®]) by following the literature procedure, see: H. Rezaei, I. Marek and J. F. Normant, *Tetrahedron*, 2001, **57**, 2477–2483. ¹H and ¹³C NMR spectra of **2d** are provided in section K.

monotriazole **3d** (70% isolated yield) as a pure compound and 59 mg of axially and centrally chiral 5,5'-bistriazole **4d** (8% isolated yield) as a 53:47 mixture of atropisomeric diastereomers [(*S,S,R_a*)-**4d** and (*S,S,S_a*)-**4d**] which could not be isolated separately in that manner. Owing to this, the two individual diastereomers of **4d** could not be fully characterized at this stage although ¹H and ¹³C NMR spectra are provided for the isolated 53:47 mixture of diastereomers (see section K).

Characterization data for **3d**: White solid; TLC *R_f* = 0.48 (EtOAc); mp = 83.5–86.3 °C; [α]_D²⁶ = –20.2 (*c* 0.97, CHCl₃); IR absorption (neat) ν_{max} 3111, 3069 and 3030 (C_{sp2}–H), 1600 (C=C), 1551 (C_{Ar}=C_{Ar}), 1491 (N=N), 1245, 1216, 1126, 1050 and 1031 (C–N); ¹H NMR (500 MHz, CDCl₃) δ 1.42 (d, 3H, *J* = 6.7, CH–*Me*), 2.22 (s, 3H, *NMe*), 3.58 (d, 1H, *J* = 14.1, CHH–N), 3.59 (q, 1H, *J* = 6.7, CH–*Me*), 3.76 (d, 1H, *J* = 14.1, CHH–N), 5.51 (d, 1H, *J* = 14.9, CHH–Ph), 5.55 (d, 1H, *J* = 14.9, CHH–Ph), 7.21–7.45 (m, 11H, 2*Ph* and C=CH); ¹³C{¹H} NMR (125 MHz, CDCl₃) δ 19.0 (CH*Me*), 38.8 (*NMe*), 49.6 (CH₂N), 54.1 (CH₂Ph), 62.9 (CH*Me*), 122.3 (NCH₂C=CH), 126.9 (CH_{Ar}), 127.6 (CH_{Ar}), 128.0 (CH_{Ar}), 128.2 (CH_{Ar}), 128.6 (CH_{Ar}), 129.1 (CH_{Ar}), 134.9 (C_{Ar}), 143.8 (C_{Ar}), 146.4 (NCH₂C=CH); HRMS (ESI⁺): *m/z* [M+H]⁺ calcd for C₁₉H₂₃N₄ 307.1917, found 307.1919.

E8 Resolution of (*S,S,R_a*/*S_a*)-4d** by semi-preparative chiral HPLC (see Scheme 7)**

Semi-preparative chiral HPLC conditions for (*S,S,R_a*/*S_a*)-**4d** (53:47 dr): Daicel Chiralpak[®] IA (25 cm x 0.46 cm x 5 μ m), 50:50:0.1 *n*-hexane/2-propanol/diethylamine, 1.0 mL/min, 254 nm, *t_R*(**4d-1**) = 7.5 min, *t_R*(**4d-2**) = 12.9 min (Fig. SI-7). Loading studies led to injection volumes up to 100 μ L at 15 mg/mL sample concentration. Under such conditions, around 40 mg of diastereomeric mixture of **4d** (53:47 dr) were easily separated and, after removal of solvents, furnished 14 mg of the 1st eluting diastereomer **4d-1** and 15 mg of the 2nd eluting diastereomer **4d-2** which were both obtained as chemically pure single stereoisomers and could be thus fully characterized (*vide infra*).²⁰

²⁰ Compounds **4d-1** and **4d-2** were both isolated as oils, precluding the possible assignment of the axial chirality of the bistriazole core of each diastereomer through SCXRD.

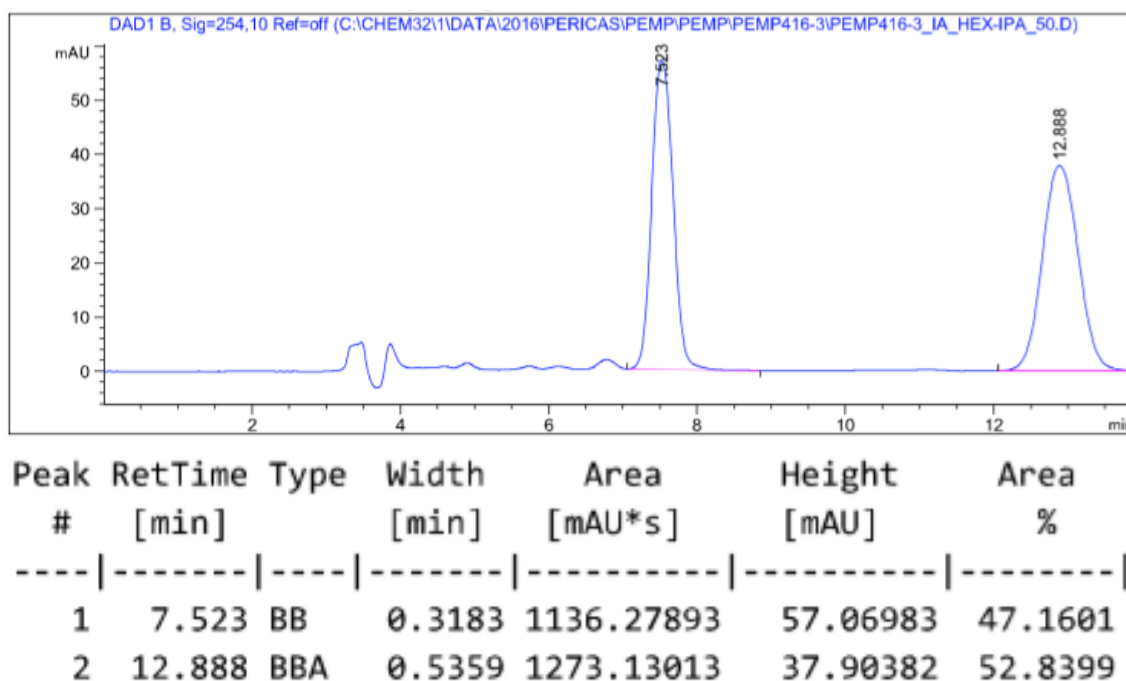


Fig. SI-10 Semi-preparative chiral HPLC analysis of (*S,S,R_a/S_a*)-**4d** (53:47 dr).

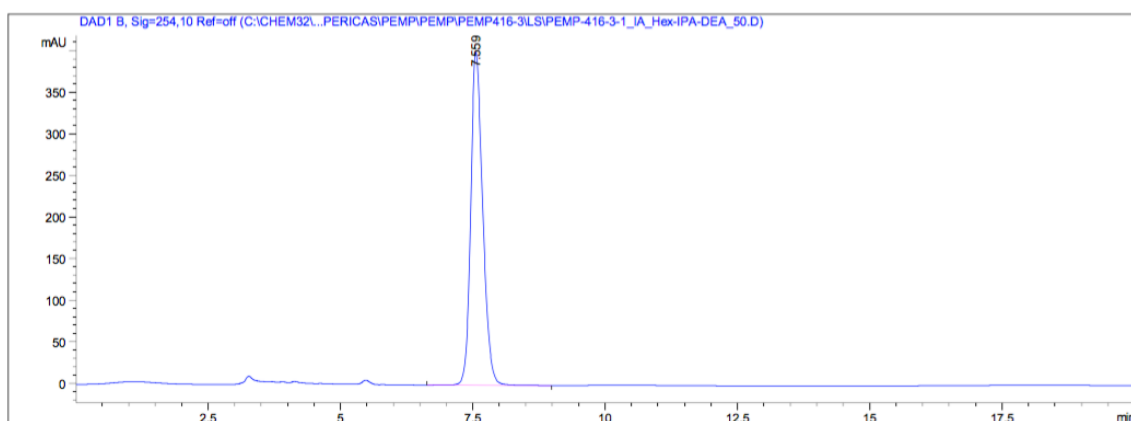


Fig. SI-11 Diastereomeric purity analysis of the 1st eluting diastereomer **4d-1** after 24 h (100:0 dr).

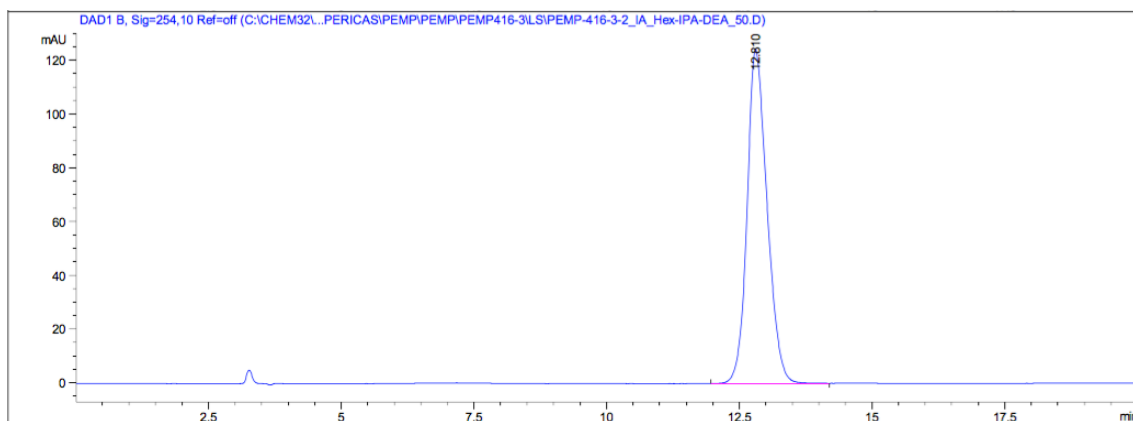


Fig. SI-12 Diastereomeric purity analysis of the 2nd eluting diastereomer **4d-2** after 24 h (0:100 dr).

Characterization data for the 1st eluting diastereomer **4d-1**: Sticky whitish oil; TLC $R_f = 0.86$ (EtOAc); $[\alpha]_D^{24} = +23.2$ (c 0.70, CHCl_3); IR absorption (neat) ν_{max} 3084, 3061 and 3030 ($\text{C}_{\text{sp}2}\text{-H}$), 1603 ($\text{C}=\text{C}$), 1586 ($\text{C}_{\text{Ar}}=\text{C}_{\text{Ar}}$), 1494 ($\text{N}=\text{N}$), 1214, 1153, 1120, 1074, 1050 and 1030 (C-N); ^1H NMR (500 MHz, CDCl_3) δ 1.15 (d, 6H, $J = 6.7$, 2CH-Me), 2.07 (s, 6H, 2NMe), 2.80 (d, 2H, $J = 13.1$, 2CHH-N), 3.15 (d, 2H, $J = 13.1$, 2CHH-N), 3.35 (q, 2H, $J = 6.7$, 2CH-Me), 4.42 (d, 2H, $J = 14.6$, 2CHH-Ph), 4.94 (d, 2H, $J = 14.6$, 2CHH-Ph), 6.73–6.81 (m, 4H, H_{Ar}), 6.97–7.03 (m, 4H, H_{Ar}), 7.13–7.31 (m, 12H, H_{Ar}); $^{13}\text{C}\{^1\text{H}\}$ NMR (125 MHz, CDCl_3) δ 18.2 (CHMe), 38.6 (NMe), 48.4 (CH_2N), 52.6 (CH_2Ph), 64.0 (CHMe), 122.2 ($\text{NCH}_2\text{C}=\text{C}$), 127.0 (CH_{Ar}), 127.2 (CH_{Ar}), 128.2 (CH_{Ar}), 128.3 (CH_{Ar}), 128.6 (CH_{Ar}), 129.0 (CH_{Ar}), 134.0 (C_{Ar}), 143.3 (C_{Ar}), 148.4 ($\text{NCH}_2\text{C}=\text{C}$); HRMS (ESI^+): m/z $[\text{M}+\text{H}]^+$ calcd for $\text{C}_{38}\text{H}_{43}\text{N}_8$ 611.3605, found 611.3591.

Characterization data for the 2nd eluting diastereomer **4d-2**: Sticky whitish oil; TLC $R_f = 0.86$ (EtOAc); $[\alpha]_D^{26} = -8.8$ (c 0.80, CHCl_3); IR absorption (neat) ν_{max} 3084, 3061 and 3030 ($\text{C}_{\text{sp}2}\text{-H}$), 1603 ($\text{C}=\text{C}$), 1586 ($\text{C}_{\text{Ar}}=\text{C}_{\text{Ar}}$), 1494 ($\text{N}=\text{N}$), 1214, 1153, 1120, 1074, 1050 and 1030 (C-N); ^1H NMR (500 MHz, CDCl_3) δ 1.11 (d, 6H, $J = 6.7$, 2CH-Me), 1.94 (s, 6H, 2NMe), 2.65 (d, 2H, $J = 13.1$, 2CHH-N), 3.09 (d, 2H, $J = 13.1$, 2CHH-N), 3.22 (q, 2H, $J = 6.7$, 2CH-Me), 4.51 (d, 2H, $J = 14.9$, 2CHH-Ph), 5.03 (d, 2H, $J = 14.9$, 2CHH-Ph), 6.87–6.94 (m, 8H, H_{Ar}), 7.13–7.31 (m, 12H, H_{Ar}); $^{13}\text{C}\{^1\text{H}\}$ NMR (125 MHz, CDCl_3) δ 18.8 (CHMe), 38.3 (NMe), 48.6 (CH_2N), 52.5 (CH_2Ph), 64.1 (CHMe), 122.2 ($\text{NCH}_2\text{C}=\text{C}$), 126.9 (CH_{Ar}), 127.1 (CH_{Ar}), 128.2 (CH_{Ar}), 128.3 (CH_{Ar}), 128.7 (CH_{Ar}), 129.0 (CH_{Ar}), 134.1 (C_{Ar}), 143.2 (C_{Ar}), 148.1 ($\text{NCH}_2\text{C}=\text{C}$); HRMS (ESI^+): m/z $[\text{M}+\text{H}]^+$ calcd for $\text{C}_{38}\text{H}_{43}\text{N}_8$ 611.3605, found 611.3597.

(F) Determination of rotational energy barriers and half-life times

F1 Configurational stability of axially chiral 5,5'-bistriazole 4a

F1.1 Results for the 1st eluting enantiomer 4a-1 (see Scheme 5)

Table SI-1 Changes on the enantiomeric ratio of **4a-1** at 25 °C^a

Time (s)	ee(%)	er (B:A)
0	100	100:0
600	94	97:3
86400	16	58:42

^a Determined by chiral HPLC analysis in *n*-hexane/EtOH/HNEt₂ (85:15:0.1).

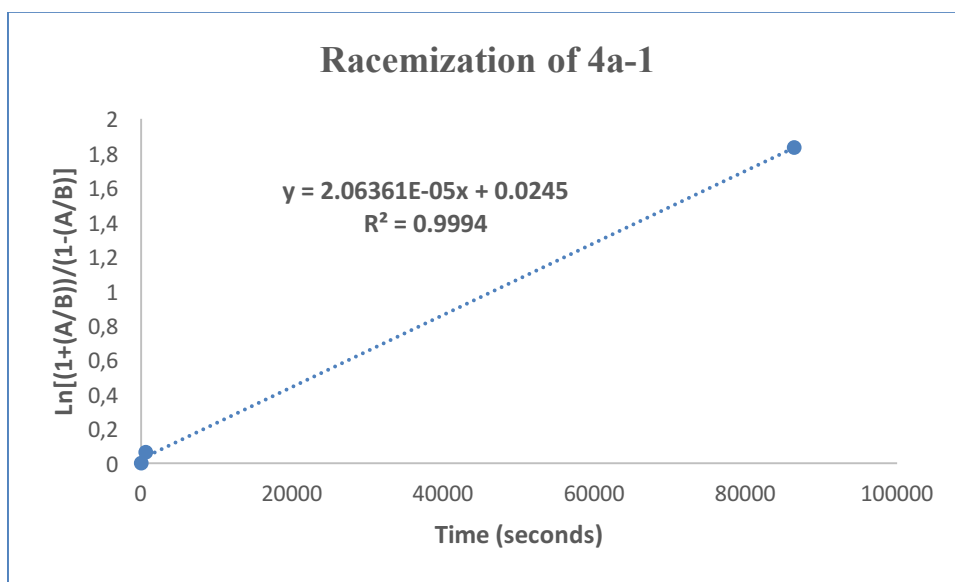


Fig. SI-13 Analysis of racemization kinetics of the 1st eluting enantiomer **4a-1**.

$$\text{slope} = 2.06361 \times 10^{-5} = 2k_{\text{rot}}$$

$$k_{\text{rot}} = 1.0318 \times 10^{-5} \text{ s}^{-1}$$

$$\text{Eyring equation: } \Delta G_{\text{rot}}^{\ddagger} = -RT \ln K_{\text{rot}} \text{ with } K_{\text{rot}} = k_{\text{rot}}/k_{\text{B}}T$$

$$\text{Ideal gas constant: } R = 8.3145 \text{ J/mol} = 0.0083145 \text{ kJ/mol}$$

$$T = 25 \text{ }^{\circ}\text{C} = 298 \text{ K}$$

$$\text{Planck constant: } h = 6.626 \times 10^{-34} \text{ J}\cdot\text{s}$$

$$\text{Boltzmann constant: } k_{\text{B}} = 1.381 \times 10^{-23} \text{ J/K}$$

$$K_{\text{rot}} = 1.6612 \times 10^{-14}$$

$$\Delta G_{\text{rot}}^{\ddagger} = \Delta G_{\text{rac}}^{\ddagger} = 78.6 \text{ kJ/mol} = 18.8 \pm 0.1 \text{ kcal/mol}$$

$$\tau_{1/2\text{rac}} = (\text{Ln } 2)/k_{\text{rac}}$$

$$k_{\text{rac}} = 2k_{\text{rot}}$$

$$k_{\text{rac}} = 2.06361 \times 10^{-5} \text{ s}^{-1} \text{ at } 25^\circ\text{C}$$

$$\tau_{1/2\text{rac}} = 33589 \text{ s} = 560 \text{ min} = 9.3 \text{ h at } 25^\circ\text{C}$$

F1.2 Results for the 2nd eluting enantiomer 4a-2 (see Scheme 5)

Table SI-2 Changes on the enantiomeric ratio of **4a-2** at 25 °C^a

Time (s)	ee(%)	er (B:A)
0	100	100:0
600	96	98:2
86400	14	57:43

^a Determined by chiral HPLC analysis in *n*-hexane/EtOH/HNEt₂ (85:15:0.1).

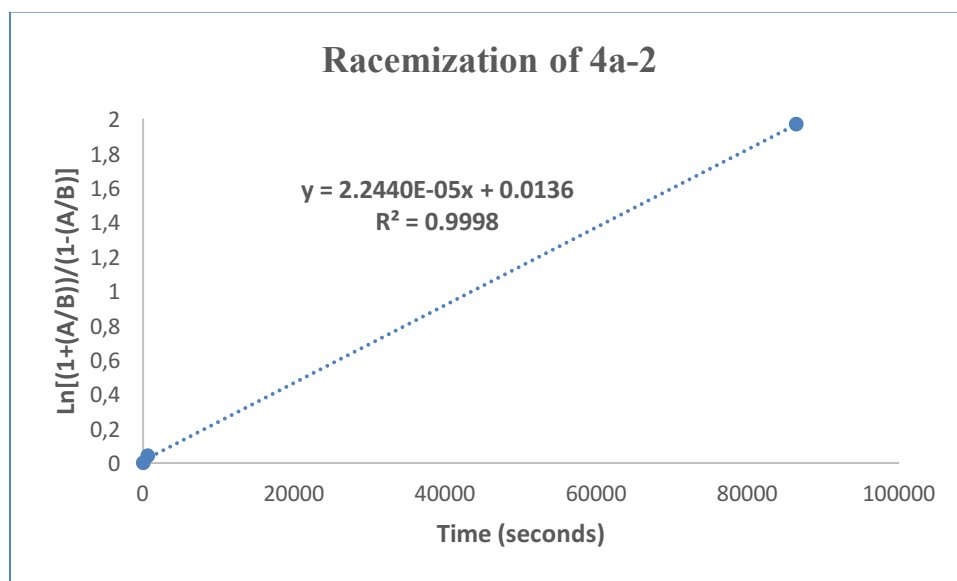


Fig. SI-14 Analysis of racemization kinetics of the 2nd eluting enantiomer **4a-2**.

$$\text{slope} = 2.2440 \times 10^{-5} = 2k_{\text{rot}}$$

$$k_{\text{rot}} = 1.1122 \times 10^{-5} \text{ s}^{-1}$$

$$\text{Eyring equation: } \Delta G_{\text{rot}}^{\ddagger} = -RT \text{Ln } K_{\text{rot}} \text{ with } K_{\text{rot}} = k_{\text{rot}}h/k_{\text{B}}T$$

$$\text{Ideal gas constant: } R = 8.3145 \text{ J/mol} = 0.0083145 \text{ kJ/mol}$$

$$T = 25^\circ\text{C} = 298 \text{ K}$$

$$\text{Planck constant: } h = 6.626 \times 10^{-34} \text{ J}\cdot\text{s}$$

$$\text{Boltzmann constant: } k_{\text{B}} = 1.381 \times 10^{-23} \text{ J/K}$$

$$K_{\text{rot}} = 1.7907 \times 10^{-14}$$

$$\Delta G_{\text{rot}}^{\ddagger} = \Delta G_{\text{rac}}^{\ddagger} = 78.4 \text{ kJ/mol} = 18.8 \pm 0.1 \text{ kcal/mol}$$

$$\tau_{1/2\text{rac}} = (\text{Ln } 2)/k_{\text{rac}}$$

$$k_{\text{rac}} = 2k_{\text{rot}}$$

$$k_{\text{rac}} = 2.2440 \times 10^{-5} \text{ s}^{-1} \text{ at } 25^\circ\text{C}$$

$$\tau_{1/2\text{rac}} = 30888 \text{ s} = 515 \text{ min} = 8.6 \text{ h at } 25^\circ\text{C}$$

F2 Configurational stability of axially and centrally chiral diastereomeric 5,5'-bistriazoles **4d-1** and **4d-2**

F2.1 Epimerization of the 1st eluting diastereomer **4d-1** as a function on the temperature

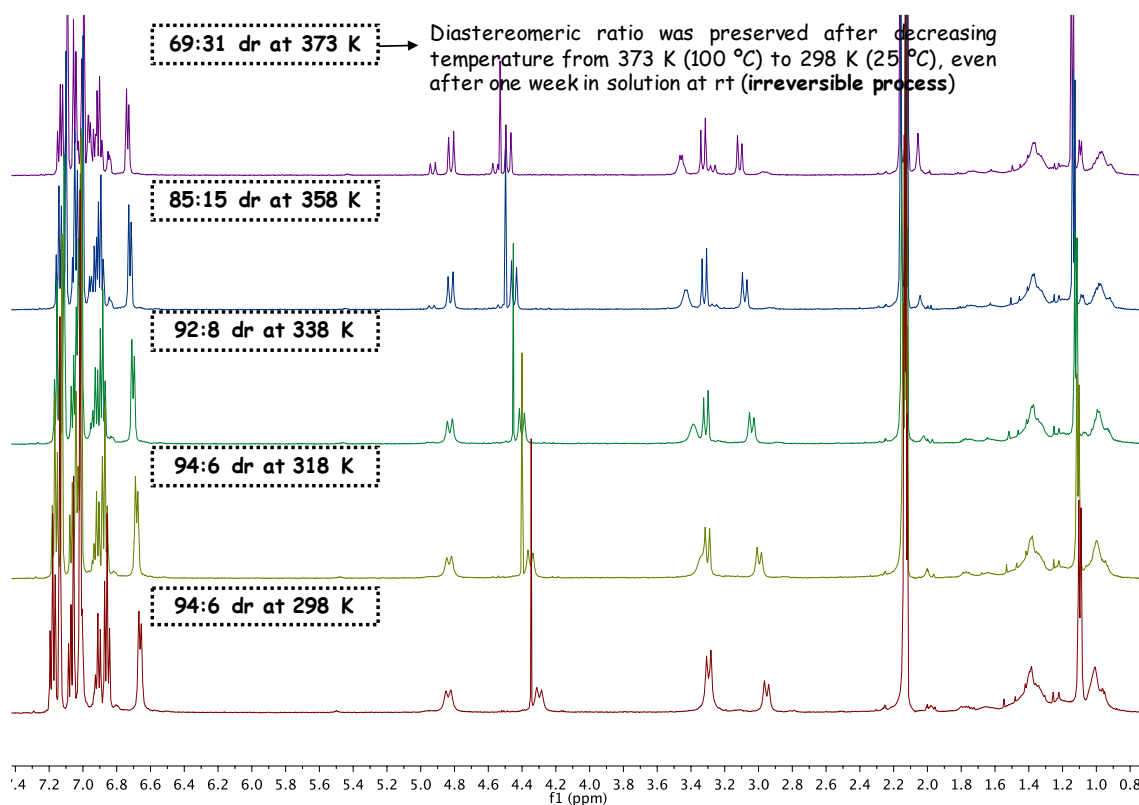


Fig. SI-15 Changes on the diastereomeric ratio (given as **4d-1/4d-2** ratio) of the 1st eluting diastereomer **4d-1** as monitored through VT-¹H NMR analyses in toluene-*d*₈.

F2.2 Epimerization of the 2nd eluting diastereomer **4d-2** as a function on the temperature

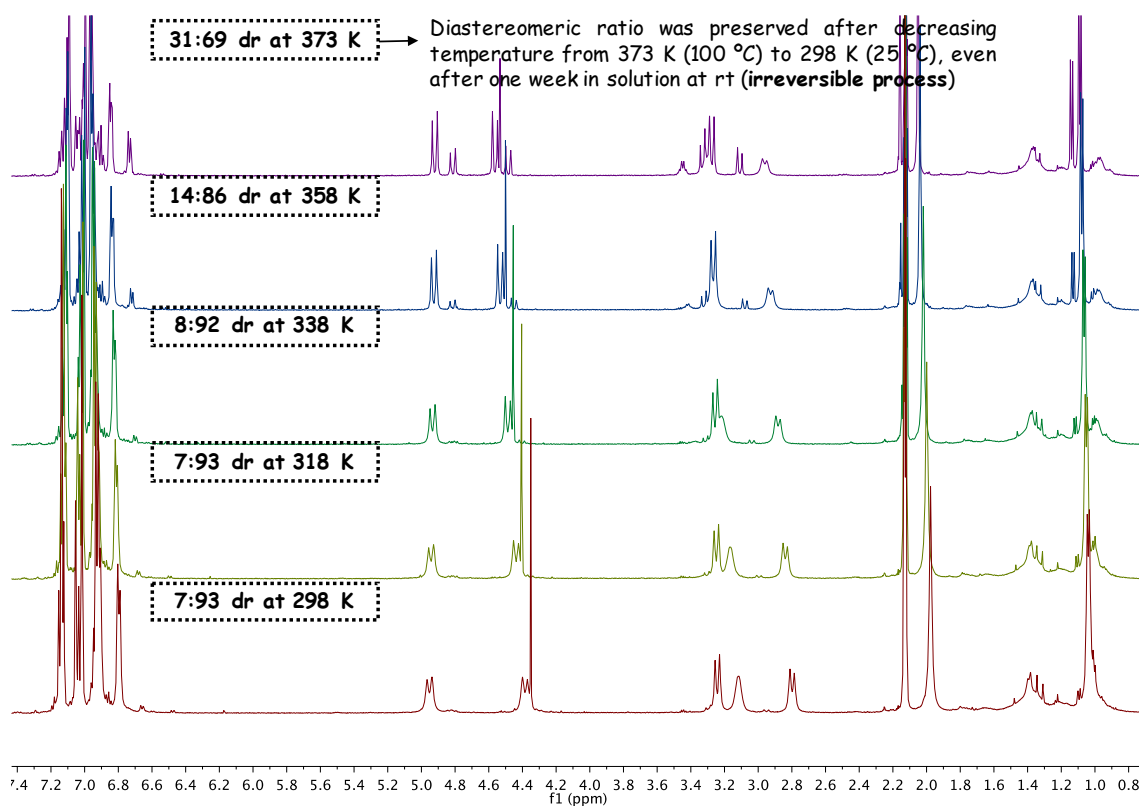


Fig. SI-16 Changes on the diastereomeric ratio (given as **4d-1/4d-2** ratio) of the 2nd eluting diastereomer **4d-2** as monitored through VT-¹H NMR analyses in toluene-*d*₈.

F2.3 Results for the 1st eluting diastereomer **4d-1** (see Scheme 8)

Table SI-3 Changes on the diastereomeric ratio of **4d-1** at 75 °C^a

Time (s)	de(%)	dr (B:A)
300	34	67:33
1200	32	66:34
2100	30	65:35
3000	28	64:36
3600	26	63:37
4200	24	62:38
4500	22	61:39
5700	20	60:40
6300	18	59:41

6900	16	58:42
8100	14	57:43
9000	12	56:44
10200	10	55:45
11400	8	54:46
12900	6	53:47
15000	4	52:48
17100	2	51:49

^a Determined by ¹H NMR analysis in toluene-*d*₈. Selected data from multiple ¹H NMR spectra recorded every 5 min during around 5 h.

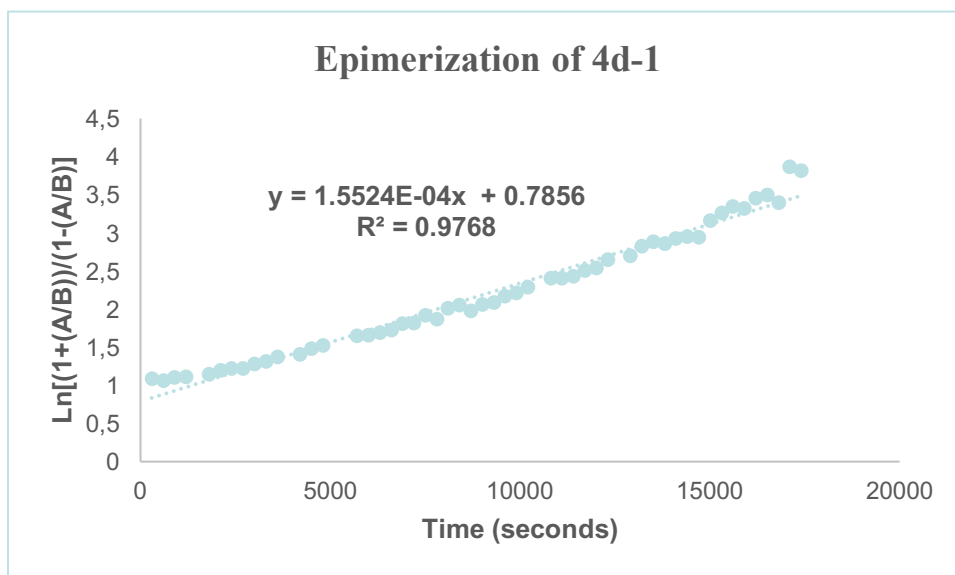


Fig. SI-17 Analysis of epimerization kinetics of the 1st eluting diastereomer **4d-1**.

$$\text{slope} = 1.5524 \times 10^{-4} = 2k_{\text{rot}}$$

$$k_{\text{rot}} = 7.7622 \times 10^{-5} \text{ s}^{-1}$$

$$\text{Eyring equation: } \Delta G_{\text{rot}}^{\ddagger} = -RT \ln K_{\text{rot}} \text{ with } K_{\text{rot}} = k_{\text{rot}}/k_{\text{B}}T$$

$$\text{Ideal gas constant: } R = 8.3145 \text{ J/mol} = 0.0083145 \text{ kJ/mol}$$

$$T = 75 \text{ }^{\circ}\text{C} = 348 \text{ K}$$

$$\text{Planck constant: } h = 6.626 \times 10^{-34} \text{ J}\cdot\text{s}$$

$$\text{Boltzmann constant: } k_{\text{B}} = 1.381 \times 10^{-23} \text{ J/K}$$

$$K_{\text{rot}} = 1.0702 \times 10^{-17}$$

$$\Delta G_{\text{rot}}^{\ddagger} = \Delta G_{\text{epim}}^{\ddagger} = 113.1 \text{ kJ/mol} = 27.0 \pm 0.1 \text{ kcal/mol}$$

$$\tau_{1/2\text{epim}} = (\ln 2)/k_{\text{epim}}$$

$$k_{\text{epim}} = 2k_{\text{rot}}$$

$$k_{\text{epim}} = 1.5524 \times 10^{-4} \text{ s}^{-1} \text{ at } 75 \text{ }^{\circ}\text{C}$$

$$\tau_{1/2\text{epim}} = 4465 \text{ s} = 74 \text{ min} = 1.2 \text{ h at } 75 \text{ }^{\circ}\text{C}$$

$$\Delta S_{\text{epim}}^{\ddagger} \approx 0 \Rightarrow \Delta G_{\text{epim}}^{\ddagger} \approx \Delta H_{\text{epim}}^{\ddagger} \quad (\Delta G_{\text{epim}}^{\ddagger} = \Delta H_{\text{epim}}^{\ddagger} - T\Delta S_{\text{epim}}^{\ddagger})$$

$$\text{Eyring equation: } k_{\text{epim}} = (2k_{\text{B}}T/h)\text{e}(-\Delta G_{\text{epim}}^{\ddagger}/RT)$$

$$k_{\text{epim}} = 1.8600 \times 10^{-7} \text{ s}^{-1} \text{ at } 25 \text{ }^{\circ}\text{C}$$

$$\tau_{1/2\text{epim}} = 3726598 \text{ s} = 62110 \text{ min} = 1035 \text{ h} = 43.1 \text{ days at } 25 \text{ }^{\circ}\text{C}$$

F2.4 Results for the 2nd eluting diastereomer 4d-2 (see Scheme 8)

Table SI-4 Changes on the diastereomeric ratio of **4d-2** at 75 °C^a

Time (s)	de(%)	dr (B:A)
300	32	66:34
1200	30	65:35
2100	28	64:36
3000	26	63:37
3900	24	62:38
5100	22	61:39
7200	20	60:40
8400	18	59:41
10800	16	58:42
14400	14	57:43
19200	12	56:44
24000	12	56:44

^a Determined by ¹H NMR analysis in toluene-*d*₈. Selected data from multiple ¹H NMR spectra recorded every 5 min during around 7 h.

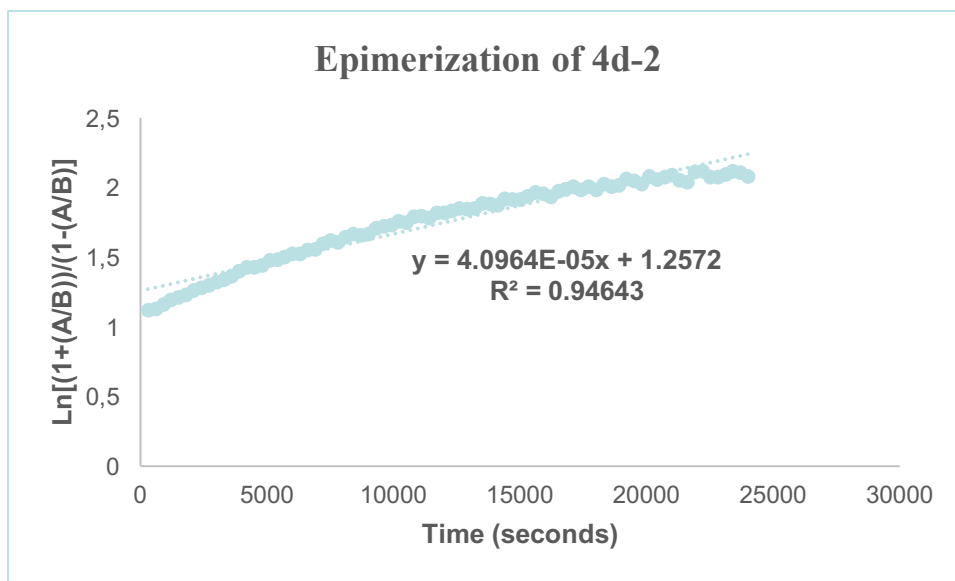


Fig. SI-18 Analysis of epimerization kinetics of the 2nd eluting diastereomer **4d-2**.

$$\text{slope} = 4.0964 \times 10^{-5} = 2k_{\text{rot}}$$

$$k_{\text{rot}} = 2.0482 \times 10^{-5} \text{ s}^{-1}$$

$$\text{Eyring equation: } \Delta G_{\text{rot}}^{\ddagger} = -RT \ln K_{\text{rot}} \text{ with } K_{\text{rot}} = k_{\text{rot}} h / k_B T$$

$$\text{Ideal gas constant: } R = 8.3145 \text{ J/mol} = 0.0083145 \text{ kJ/mol}$$

$$T = 75 \text{ }^{\circ}\text{C} = 348 \text{ K}$$

$$\text{Planck constant: } h = 6.626 \times 10^{-34} \text{ J}\cdot\text{s}$$

$$\text{Boltzmann constant: } k_B = 1.381 \times 10^{-23} \text{ J/K}$$

$$K_{\text{rot}} = 2.8238 \times 10^{-18}$$

$$\Delta G_{\text{rot}}^{\ddagger} = \Delta G_{\text{epim}}^{\ddagger} = 116.9 \text{ kJ/mol} = 28.0 \pm 0.1 \text{ kcal/mol}$$

$$\tau_{1/2\text{epim}} = (\ln 2) / k_{\text{epim}}$$

$$k_{\text{epim}} = 2k_{\text{rot}}$$

$$k_{\text{epim}} = 4.0964 \times 10^{-5} \text{ s}^{-1} \text{ at } 75 \text{ }^{\circ}\text{C}$$

$$\tau_{1/2\text{epim}} = 16921 \text{ s} = 282 \text{ min} = 4.7 \text{ h at } 75 \text{ }^{\circ}\text{C}$$

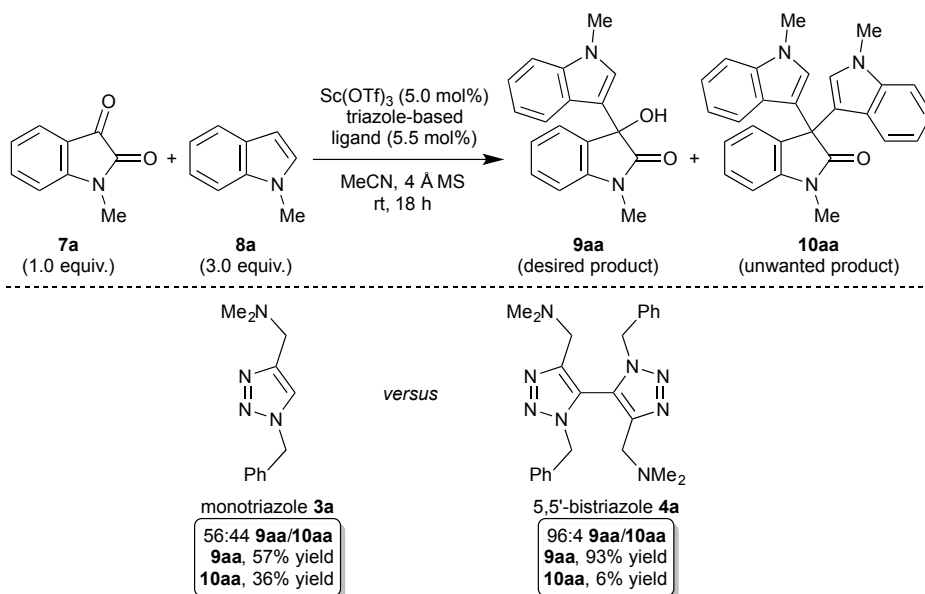
$$\Delta S_{\text{epim}}^{\ddagger} \approx 0 \Rightarrow \Delta G_{\text{epim}}^{\ddagger} \approx \Delta H_{\text{epim}}^{\ddagger} \quad (\Delta G_{\text{epim}}^{\ddagger} = \Delta H_{\text{epim}}^{\ddagger} - T \Delta S_{\text{epim}}^{\ddagger})$$

$$\text{Eyring equation: } k_{\text{epim}} = (2k_B T / h) e^{(-\Delta G_{\text{epim}}^{\ddagger} / RT)}$$

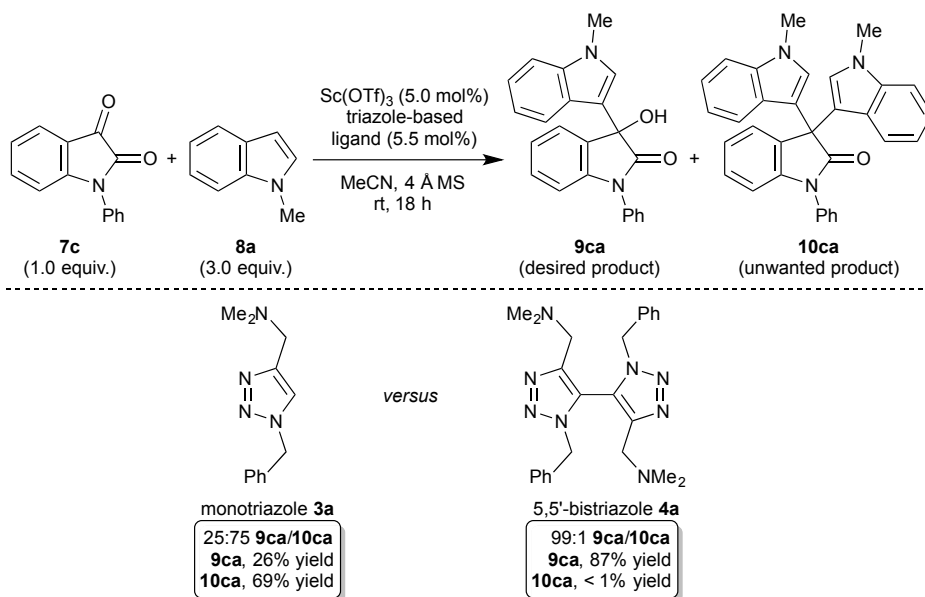
$$k_{\text{epim}} = 4.0000 \times 10^{-8} \text{ s}^{-1} \text{ at } 25 \text{ }^{\circ}\text{C}$$

$$\tau_{1/2\text{epim}} = 17328680 \text{ s} = 288811 \text{ min} = 4814 \text{ h} = 200.6 \text{ days at } 25 \text{ }^{\circ}\text{C}$$

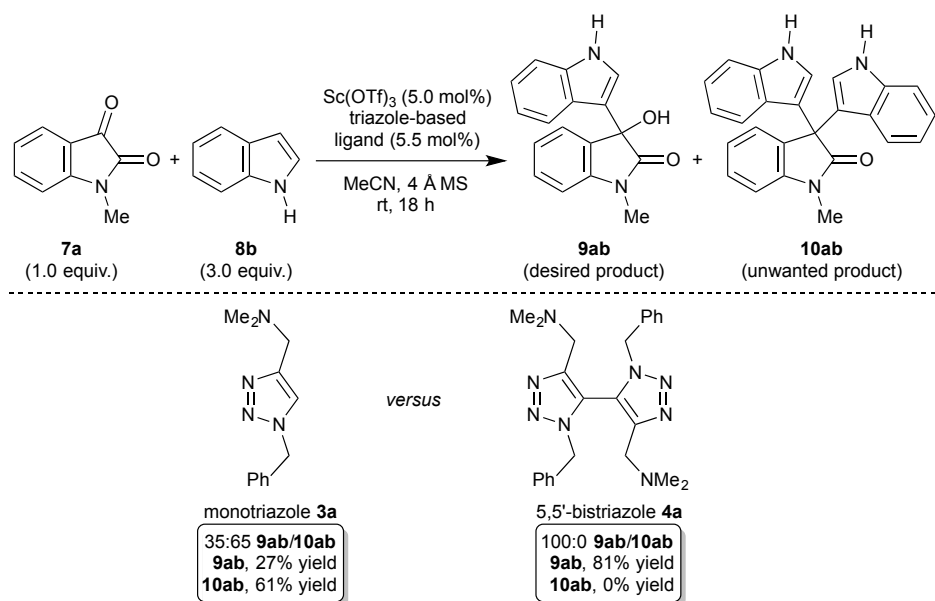
(G) Comparative FC outcomes with monotriazole 3a vs. 5,5'-bistriazole 4a



Scheme SI-3 Comparative performance in the Sc-catalyzed addition of *N*-methylindole (**8a**) to *N*-methylisatin (**7a**).



Scheme SI-4 Comparative performance in the Sc-catalyzed addition of *N*-methylindole (**8a**) to *N*-phenylisatin (**7c**).



Scheme SI-5 Comparative performance in the Sc-catalyzed addition of N-unsubstituted indole (**8b**) to N-methylisatin (**7a**).

(H) Screening of conditions for the FC reaction of N-unsubstituted isatin **7b**

Table SI-5 Screening of conditions for the Sc-catalyzed addition of N-methylindole (**8a**) to N-unsubstituted isatin (**7b**)^a

Reaction scheme showing the Sc-catalyzed addition of N-methylindole (**8a**) to N-unsubstituted isatin (**7b**). The reaction conditions are Sc(OTf)₃ (5.0 mol%), **4a** (5.5 mol%), MeCN (0.11 M), 4 Å MS, rt, 18 h. The reaction yields two products: **9ba** (desired product) and **10ba** (unwanted product).

Entry	Modifications ^a	Conv. (%) ^b	9ba/10ba ^b	9ba yield (%) ^c	10ba yield (%) ^c
1	none	62	96:4	49	2
2	10 mol% catalyst	62	82:18	51	11
3	45 h reaction time	94	20:80	n.d. ^d	n.d. ^d
4	0.03 M in MeCN	42	99:1	28	< 1
5	toluene as solvent	50	98:2	42	< 1
6	DMF as solvent	0	n.r. ^e	—	—

^a All reactions were conducted under argon atmosphere on a 0.2 mmol scale by following the standard reaction conditions shown on the reaction scheme, unless otherwise indicated. ^b Determined by ¹H NMR analysis of the crude reaction mixture. ^c Yield of isolated pure product after column chromatography. ^d Not determined. ^e No reaction.

(I) Rationalization of the FC reaction catalyzed by $4\mathbf{a}\cdot\text{Sc}(\text{OTf})_3$

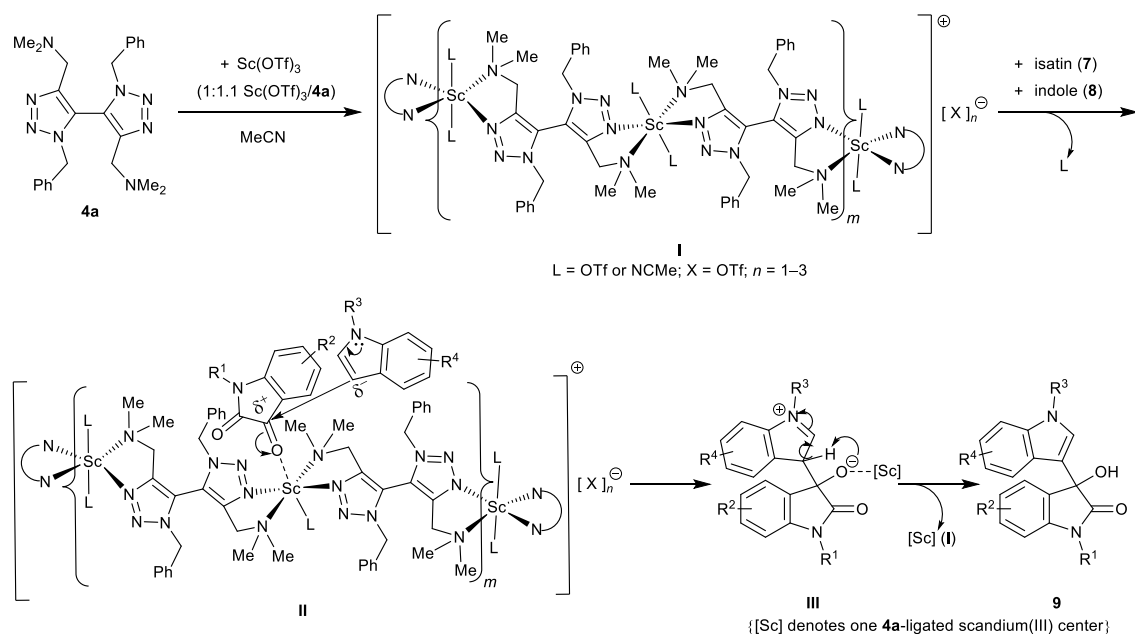
In an attempt to rationalize the product selectivity imposed by $4\mathbf{a}\cdot\text{Sc}(\text{OTf})_3$ we devoted much effort to the crystallization of this species. Unfortunately, all attempts to obtain single crystals of this material suitable for XRD analysis were unsuccessful.

In any case, both the stoichiometry (1:1) of the complex and the known tendency of scandium complexes to form polymeric networks,²¹ led us to propose for the catalyst the rather congested coordination polymeric chain structure (I) depicted in Scheme SI-6. This proposed coordination network displays each scandium center in a distorted six-coordinate octahedral geometry, connecting two $4\mathbf{a}$ units through the formation of double five-membered chelates.⁵

Upon addition of a isatin molecule ($\mathbf{7}$) to **I** and the corresponding ligand exchange, the heavily congested intermediate **II** forms, where $\mathbf{7}$ is electrophilically activated toward the nucleophilic addition of an indole nucleophile ($\mathbf{8}$). Once this attack has taken place, intermediate **III** would rapidly evolve to product $\mathbf{9}$, with regeneration of the catalyst.

In our opinion, the origin of the chemoselectivity imposed by $4\mathbf{a}\cdot\text{Sc}(\text{OTf})_3$ lies on the fact that the bulky molecules of $\mathbf{9}$ are no longer able to interact with the also congested polymer **I**. The reaction would, thus, be blocked at this stage resulting in the observed chemoselectivity. In support of this interpretation, when $3\mathbf{a}\cdot\text{Sc}(\text{OTf})_3$ is used as the catalyst and the formation of the coordination polymer is no longer possible, no steric congestion is developed around the putative scandium chelates and no chemoselectivity is observed at all.

²¹ a) C. Yan, Y. Zhang, B. Li, T. Jin and G. Xu, *Polyhedron*, 1996, **15**, 2895–2899; (b) H. R. Webb, M. J. Hardie and C. L. Raston, *Chem. – Eur. J.*, 2001, **7**, 3616–3620; (c) J. Perles, M. Iglesias, C. Ruiz-Valero and N. Snejko, *Chem. Commun.*, 2003, 346–347; (d) L. Zhang, L. Wang, P.-C. Wang, T. Song, D. Li, X. Chen, Y. Fan and J. Xu, *Eur. J. Inorg. Chem.*, 2015, 931–938.



Scheme SI-6 Proposed working model for the ligand-controlled Sc(III)-catalyzed nucleophilic single addition of indoles to isatins.

(J) Synthesis and characterization of FC reaction products

The following compounds are all commercially available chemicals which were used as received from the chemical supplier cited in parentheses: scandium(III) triflate (Sigma-Aldrich[®]), 4 Å molecular sieves (Sigma-Aldrich[®]), *N*-methylisatin (**7a**; Acros Organics[®]), isatin (**7b**; Sigma-Aldrich[®]), *N*-phenylisatin (**7c**; Sigma-Aldrich[®]), *N*-benzylisatin (**7d**; abcr[®]), *N*-allylisatin (**7f**; abcr[®]), *N*-propargylisatin (**7g**; abcr[®]), *N*-methylindole (**8a**; Sigma-Aldrich[®]), indole (**8b**; Sigma-Aldrich[®]), *N*-benzylindole (**8c**; Alfa Aesar[®]), 5-methoxyindole (**8d**; Sigma-Aldrich[®]), 5-fluoroindole (**8e**; Fluorochem[®]), 6-fluoroindole (**8f**; Fluorochem[®]), 5-bromoindole (**8g**; Acros Organics[®]) and 6-chloroindole (**8h**; Sigma-Aldrich[®]).

The following isatin substrates were prepared according to the cited literature procedures for each case: *N*-benzyl-7-trifluoromethylisatin (**7e**),²² *N*-benzyl-5-chloroisatin (**7h**)²³ and *N*-allyl-5-chloroisatin (**7i**).²⁴ Physical and spectroscopic data obtained for these substrates were in perfect agreement with the data reported in the

²² F. Shi, Z.-L. Tao, S.-W. Luo, S.-J. Tu and L.-Z. Gong, *Chem. – Eur. J.*, 2012, **18**, 6885–6894.

²³ M. Gangar, N. Kashyap, K. Kumar, S. Goyal and V. A. Nair, *Tetrahedron Lett.*, 2015, **56**, 7074–7081.

²⁴ Nisha, J. Gut, P. J. Rosenthal and V. Kumar, *Eur. J. Med. Chem.*, 2014, **84**, 566–573. For a full characterization of **7i**, see: M. Raghavender Reddy, N. Nageswara Rao, K. Ramakrishna and H. M. Meshram, *Tetrahedron Lett.*, 2014, **55**, 4758–4762.

references indicated for each case. NMR spectra of compounds **7e**, **7h** and **7i** are provided in section K.

J1 General procedure for the Sc-catalyzed addition of indole nucleophiles (8) to isatin electrophiles (7) mediated by the 5,5'-bistriazole ligand 4a (GP1)

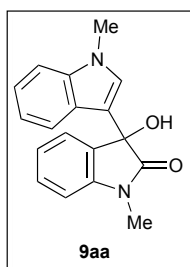
A solution of Sc(OTf)₃ (5.0 mol%; 4.9 mg, 0.010 mmol) and 5,5'-bistriazole ligand **4a** (5.5 mol%; 4.7 mg, 0.011 mmol) in anhydrous MeCN (1.0 mL) under argon atmosphere was prepared inside a 10 mL Schlenk tube containing a small stirring bar and previously loaded with activated 4 Å MS (typically one ball of sieve). Such a solution was stirred for 2 h at rt under inert atmosphere. After this period, the corresponding isatin electrophile **7** (1.0 equiv.; 0.20 mmol) was loaded as a solid added in one portion and under an argon stream over the previous solution containing the preformed scandium(III)–bistriazole **4a** complex under stirring at rt. A solution of the corresponding indole nucleophile **8** (3.0 equiv.; 0.60 mmol) in anhydrous MeCN (1.0 mL) was subsequently syringed into the reaction mixture, which was further stirred at rt under argon atmosphere for 18 h (overnight reactions). Then, the reaction mixture was diluted with DCM (5 mL) and passed through filtering paper in order to separate the molecular sieve by washing it with additional DCM (5 mL). The solvents were removed under reduced pressure. ¹H NMR analysis of the crude reaction mixture allowed determining both conversion and product selectivity given as the molar ratio between desired monoaddition product **9** and unwanted double addition product **10** (**9/10** ratio). Most of the FC reactions proceeded to completion (with full conversion) after 18 h at rt. Purification of the crude mixture by silica gel column chromatography (CombiFlash[®] system, 4 g SiO₂ cartridge, 1st eluent: cyclohexane, 2nd eluent: 10:90 EtOAc/cyclohexane, 3rd eluent: 30:70 EtOAc/cyclohexane, 4th eluent: 50:50 EtOAc/cyclohexane) furnished the very major monoaddition product **9** as a pure compound, which could be easily isolated separately from the corresponding double addition product **10** (typically formed as traces).

J2 General procedure for the Sc-catalyzed addition of indole nucleophiles (8) to isatin electrophiles (7) mediated by the monotriazole ligand 3a (GP2)

A solution of Sc(OTf)₃ (5.0 mol%; 4.9 mg, 0.010 mmol) and monotriazole ligand **3a** (5.5 mol%; 2.4 mg, 0.011 mmol) in anhydrous MeCN (1.0 mL) under argon atmosphere was prepared inside a 10 mL Schlenk tube containing a small stirring bar and previously loaded with activated 4 Å MS (typically one ball of sieve). Such a solution was stirred for 2 h at rt under inert atmosphere. After this period, the corresponding isatin

electrophile **7** (1.0 equiv.; 0.20 mmol) was loaded as a solid added in one portion and under an argon stream over the previous solution containing the preformed scandium(III)–monotriazole **3a** complex under stirring at rt. A solution of the corresponding indole nucleophile **8** (3.0 equiv.; 0.60 mmol) in anhydrous MeCN (1.0 mL) was subsequently syringed into the reaction mixture, which was further stirred at rt under argon atmosphere for 18 h (overnight reactions). Then, the reaction mixture was diluted with DCM (5 mL) and passed through filtering paper in order to separate the molecular sieve by washing it with additional DCM (5 mL). The solvents were removed under reduced pressure. ¹H NMR analysis of the crude reaction mixture allowed determining both conversion and product selectivity given as the molar ratio between desired monoaddition product **9** and unwanted double addition product **10** (**9/10** ratio). Most of the FC reactions proceeded to completion (with full conversion) after 18 h at rt. Purification of the crude mixture by silica gel column chromatography (CombiFlash[®] system, 4 g SiO₂ cartridge, 1st eluent: cyclohexane, 2nd eluent: 10:90 EtOAc/cyclohexane, 3rd eluent: 30:70 EtOAc/cyclohexane, 4th eluent: 50:50 EtOAc/cyclohexane) furnished the monoaddition product **9** and the corresponding double addition product **10**, with both products isolated separately as pure compounds.

J3 Synthesis of monoaddition product **9aa** (see Scheme 10A)



3-Hydroxy-1-methyl-3-(1-methyl-1H-indol-3-yl)indolin-2-one

(9aa)

Isolated as a crystalline yellowish solid in 93% yield by following the general procedure GP1 with *N*-methylisatin (**7a**) and *N*-methylindole (**8a**). Physical and spectroscopic data obtained for this known compound were in perfect agreement with the data reported in the literature.²⁵ ¹H and ¹³C NMR spectra of **9aa** are provided in section K. The crystal structure of **9aa** is shown within Scheme 12A of the manuscript and crystal data for **9aa** are herein given as section D7. Chiral HPLC conditions for racemic **9aa**: Daicel Chiralpak[®] AD-H (25 cm x 0.46 cm x 5 μm), 70:30 *n*-hexane/2-

²⁵ N. V. Hanhan, A. H. Sahin, T. W. Chang, J. C. Fettinger and A. K. Franz, *Angew. Chem., Int. Ed.*, 2010, **49**, 744–747.

propanol, 1.0 mL/min, 254 nm, t_R (1st eluting enantiomer) = 11.0 min, t_R (2nd eluting enantiomer) = 15.4 min (Fig. SI-19).

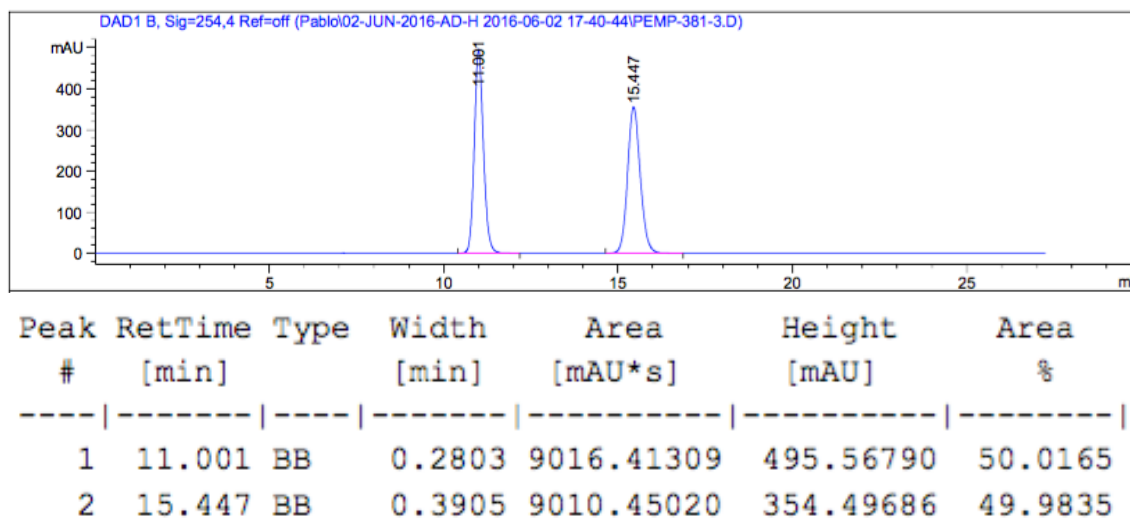
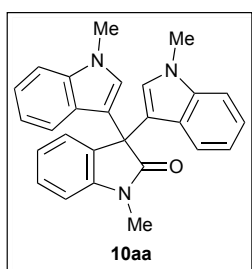


Fig. SI-19 HPLC trace for racemic monoaddition product **9aa**.

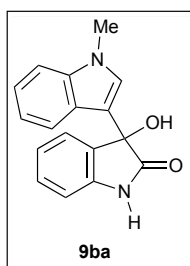
J4 Synthesis of double addition product **10aa** (see Scheme SI-3)



1,1',1''-Trimethyl-[3,3':3'',3''-terindolin]-2'-one (10aa)

Isolated as a white-yellowish solid in 36% yield by following the general procedure GP2 with *N*-methylysatine (**7a**) and *N*-methylindole (**8a**). Physical and spectroscopic data obtained for this known compound were in perfect agreement with the data reported in the literature.²⁶ ¹H and ¹³C NMR spectra of **10aa** are provided in section K.

J5 Synthesis of monoaddition product **9ba** (see Scheme 10A)



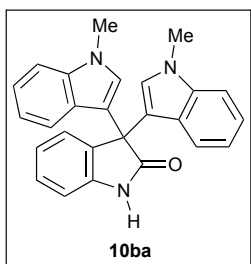
3-Hydroxy-3-(1-methyl-1H-indol-3-yl)indolin-2-one (9ba)

Isolated as a white solid in 49% yield (62% conversion) by following the general procedure GP1 with isatin (**7b**) and *N*-methylindole (**8a**). Physical and spectroscopic

²⁶ K. Tabatabaieian, M. Mamaghani, N. Mahmoodi and A. Khroshidi, *Can. J. Chem.*, 2009, **87**, 1213–1217.

data obtained for this known compound were in perfect agreement with the data reported in the literature.²⁵ ¹H and ¹³C NMR spectra of **9ba** are provided in section K.

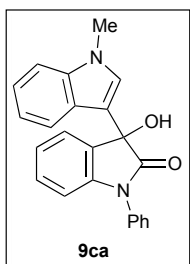
J6 Synthesis of double addition product 10ba (see Table SI-5, entry 2)



1,1''-Dimethyl-[3,3':3',3''-terindolin]-2'-one (10ba)

Isolated as a mixture containing the known double addition product **10ba**²⁷ (11% yield) along with unreacted isatin **7b** (62% conversion) in 37:63 **10ba**/**7b** molar ratio, respectively, by following the general procedure GP1 with isatin (**7b**) and *N*-methylindole (**8a**) on using 10 mol% of Sc(OTf)₃ and 11 mol% of 5,5'-bistriazole **4a**. Both compounds (**7b** and **10ba**) showed the same *R_f* value on TLC [*R_f* = 0.40 (EtOAc)] and could not be separated by column chromatography. As a consequence, NMR spectra of pure **10ba** are not provided.

J7 Synthesis of monoaddition product 9ca (see Scheme 10A)



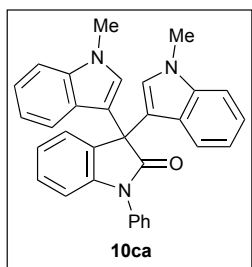
3-Hydroxy-3-(1-methyl-1*H*-indol-3-yl)-1-phenylindolin-2-one

(9ca)

Isolated as a white solid in 87% yield by following the general procedure GP1 with *N*-phenylisatin (**7c**) and *N*-methylindole (**8a**). Physical and spectroscopic data obtained for this known compound were in perfect agreement with the data reported in the literature.²⁵ ¹H and ¹³C NMR spectra of **9ca** are provided in section K.

²⁷ M. Nikpassand, M. Mamaghani, K. Tabatabaeian and H. A. Samimi, *Synth. Commun.*, 2010, **40**, 3552–3560.

J8 Synthesis of double addition product **10ca** (see Scheme SI-4)

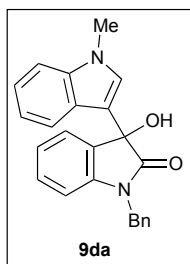


1,1''-Dimethyl-1'-phenyl-[3,3':3',3''-terindolin]-2'-one

(**10ca**)

Isolated as a white-yellowish solid in 69% yield by following the general procedure GP2 with *N*-phenylisatin (**7c**) and *N*-methylindole (**8a**). Characterization data for the hitherto unknown compound **10ca**: TLC R_f = 0.70 (1:1 EtOAc/cyclohexane); mp = 149.4–151.6 °C; IR absorption (neat) ν_{\max} 3047 ($C_{sp^2}-H$), 1720 ($C=O$), 1607 ($C=C$), 1593 ($C_{Ar}=C_{Ar}$), 1204 and 1155 ($C-N$); 1H NMR (500 MHz, $CDCl_3$) δ 3.71 (s, 6H, $2CH_3$), 6.92 (bs, 2H, $2CH_{Ar}-N$), 6.95 (bdd, 2H, $J = 7.9$ and 7.9 , H_{Ar}), 7.00 (bd, 1H, $J = 7.9$, H_{Ar}), 7.05 (bdd, 1H, $J = 7.4$ and 7.4 , H_{Ar}), 7.17 (bdd, 2H, $J = 8.3$ and 8.3 , H_{Ar}), 7.25 (bdd, 1H, $J = 7.9$ and 7.9 , H_{Ar}), 7.29 (bd, 2H, $J = 8.3$, H_{Ar}), 7.35–7.42 (m, 1H, H_{Ar}), 7.41 (bd, 2H, $J = 7.8$, H_{Ar}), 7.48 (bd, 1H, $J = 7.5$, H_{Ar}), 7.49–7.55 (m, 4H, H_{Ar}); $^{13}C\{^1H\}$ NMR (125 MHz, $CDCl_3$) δ 32.8 (CH_3), 52.9 (C_q), 109.4 (CH_{Ar}), 109.5 (CH_{Ar}), 113.8 (C_{Ar}), 119.0 (CH_{Ar}), 121.4 (CH_{Ar}), 121.6 (CH_{Ar}), 123.1 (CH_{Ar}), 125.6 (CH_{Ar}), 126.4 (CH_{Ar}), 126.7 (CH_{Ar}), 127.9 (CH_{Ar}), 128.9 (CH_{Ar}), 129.5 (CH_{Ar}), 134.0 (C_{Ar}), 135.0 (C_{Ar}), 137.8 (x 2, C_{Ar}), 142.8 (C_{Ar}), 177.0 ($C=O$); HRMS (ESI $^+$): m/z $[M+H]^+$ calcd for $C_{32}H_{25}N_3NaO$ 490.1890, found 490.1890.

J9 Synthesis of monoaddition product **9da** (see Scheme 10A)



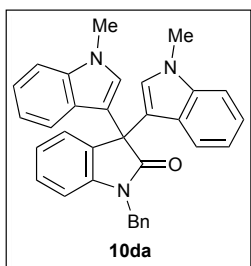
1-Benzyl-3-hydroxy-3-(1-methyl-1*H*-indol-3-yl)indolin-2-one

(**9da**)

Isolated as a white solid in 88% yield by following the general procedure GP1 with *N*-benzylisatin (**7d**) and *N*-methylindole (**8a**). Physical and spectroscopic data obtained

for this known compound were in perfect agreement with the data reported in the literature.²⁸ ¹H and ¹³C NMR spectra of **9da** are provided in section K.

J10 Synthesis of double addition product **10da** (see Scheme 10A)

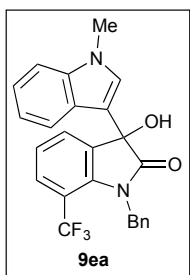


1'-Benzyl-1,1''-dimethyl-[3,3':3',3''-terindolin]-2'-one

(10da)

Isolated as a mixture containing the known double addition product **10da**²⁹ (6% yield) along with unreacted *N*-benzylisatin **7d** (*ca.* 95% conversion) in 81:19 **10da**/**7d** molar ratio, respectively, by following the general procedure GP1 with *N*-benzylisatin (**7d**) and *N*-methylindole (**8a**). Both compounds (**7d** and **10da**) showed the same *R_f* value on TLC [*R_f* = 0.71 (1:1 EtOAc/cyclohexane)] and could not be separated by column chromatography although ¹H and ¹³C NMR spectra for the isolated 81:19 **10da**/**7d** mixture are provided in section K. Spectroscopic data of **10da** were in perfect agreement with the data reported in the literature.²⁹

J11 Synthesis of monoaddition product **9ea** (see Scheme 10A)



1-Benzyl-3-hydroxy-3-(1-methyl-1*H*-indol-3-yl)indolin-2-one

(9ea)

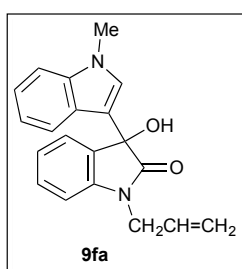
Isolated as a white solid in 100% yield by following the general procedure GP1 with *N*-benzyl-7-trifluoromethylisatin²² (**7e**) and *N*-methylindole (**8a**). Characterization data for the hitherto unknown compound **9ea**: TLC *R_f* = 0.20 (3:7 EtOAc/cyclohexane); mp = 107.5–110.3 °C; IR absorption (neat) *v*_{max} 3403 (O–H), 3056 and 3033 (C_{sp2}–H), 1715 (C=O), 1614 (C=C), 1596 and 1542 (C_{Ar}=C_{Ar}), 1157, 1119, 1095, 1076 and 1013 (C–F, C–N and C–O); ¹H NMR (500 MHz, CDCl₃) δ 3.55 (s, 1H, OH), 3.73 (s, 3H, NMe), 5.24 (d, 1H, *J* = 16.9, NCHHPh), 5.30 (d, 1H, *J* = 16.9, NCHHPh), 6.91 (s, 1H,

²⁸ P. K. Vuram, C. Kabilan and A. Chadha, *Int. J. Org. Chem.*, 2015, **5**, 108–118.

²⁹ K. Alimohammadi, Y. Sarrafi and M. Tajbakhsh, *Monatsh. Chem.*, 2008, **139**, 1037–1039.

H_{Ar}), 7.10–7.31 (m, 8H, H_{Ar}), 7.33 (bd, 1H, $J = 8.3$, H_{Ar}), 7.64 (dd, 1H, $J = 8.2$ and 1.1, H_{Ar}), 7.75 (bd, 1H, $J = 8.0$, H_{Ar}), 7.81 (dd, 1H, $J = 7.2$ and 0.9, H_{Ar}); $^{13}C\{^1H\}$ NMR (125 MHz, $CDCl_3$) δ 32.9 (CH_2), 45.7 (q, $^5J_{C-F} = 4.9$, CH_2), 73.7 ($C-OH$), 109.8 (CH_{Ar}), 113.2 (C_{Ar}), 113.4 (q, $^2J_{C-F} = 32.3$, C_{Ar}), 120.1 (CH_{Ar}), 120.6 (CH_{Ar}), 122.4 (CH_{Ar}), 122.9 (CH_{Ar}), 123.3 (q, $^1J_{C-F} = 272.2$, CF_3), 125.2 (CH_{Ar}), 125.8 (CH_{Ar}), 126.9 (CH_{Ar}), 127.7 (q, $^3J_{C-F} = 5.9$, C_{Ar}), 127.8 (CH_{Ar}), 128.4 (CH_{Ar}), 128.8 (CH_{Ar}), 134.1 (C_{Ar}), 136.0 (C_{Ar}), 137.8 (C_{Ar}), 140.6 (C_{Ar}), 178.7 ($C=O$); $^{19}F\{^1H\}$ NMR (376 MHz, $CDCl_3$) δ –55.0; HRMS (ESI $^+$): m/z $[M+Na]^+$ calcd for $C_{25}H_{19}F_3N_2NaO_2$ 459.1291, found 459.1295.

J12 Synthesis of monoaddition product **9fa** (see Scheme 10A)

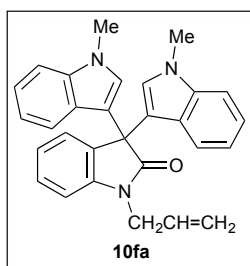


1-Allyl-3-hydroxy-3-(1-methyl-1H-indol-3-yl)indolin-2-one

(**9fa**)

Isolated as a crystalline white-yellowish solid in 89% yield by following the general procedure GP1 with *N*-allylisatin (**7f**) and *N*-methylindole (**8a**). Physical and spectroscopic data obtained for this known compound were in perfect agreement with the data reported in the literature.²⁸ 1H and ^{13}C NMR spectra of **9fa** are provided in section K. The crystal structure of **9fa** is shown within Scheme 10A of the manuscript and crystal data for **9fa** are herein given as section D8.

J13 Synthesis of double addition product **10fa** (see Scheme 10A)

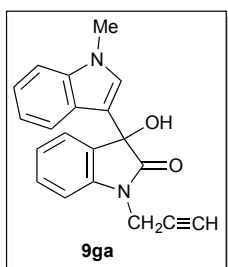


1'-Allyl-1,1''-dimethyl-[3,3':3',3''-terindolin]-2'-one (10fa)

Isolated as a white-yellowish solid in 11% yield by following the general procedure GP1 with *N*-allylisatin (**7f**) and *N*-methylindole (**8a**). Characterization data for the hitherto unknown compound **10fa**: TLC $R_f = 0.37$ (3:7 EtOAc/cyclohexane); mp = 86.5–88.3 °C (decomp.); IR absorption (neat) ν_{max} 3050 and 3019 ($C_{sp2}-H$), 1708

(C=O), 1645 (C=C), 1608 ($C_{Ar}=C_{Ar}$), 1193, 1156, 1131, 1094 and 1076 (C–N); 1H NMR (500 MHz, $CDCl_3$) δ 3.72 (s, 6H, $2CH_3$), 4.50 (dt, 2H, $J = 5.3$ and 1.6 , $CH_2CH=CH_2$), 5.26 (dtd, 1H, $J = 10.4$, 1.6 and 1.3 , $CH_2CH=CHH$), 5.32 (dtd, 1H, $J = 17.2$, 1.6 and 1.1 , $CH_2CH=CHH$), 5.93 (ddt, 1H, $J = 17.2$, 10.4 and 5.3 , $CH_2CH=CH_2$), 6.88 (bs, 2H, $2CH_{Ar-N}$), 6.94 (ddd, 2H, $J = 7.8$, 7.8 and 1.2 , H_{Ar}), 7.00 (bd, 1H, $J = 7.8$, H_{Ar}), 7.06 (ddd, 1H, $J = 7.6$, 7.6 and 1.0 , H_{Ar}), 7.14–7.22 (m, 2H, H_{Ar}), 7.24–7.35 (m, 5H, H_{Ar}), 7.49 (bd, 1H, $J = 7.4$, H_{Ar}); $^{13}C\{^1H\}$ NMR (125 MHz, $CDCl_3$) δ 32.8 (CH_3), 42.7 (CH_2), 52.7 (C_q), 109.1 (CH_{Ar}), 109.3 (CH_{Ar}), 113.8 (C_{Ar}), 117.7 ($CH=CH_2$), 119.0(CH_{Ar}), 121.4 (CH_{Ar}), 121.5 (CH_{Ar}), 122.6 (CH_{Ar}), 125.4 (CH_{Ar}), 126.4 (C_{Ar}), 127.8 (CH_{Ar}), 128.7 (CH_{Ar}), 131.8 ($CH=CH_2$), 134.3 (C_{Ar}), 137.7 (C_{Ar}), 142.0 (C_{Ar}), 177.4 (C=O); HRMS (ESI $^+$): m/z $[M+Na]^+$ calcd for $C_{29}H_{25}N_3NaO$ 454.1890, found 454.1900.

J14 Synthesis of monoaddition product **9ga** (see Scheme 10A)

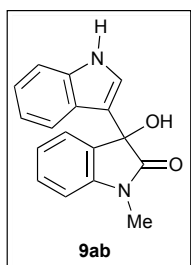


3-Hydroxy-3-(1-methyl-1H-indol-3-yl)-1-(prop-2-yn-1-

yl)indolin-2-one (9ga)

Isolated as a white solid in 89% yield by following the general procedure GP1 with *N*-propargylisatin (**7g**) and *N*-methylindole (**8a**). Physical and spectroscopic data obtained for this known compound were in perfect agreement with the data reported in the literature.²⁸ 1H and ^{13}C NMR spectra of **9ga** are provided in section K.

J15 Synthesis of monoaddition product **9ab** (see Scheme 10B)

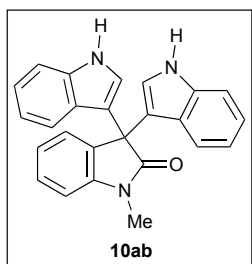


3-Hydroxy-3-(1H-indol-3-yl)-1-methylindolin-2-one (9ab)

Isolated as a white solid in 81% yield by following the general procedure GP1 with *N*-methylisatin (**7a**) and indole (**8b**). Physical and spectroscopic data obtained for this

known compound were in perfect agreement with the data reported in the literature.³⁰ ¹H and ¹³C NMR spectra of **9ab** are provided in section K.

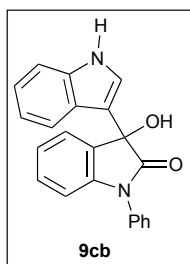
J16 Synthesis of double addition product 10ab (see Scheme SI-5)



1'-Methyl-[3,3':3',3''-terindolin]-2'-one (10ab)

Isolated as a white-pinkish solid in 61% yield by following the general procedure GP2 with *N*-methyloisatin (**7a**) and indole (**8b**). Physical and spectroscopic data obtained for this known compound were in perfect agreement with the data reported in the literature.³¹ ¹H and ¹³C NMR spectra of **10ab** are provided in section K.

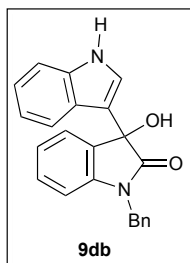
J17 Synthesis of monoaddition product 9cb (see Scheme 10B)



3-Hydroxy-3-(1*H*-indol-3-yl)-1-phenylindolin-2-one (9cb)

Isolated as a white solid in 79% yield by following the general procedure GP1 with *N*-phenyloisatin (**7c**) and indole (**8b**). Physical and spectroscopic data obtained for this known compound were in perfect agreement with the data reported in the literature.³² ¹H and ¹³C NMR spectra of **9cb** are provided in section K.

J18 Synthesis of monoaddition product 9db (see Scheme 10B)



1-Benzyl-3-hydroxy-3-(1*H*-indol-3-yl)indolin-2-one (9db)

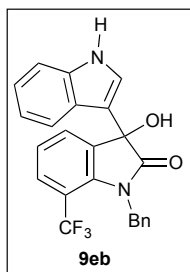
³⁰ P. Chauhan and S. S. Chimni, *Chem. – Eur. J.*, 2010, **16**, 7709–7713.

³¹ J. Azizian, A. A. Mohammadi, N. Karimi, M. R. Mohammadzadeh and A. R. Karimi, *Catal. Commun.*, 2006, **7**, 752–755.

³² F.-L. Zhang, X. Zhu and S. Chiba, *Org. Lett.*, 2015, **17**, 3138–3141.

Isolated as a white solid in 84% yield by following the general procedure GP1 with *N*-benzylisatin (**7d**) and indole (**8b**). Physical and spectroscopic data obtained for this known compound were in perfect agreement with the data reported in the literature.³⁰ ¹H and ¹³C NMR spectra of **9db** are provided in section K.

J19 Synthesis of monoaddition product 9eb (see Scheme 10B)

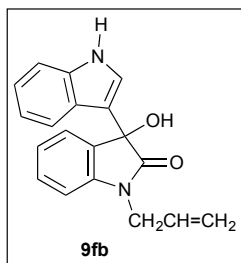


1-Benzyl-3-hydroxy-3-(1*H*-indol-3-yl)-7-

(trifluoromethyl)indolin-2-one (9eb)

Isolated as a crystalline white solid in 96% yield by following the general procedure GP1 with *N*-benzyl-7-trifluoromethylisatin²² (**7e**) and indole (**8b**). Physical and spectroscopic data obtained for this known compound were in perfect agreement with the data reported in the literature.³² ¹H, ¹³C and ¹⁹F NMR spectra of **9eb** are provided in section K. The crystal structure of **9eb** is shown within Scheme 10B of the manuscript and crystal data for **9eb** are herein given as section D9.

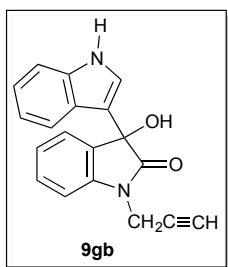
J20 Synthesis of monoaddition product 9fb (see Scheme 10B)



1-Allyl-3-hydroxy-3-(1*H*-indol-3-yl)indolin-2-one (9fb)

Isolated as a white solid in 100% yield by following the general procedure GP1 with *N*-allylisatin (**7f**) and indole (**8b**). Physical and spectroscopic data obtained for this known compound were in perfect agreement with the data reported in the literature.²⁸ ¹H and ¹³C NMR spectra of **9fb** are provided in section K.

J21 Synthesis of monoaddition product **9gb** (see Scheme 10B)

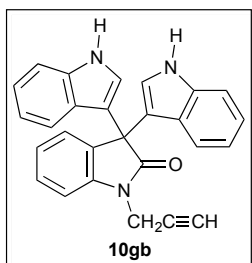


3-Hydroxy-3-(1*H*-indol-3-yl)-1-(prop-2-yn-1-yl)indolin-2-one

(9gb)

Isolated as a foamy white solid in 84% yield by following the general procedure GP1 with *N*-propargylisatin (**7g**) and indole (**8b**). Characterization data for the hitherto unknown compound **9gb**: TLC R_f = 0.09 (3:7 EtOAc/cyclohexane); mp = 77.4–78.9 °C (decomp.); IR absorption (neat) ν_{\max} 3384 (N–H, stretching), 3283 (O–H), 3058 (C_{sp^2} –H), 2166 ($C\equiv C$), 1705 ($C=O$), 1653 (N–H, bending), 1612 ($C=C$), 1544 ($C_{Ar}=C_{Ar}$), 1175, 1104 and 1004 (C–N and C–O); 1H NMR (500 MHz, $CDCl_3$) δ 2.29 (dd, 1H, J = 2.6 and 2.4, $CH_2C\equiv CH$), 3.77 (s, 1H, OH), 4.41 (dd, 1H, J = 17.7 and 2.4, $CHHC\equiv CH$), 4.64 (dd, 1H, J = 17.7 and 2.6, $CHHC\equiv CH$), 6.99 (bd, 1H, J = 2.6, H_{Ar}), 7.05 (ddd, 1H, J = 8.2, 7.1 and 1.0, H_{Ar}), 7.11 (ddd, 1H, J = 8.2, 7.1 and 1.0, H_{Ar}), 7.15 (bd, 1H, J = 7.8, H_{Ar}), 7.16 (ddd, 1H, J = 8.2, 7.1 and 1.1, H_{Ar}), 7.29 (bd, 1H, J = 8.2, H_{Ar}), 7.39 (ddd, 1H, J = 9.0, 7.8 and 1.2, H_{Ar}), 7.46 (bdd, 1H, J = 7.4 and 0.9, H_{Ar}), 7.57 (bd, 1H, J = 8.2, H_{Ar}), 8.32 (s, 1H, NH); $^{13}C\{^1H\}$ NMR (125 MHz, $CDCl_3$) δ 29.6 (CH_2), 72.7 ($C\equiv CH$), 75.7 (C–OH), 76.7 ($C\equiv CH$), 109.6 (CH_{Ar}), 111.5 (CH_{Ar}), 115.0 (C_{Ar}), 120.1 (CH_{Ar}), 120.4 (CH_{Ar}), 122.4 (CH_{Ar}), 123.4 (CH_{Ar}), 123.7 (CH_{Ar}), 124.6 (CH_{Ar}), 125.0 (C_{Ar}), 129.8 (CH_{Ar}), 131.0 (C_{Ar}), 136.9 (C_{Ar}), 141.3 (C_{Ar}), 176.3 ($C=O$); HRMS (ESI $^+$): m/z $[M+Na]^+$ calcd for $C_{19}H_{14}N_2NaO_2$ 325.0947, found 325.0952.

J22 Synthesis of double addition product **10gb** (see Scheme 10B)

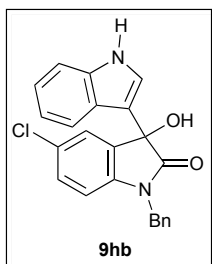


1'-(Prop-2-yn-1-yl)-[3,3':3',3''-terindolin]-2'-one (10gb)

Isolated as a brownish solid in 2% yield by following the general procedure GP1 with *N*-propargylisatin (**7g**) and indole (**8b**). Physical and spectroscopic data obtained

for this known compound were in perfect agreement with the data reported in the literature.³³ ¹H and ¹³C NMR spectra of **10gb** are provided in section K.

J23 Synthesis of monoaddition product **9hb** (see Scheme 10B)

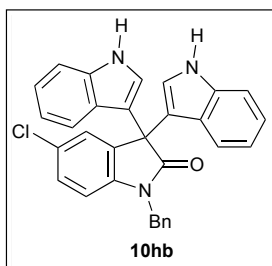


1-Benzyl-5-chloro-3-hydroxy-3-(1*H*-indol-3-yl)indolin-2-one

(9hb)

Isolated as a white solid in 78% yield by following the general procedure GP1 with *N*-benzyl-5-chloroisatin²³ (**7h**) and indole (**8b**). Physical and spectroscopic data obtained for this known compound were in perfect agreement with the data reported in the literature.³⁴ ¹H and ¹³C NMR spectra of **9hb** are provided in section K.

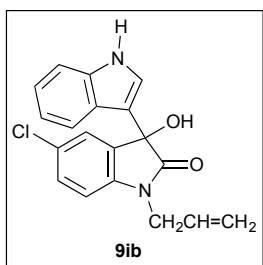
J24 Synthesis of double addition product **10hb** (see Scheme 10B)



1'-Benzyl-5'-chloro-[3,3':3',3''-terindolin]-2'-one (10hb)

Isolated as a white solid in 19% yield by following the general procedure GP1 with *N*-benzyl-5-chloroisatin²³ (**7h**) and indole (**8b**). Physical and spectroscopic data obtained for this known compound were in perfect agreement with the data reported in the literature.³³ ¹H and ¹³C NMR spectra of **10hb** are provided in section K.

J25 Synthesis of monoaddition product **9ib** (see Scheme 10B)



1-Allyl-5-chloro-3-hydroxy-3-(1*H*-indol-3-yl)indolin-2-one

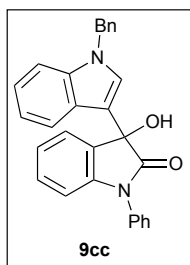
(9ib)

³³ E. Mehrasbi, Y. Sarrafi and M. Tajbakhsh, *Res. Chem. Intermed.*, 2015, **41**, 6777–6787.

³⁴ P. S. Prathima, P. Rajesh, J. V. Rao, U. S. Kailash, B. Sridhar and M. M. Rao, *Eur. J. Med. Chem.*, 2014, **84**, 155–159.

Isolated as a crystalline white solid in 95% yield by following the general procedure GP1 with *N*-allyl-5-chloroisatin²⁴ (**7i**) and indole (**8b**). Characterization data for the hitherto unknown compound **9ib**: TLC R_f = 0.43 (1:1 EtOAc/cyclohexane); mp = 169.5–172.7 °C; IR absorption (neat) ν_{\max} 3402 (N–H), 3317 (O–H), 3057 (C_{sp^2} –H), 1695 (C=O), 1605 (C=C), 1543 (C_{Ar} = C_{Ar}), 1249, 1172 and 1105 (C–N and C–O), 1073 (C_{Ar} –Cl); 1H NMR (400 MHz, $CDCl_3$) δ 3.59 (bs, 1H, OH), 4.31 (dddd, 1H, J = 16.3, 5.3, 1.6 and 1.6, NCHHCH=CH₂), 4.47 (dddd, 1H, J = 16.3, 5.2, 1.8 and 1.8, NCHHCH=CH₂), 5.23–5.33 (m, 2H, NCHHCH=CH₂), 5.87 (dddd, 1H, J = 15.7, 10.4, 5.3 and 5.2, NCHHCH=CH₂), 6.86 (d, 1H, J = 8.5, H_{Ar}), 7.09 (d, 1H, J = 2.7, H_{Ar}), 7.12 (ddd, 1H, J = 7.9, 7.1 and 0.8, H_{Ar}), 7.22 (ddd, 1H, J = 8.2, 7.0 and 1.1, H_{Ar}), 7.31 (dd, 1H, J = 8.2 and 2.0, H_{Ar}), 7.37 (bd, 1H, J = 8.1, H_{Ar}), 7.48 (d, 1H, J = 1.9, H_{Ar}), 7.66 (bd, 1H, J = 8.0, H_{Ar}), 8.27 (bs, 1H, NH); $^{13}C\{^1H\}$ NMR (100 MHz, $CDCl_3$) δ 42.7 (CH₂), 75.5 (C–OH), 110.5 (CH_{Ar}), 111.6 (CH_{Ar}), 115.0 (C_{Ar}), 118.2 (CH=CH₂), 120.38 (CH_{Ar}), 120.42 (CH_{Ar}), 122.8 (CH_{Ar}), 123.1 (CH_{Ar}), 124.6 (C_{Ar}), 125.5 (CH_{Ar}), 128.7 (C_{Ar}), 129.6 (CH_{Ar}), 130.8 (CH=CH₂), 132.6 (C_{Ar}), 136.9 (C_{Ar}), 140.9 (C_{Ar}), 176.5 (C=O); HRMS (ESI⁺): m/z $[M+Na]^+$ calcd for C₁₉H₁₅ClN₂NaO₂ 361.0714, found 361.0718. The crystal structure of **9ib** is shown within Scheme 10B of the manuscript and crystal data for **9ib** are herein given as section D10.

J26 Synthesis of monoaddition product **9cc** (see Scheme 11Aa)

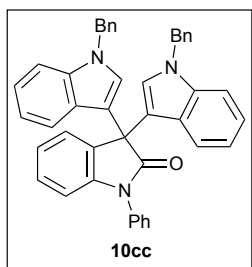


3-(1-Benzyl-1*H*-indol-3-yl)-3-hydroxy-1-phenylindolin-2-one

(9cc)

Isolated as a crystalline white solid in 42% yield (50% conversion) by following the general procedure GP1 with *N*-phenylisatin (**7c**) and *N*-benzylindole (**8c**). Physical and spectroscopic data obtained for this known compound were in perfect agreement with the data reported in the literature.³² 1H and ^{13}C NMR spectra of **9cc** are provided in section K. The crystal structure of **9cc** is shown within Scheme 11Aa of the manuscript and crystal data for **9cc** are herein given as section D11.

J27 Synthesis of double addition product **10cc** (see Scheme 11Ab)

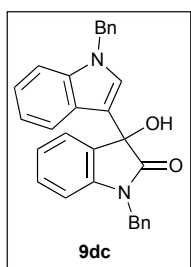


1,1''-Dibenzyl-1'-phenyl-[3,3':3',3''-terindolin]-2'-one

(**10cc**)

Isolated as a foamy white-yellowish solid in 65% yield (86% conversion) by following the general procedure GP1 with *N*-phenylisatin (**7c**) and *N*-benzylindole (**8c**) on using 10 mol% of Sc(OTf)₃ and 11 mol% of 5,5'-bistriazole **4a**. Characterization data for the hitherto unknown compound **10cc**: TLC R_f = 0.49 (3:7 EtOAc/cyclohexane); mp = 116.7–119.5 °C; IR absorption (neat) ν_{\max} 3055 and 3029 (C_{sp2}–H), 1722 (C=O), 1607 (C=C), 1594 (C_{Ar}=C_{Ar}), 1173 and 1156 (C–N); ¹H NMR (500 MHz, CDCl₃) δ 5.29 (s, 4H, 2CH₂), 6.98 (ddd, 2H, J = 8.0, 7.1 and 1.0, H_{Ar}), 7.04 (bd, 1H, J = 7.8, H_{Ar}), 7.06–7.16 (m, 9H, H_{Ar}), 7.25 (bd, 2H, J = 8.3, H_{Ar}), 7.26–7.35 (m, 7H, H_{Ar}), 7.39–7.44 (m, 1H, H_{Ar}), 7.49–7.58 (m, 7H, H_{Ar}); ¹³C{¹H} NMR (125 MHz, CDCl₃) δ 50.1 (CH₂), 53.0 (C_q), 109.6 (CH_{Ar}), 109.9 (CH_{Ar}), 114.7 (C_{Ar}), 119.4 (CH_{Ar}), 121.7 (CH_{Ar}), 121.8 (CH_{Ar}), 123.2 (CH_{Ar}), 125.7 (CH_{Ar}), 126.6 (CH_{Ar}), 126.7 (CH_{Ar}), 126.8 (C_{Ar}), 127.5 (CH_{Ar}), 127.8 (CH_{Ar}), 127.9 (CH_{Ar}), 128.5 (CH_{Ar}), 128.7 (CH_{Ar}), 129.5 (CH_{Ar}), 133.7 (C_{Ar}), 135.0 (C_{Ar}), 137.4 (C_{Ar}), 137.5 (C_{Ar}), 142.9 (C_{Ar}), 176.8 (C=O); HRMS (ESI⁺): m/z [M+Na]⁺ calcd for C₄₄H₃₃N₃NaO 642.2516, found 642.2522.

J28 Synthesis of monoaddition product **9dc** (see Scheme 11Ba)



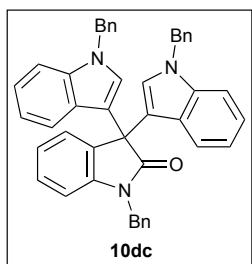
1-Benzyl-3-(1-benzyl-1*H*-indol-3-yl)-3-hydroxyindolin-2-one

(**9dc**)

Isolated as a white solid in 32% yield (35% conversion) by following the general procedure GP1 with *N*-benzylisatin (**7d**) and *N*-benzylindole (**8c**). Physical and spectroscopic data obtained for this known compound were in perfect agreement with

the data reported in the literature.³² ^1H and ^{13}C NMR spectra of **9dc** are provided in section K.

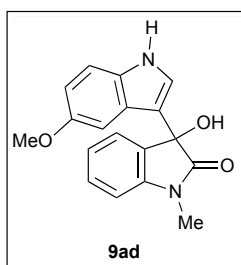
J29 Synthesis of double addition product **10dc** (see Scheme 11Bb)



1,1',1''-Tribenzyl-[3,3':3',3''-terindolin]-2'-one (10dc**)**

Isolated as a crystalline white solid in 48% yield (70% conversion) by following the general procedure GP1 with *N*-benzylisatin (**7d**) and *N*-benzylindole (**8c**) on using 10 mol% of $\text{Sc}(\text{OTf})_3$ and 11 mol% of 5,5'-bistriazole **4a**. Characterization data for the hitherto unknown compound **10dc**: TLC R_f = 0.65 (3:7 EtOAc/cyclohexane); mp = 104.7–106.5 °C; IR absorption (neat) ν_{max} 3058 and 3031 ($\text{C}_{\text{sp}2}\text{-H}$), 1712 (C=O), 1608 (C=C), 1538 ($\text{C}_{\text{Ar}}=\text{C}_{\text{Ar}}$), 1172 and 1079 (C-N); ^1H NMR (400 MHz, CDCl_3) δ 5.07 (s, 2H, CH_2), 5.27 (s, 4H, 2 CH_2), 6.86–6.96 (m, 3H, H_{Ar}), 6.96–7.04 (m, 3H, H_{Ar}), 7.04–7.14 (m, 6H, H_{Ar}), 7.19–7.43 (m, 16H, H_{Ar}), 7.47 (bdd, 1H, J = 7.5 and 0.9, H_{Ar}); $^{13}\text{C}\{^1\text{H}\}$ NMR (100 MHz, CDCl_3) δ 44.1 (CH_2), 50.1 (CH_2), 52.8 (C_q), 109.3 (CH_{Ar}), 109.9 (CH_{Ar}), 114.6 (C_{Ar}), 119.2 (CH_{Ar}), 121.77 (CH_{Ar}), 121.80 (CH_{Ar}), 122.7 (CH_{Ar}), 125.4 (CH_{Ar}), 126.6 (CH_{Ar}), 126.7 (CH_{Ar}), 127.47 (CH_{Ar}), 127.53 (C_{Ar}), 127.6 (CH_{Ar}), 127.9 (CH_{Ar}), 128.3 (CH_{Ar}), 128.7 (x 2, CH_{Ar}), 133.9 (C_{Ar}), 136.1 (C_{Ar}), 137.4 (C_{Ar}), 137.5 (C_{Ar}), 142.1 (C_{Ar}), 177.7 (C=O); HRMS (ESI^+): m/z $[\text{M}+\text{Na}]^+$ calcd for $\text{C}_{45}\text{H}_{35}\text{N}_3\text{NaO}$ 656.2672, found 656.2680. The crystal structure of **10dc** is shown within Scheme 11Bb of the manuscript and crystal data for **10dc** are herein given as section D13.

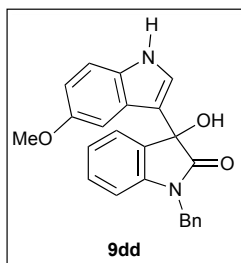
J30 Synthesis of monoaddition product **9ad** (see Scheme 12)



3-Hydroxy-3-(5-methoxy-1H-indol-3-yl)-1-methylindolin-2-one (9ad**)**

Isolated as a white solid in 97% yield by following the general procedure GP1 with *N*-methylisatin (**7a**) and 5-methoxyindole (**8d**). Physical and spectroscopic data obtained for this known compound were in perfect agreement with the data reported in the literature.²⁸ ¹H and ¹³C NMR spectra of **9ad** are provided in section K.

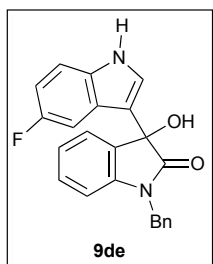
J31 Synthesis of monoaddition product 9dd (see Scheme 12)



1-Benzyl-3-hydroxy-3-(5-methoxy-1*H*-indol-3-yl)indolin-2-one (9dd)

Isolated as a white solid in 100% yield by following the general procedure GP1 with *N*-benzylisatin (**7d**) and 5-methoxyindole (**8d**). Physical and spectroscopic data obtained for this known compound were in perfect agreement with the data reported in the literature.²⁸ ¹H and ¹³C NMR spectra of **9dd** are provided in section K.

J32 Synthesis of monoaddition product 9de (see Scheme 12)

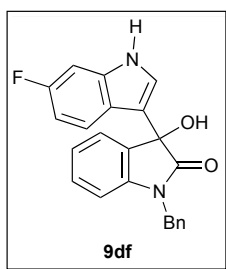


1-Benzyl-3-(5-fluoro-1*H*-indol-3-yl)-3-hydroxyindolin-2-one

(9de)

Isolated as a white solid in 71% yield by following the general procedure GP1 with *N*-benzylisatin (**7d**) and 5-fluoroindole (**8e**). Physical and spectroscopic data obtained for this known compound were in perfect agreement with the data reported in the literature.³² ¹H, ¹³C and ¹⁹F NMR spectra of **9de** are provided in section K.

J33 Synthesis of monoaddition product **9df** (see Scheme 12)

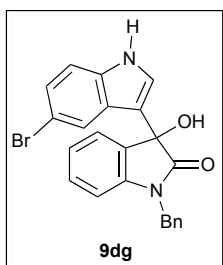


1-Benzyl-3-(6-fluoro-1H-indol-3-yl)-3-hydroxyindolin-2-one

(9df)

Isolated as a white solid in 71% yield by following the general procedure GP1 with *N*-benzylisatin (**7d**) and 6-fluoroindole (**8f**). Characterization data for the hitherto unknown compound **9df**: TLC R_f = 0.44 (1:1 EtOAc/cyclohexane); mp = 209.7–213.2 °C (decomp.); IR absorption (neat) ν_{\max} 3407 (N–H and O–H), 3061 and 3028 (C_{sp^2} –H), 1687 (C=O), 1613 (C=C), 1591 ($C_{Ar}=C_{Ar}$), 1180 (C_{Ar} –F), 1092 and 1067 (C–N and C–O); 1H NMR (500 MHz, DMSO- d_6) δ 4.89 (d, 1H, J = 15.9, $CHHPh$), 4.93 (d, 1H, J = 15.9, $CHHPh$), 6.62 (bs, 1H, OH), 6.74 (ddd, 1H, J = 8.2, 8.2 and 1.9, H_{Ar}), 6.98 (bd, 1H, J = 8.2, H_{Ar}), 7.00–7.09 (m, 2H, H_{Ar}), 7.14 (dd, 1H, J = 9.2 and 2.2, H_{Ar}), 7.21–7.47 (m, 8H, H_{Ar}), 11.1 (bs, 1H, NH); $^{13}C\{^1H\}$ NMR (125 MHz, DMSO- d_6) δ 43.1 (CH_2), 75.0 (C–OH), 97.9 (d, $^2J_{C-F}$ = 25.3, CH_{Ar}), 107.5 (d, $^2J_{C-F}$ = 24.1, CH_{Ar}), 109.7 (CH_{Ar}), 115.9 (C_{Ar}), 122.2 (d, $^3J_{C-F}$ = 10.0, CH_{Ar}), 122.3 (C_{Ar}), 123.0 (CH_{Ar}), 124.8 (d, $^5J_{C-F}$ = 3.4, CH_{Ar} –NH), 125.0 (CH_{Ar}), 127.8 (CH_{Ar}), 127.9 (CH_{Ar}), 129.0 (CH_{Ar}), 129.6 (CH_{Ar}), 132.9 (C_{Ar}), 136.8 (C_{Ar}), 137.2 (d, $^3J_{C-F}$ = 13.0, C_{Ar}), 142.6 (C_{Ar}), 159.2 (d, $^1J_{C-F}$ = 235.0, C_{Ar} –F), 177.1 (C=O); $^{19}F\{^1H\}$ NMR (376 MHz, DMSO- d_6) δ –121.9; HRMS (ESI $^+$): m/z $[M+Na]^+$ calcd for $C_{23}H_{17}FN_2NaO_2$ 395.1166, found 395.1163.

J34 Synthesis of monoaddition product **9dg** (see Scheme 12)



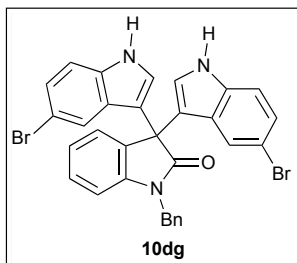
1-Benzyl-3-(5-bromo-1H-indol-3-yl)-3-hydroxyindolin-2-one

(9dg)

Isolated as a white solid in 66% yield (75% conversion) by following the general procedure GP1 with *N*-benzylisatin (**7d**) and 5-bromoindole (**8g**) on using 10 mol% of

Sc(OTf)₃ and 11 mol% of 5,5'-bistriazole **4a**. Physical and spectroscopic data obtained for this known compound were in perfect agreement with the data reported in the literature.³⁵ ¹H and ¹³C NMR spectra of **9dg** are provided in section K.

J35 Synthesis of double addition product **10dg** (see Scheme 12)

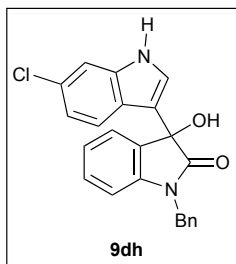


1'-Benzyl-5,5''-dibromo-[3,3':3',3''-terindolin]-2'-one

(**10dg**)

Isolated as a white solid in 9% yield (75% conversion) by following the general procedure GP1 with *N*-benzylisatin (**7d**) and 5-bromoindole (**8g**) on using 10 mol% of Sc(OTf)₃ and 11 mol% of 5,5'-bistriazole **4a**. Characterization data for the hitherto unknown compound **10dg**: TLC *R_f* = 0.56 (1:1 EtOAc/cyclohexane); IR absorption (neat) ν_{\max} 3254 (N–H), 3063 and 3030 (C_{sp2}–H), 1707 (C=O), 1610 (C=C), 1563 (C_{Ar}=C_{Ar}), 1167, 1157, 1105, 1048, 1023 and 1005 (C–N and C_{Ar}–Br); ¹H NMR (500 MHz, DMSO-*d*₆) δ 5.01 (s, 2H), 6.94 (bd, 2H, *J* = 2.6, C=CH_{Ar}–NH), 7.06 (ddd, 1H, *J* = 8.4, 7.6 and 0.9, *H*_{Ar}), 7.13 (bd, 1H, *J* = 7.8, *H*_{Ar}), 7.16 (dd, 2H, *J* = 8.6 and 2.0, *H*_{Ar}), 7.25–7.40 (m, 11H, *H*_{Ar}), 11.3 (bd, 2H, *J* = 2.6, 2C=CH_{Ar}–NH); ¹³C {¹H} NMR (125 MHz, DMSO-*d*₆) δ 43.6 (CH₂), 52.4 (C_q), 110.1 (CH_{Ar}), 111.2 (C_{Ar}), 114.0 (CH_{Ar}), 114.4 (CH_{Ar}), 123.0 (CH_{Ar}), 123.1 (CH_{Ar}), 124.2 (CH_{Ar}), 125.2 (CH_{Ar}), 126.5 (CH_{Ar}), 127.6 (CH_{Ar}), 127.8 (CH_{Ar}), 128.0 (C_{Ar}), 128.8 (C_{Ar}), 129.2 (CH_{Ar}), 133.2 (C_{Ar}), 136.2 (C_{Ar}), 136.9 (C_{Ar}), 142.1 (C_{Ar}), 177.2 (C=O); HRMS (ESI[–]): *m/z* [M–H][–] calcd for C₃₁H₂₀Br₂N₃O 607.9979, found 608.0002.

J36 Synthesis of monoaddition product **9dh** (see Scheme 12)



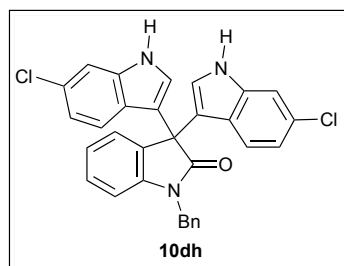
1-Benzyl-3-(6-chloro-1H-indol-3-yl)-3-hydroxyindolin-2-one

(**9dh**)

³⁵ G. Shanthi, N. Vidhya Lakshmi and P. T. Perumal, *ARKIVOC*, 2009, (x), 121–130.

Isolated as a crystalline white solid in 37% yield (80% conversion) by following the general procedure GP1 with *N*-benzylisatin (**7d**) and 6-chloroindole (**8h**) on using 10 mol% of Sc(OTf)₃ and 11 mol% of 5,5'-bistriazole **4a**. Characterization data for the hitherto unknown compound **9dh**: TLC R_f = 0.41 (1:1 EtOAc/cyclohexane); mp = 205.8–207.9 °C (decomp.); IR absorption (neat) ν_{\max} 3373 (N–H), 3296 (O–H), 3054 and 3030 (C_{sp2}–H), 1693 (C=O), 1611 (C=C), 1587 (C_{Ar}=C_{Ar}), 1174 and 1126 (C–N and C–O), 1066 (C_{Ar}–Cl); ¹H NMR (500 MHz, DMSO-*d*₆) δ 4.89 (d, 1H, J = 16.4, *CHHPh*), 4.93 (d, 1H, J = 16.4, *CHHPh*), 6.64 (s, 1H, *OH*), 6.88 (dd, 1H, J = 8.5 and 1.7, H_{Ar}), 6.98 (bd, 1H, J = 7.8, H_{Ar}), 7.02–7.10 (m, 2H, H_{Ar}), 7.23–7.46 (m, 9H, H_{Ar}), 11.2 (bs, 1H, *NH*); ¹³C{¹H} NMR (125 MHz, DMSO-*d*₆) δ 43.1 (CH₂), 75.0 (C–OH), 109.7 (CH_{Ar}), 111.6 (CH_{Ar}), 116.0 (C_{Ar}), 119.3 (CH_{Ar}), 122.5 (CH_{Ar}), 123.0 (CH_{Ar}), 124.2 (C_{Ar}), 125.0 (CH_{Ar}), 125.2 (CH_{Ar}), 126.4 (C_{Ar}), 127.8 (CH_{Ar}), 127.9 (CH_{Ar}), 129.0 (CH_{Ar}), 129.7 (CH_{Ar}), 132.8 (C_{Ar}), 136.8 (C_{Ar}), 137.7 (C_{Ar}), 142.5 (C_{Ar}), 177.0 (C=O); HRMS (ESI⁺): m/z [M+Na]⁺ calcd for C₂₃H₁₇ClN₂NaO₂ 411.0871, found 411.0882. The crystal structure of **9dh** is shown within Scheme 12 of the manuscript and crystal data for **9dh** are herein given as section D12.

J37 Synthesis of double addition product **10dh** (see Scheme 12)



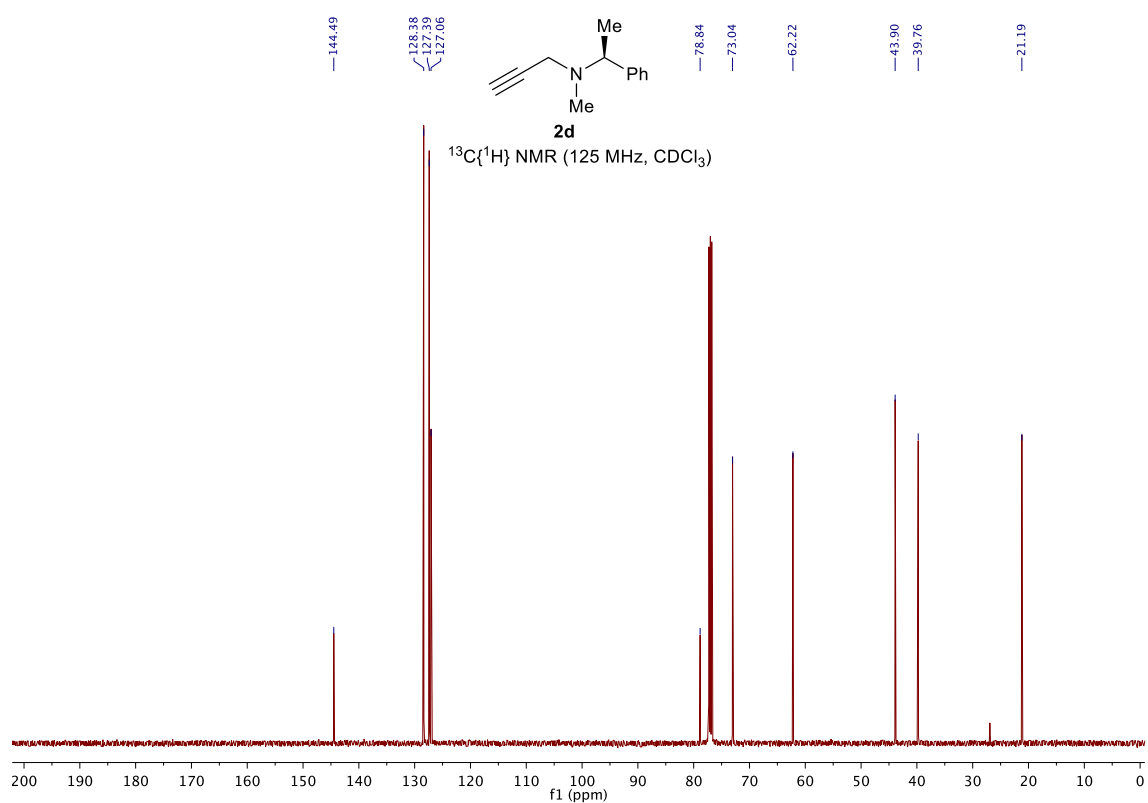
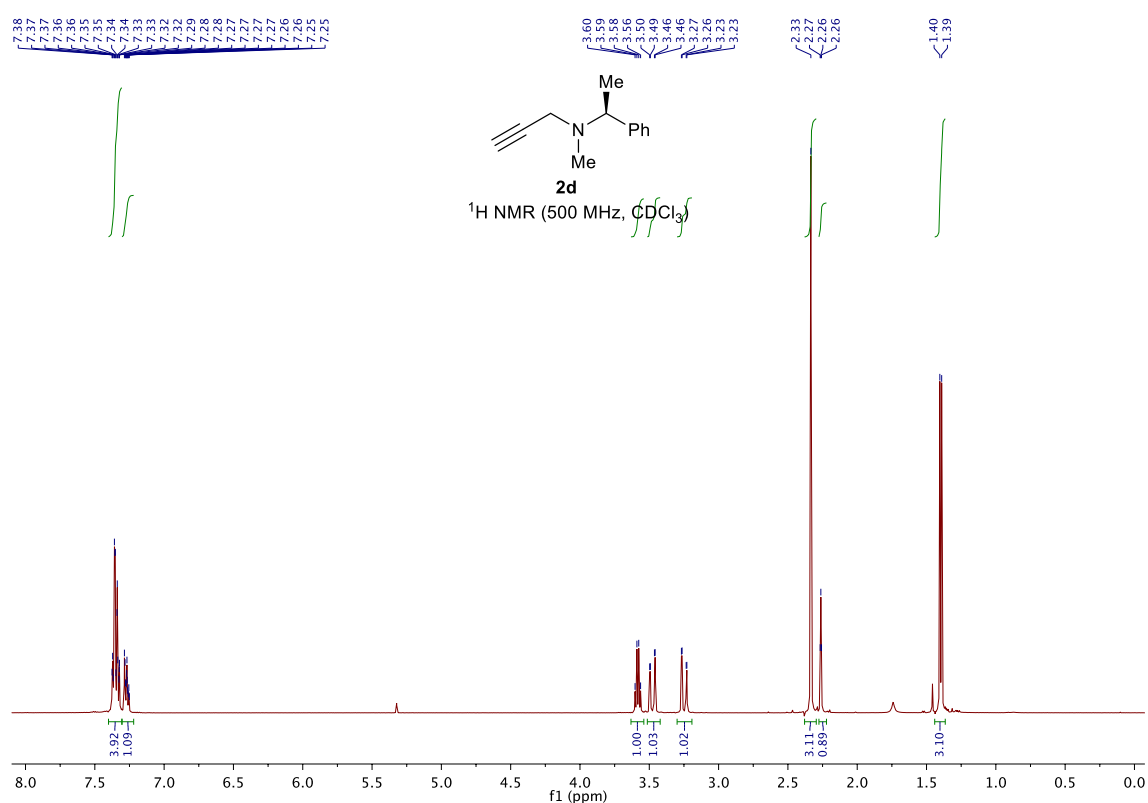
1'-Benzyl-6,6''-dichloro-[3,3':3',3''-terindolin]-2'-

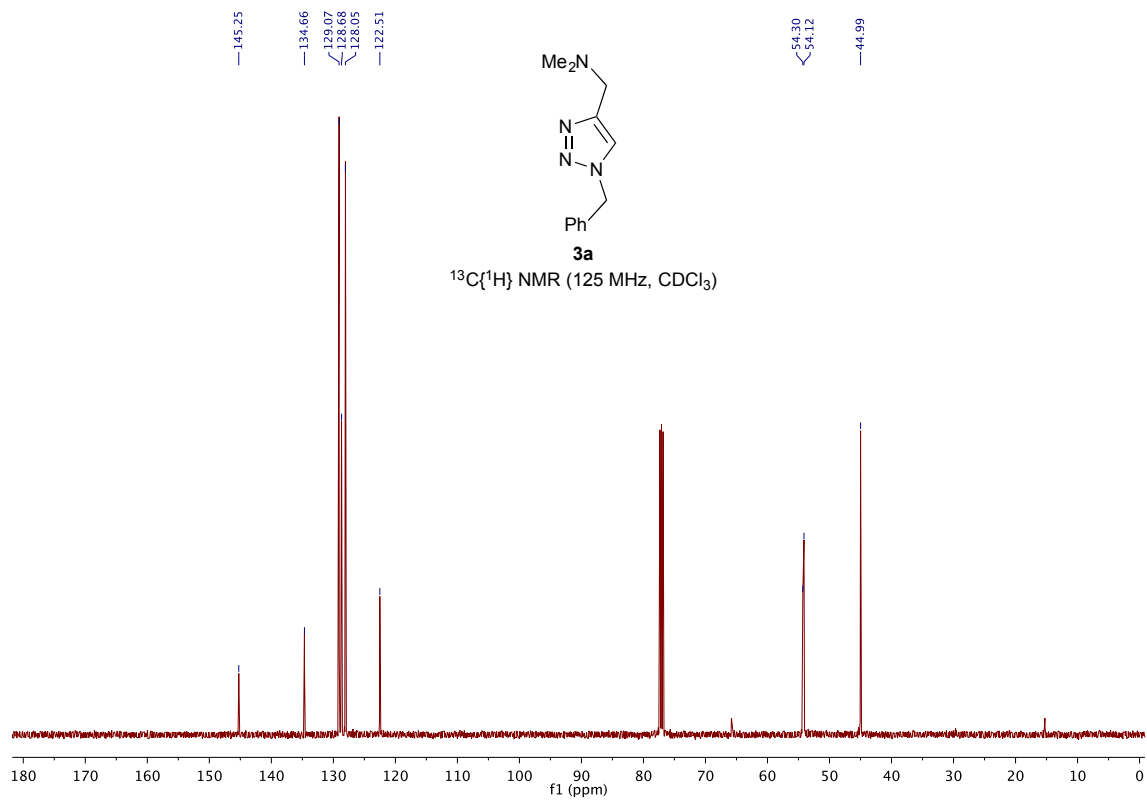
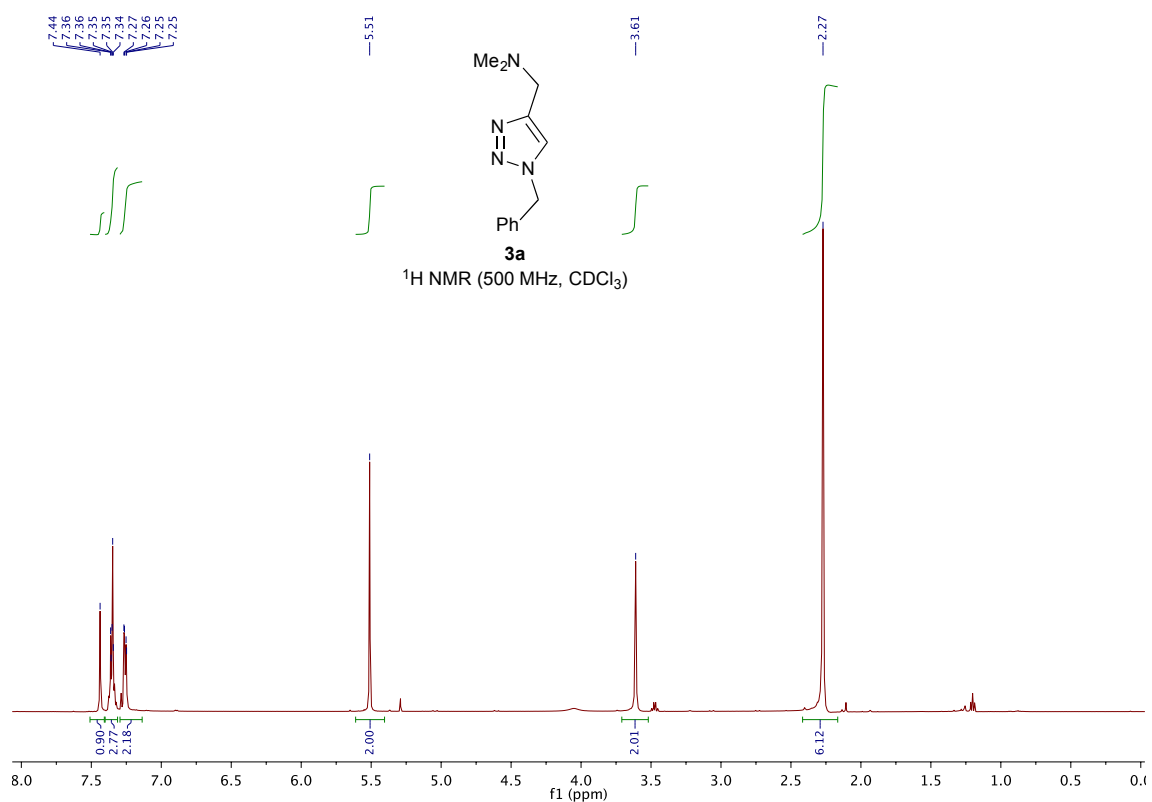
one (10dh)

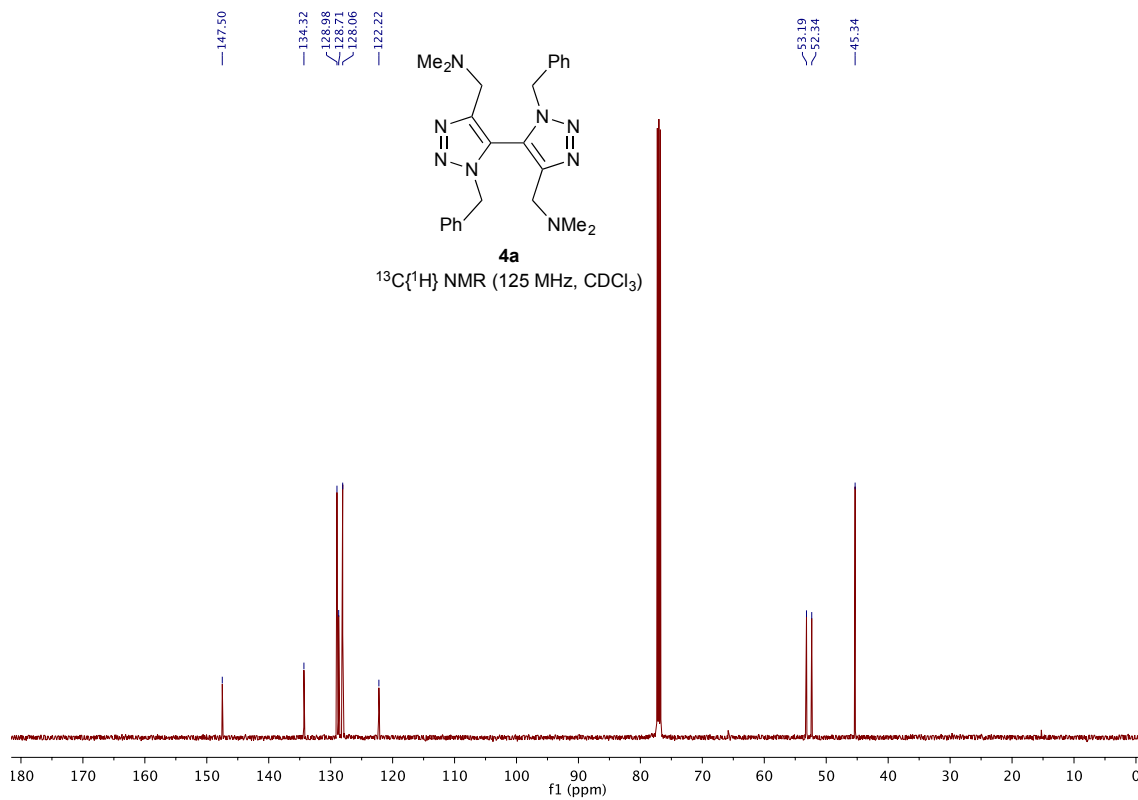
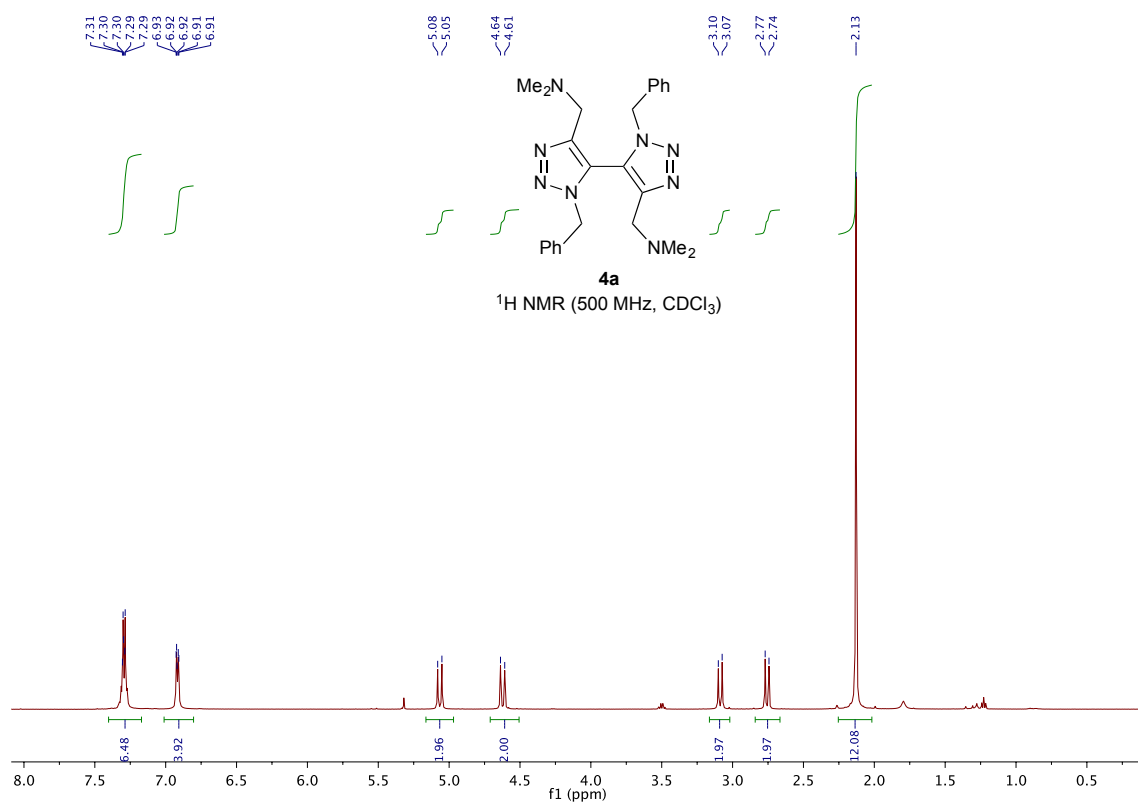
Isolated as a white-yellowish solid in 42% yield (80% conversion) by following the general procedure GP1 with *N*-benzylisatin (**7d**) and 6-chloroindole (**8h**) on using 10 mol% of Sc(OTf)₃ and 11 mol% of 5,5'-bistriazole **4a**. Characterization data for the hitherto unknown compound **10dh**: TLC R_f = 0.71 (1:1 EtOAc/cyclohexane); mp = 302.1–305.0 °C (decomp.); IR absorption (neat) ν_{\max} 3207 (N–H), 3094 and 3035 (C_{sp2}–H), 1705 (C=O), 1608 (C=C), 1211, 1167 and 1111 (C–N and C–O), 1049 (C_{Ar}–Cl); ¹H NMR (500 MHz, DMSO-*d*₆) δ 5.01 (s, 2H, NCH₂Ph), 6.78 (dd, 2H, J = 8.8 and 1.4, H_{Ar}), 6.93 (bd, 2H, J = 2.2, H_{Ar}), 7.02 (dd, 1H, J = 7.6 and 7.6, H_{Ar}), 7.09 (bd, 2H, J = 8.5, H_{Ar}), 7.14 (bd, 1H, J = 7.7, H_{Ar}), 7.22–7.39 (m, 7H, H_{Ar}), 7.42 (bd, 2H, J = 1.2, H_{Ar}), 11.2 (bs, 2H, 2*NH*); ¹³C{¹H} NMR (125 MHz, DMSO-*d*₆) δ 43.5 (CH₂),

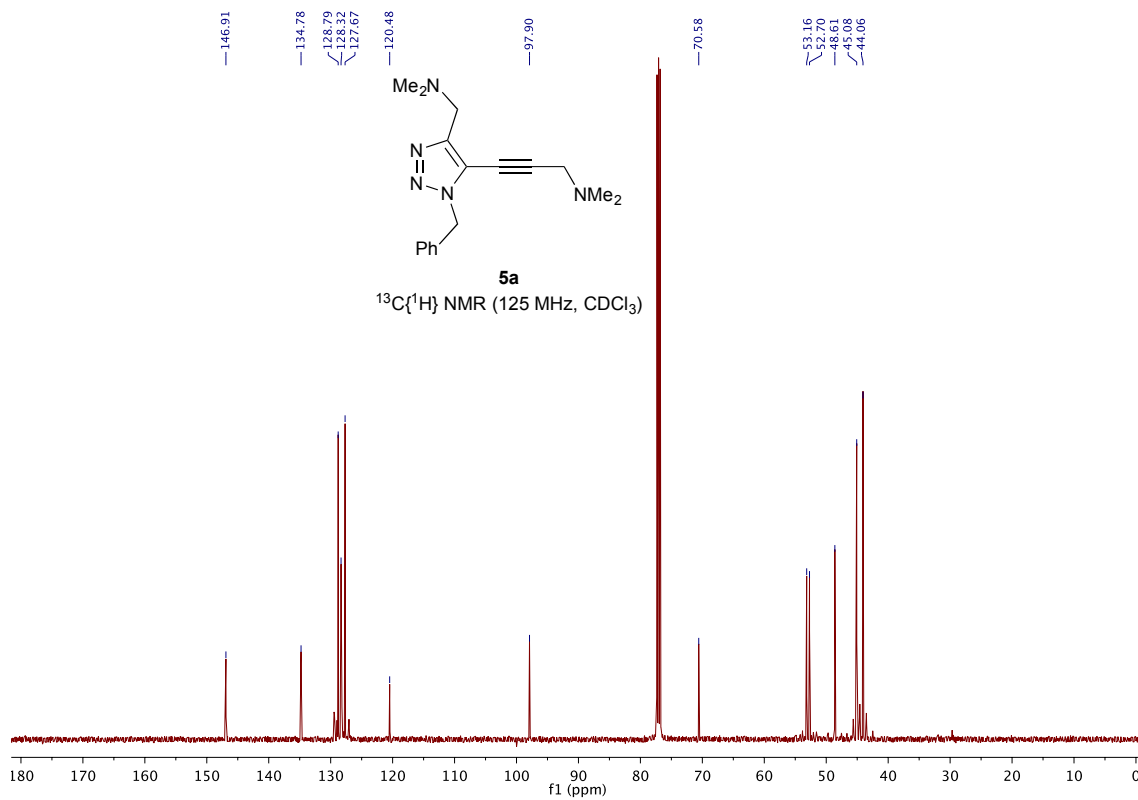
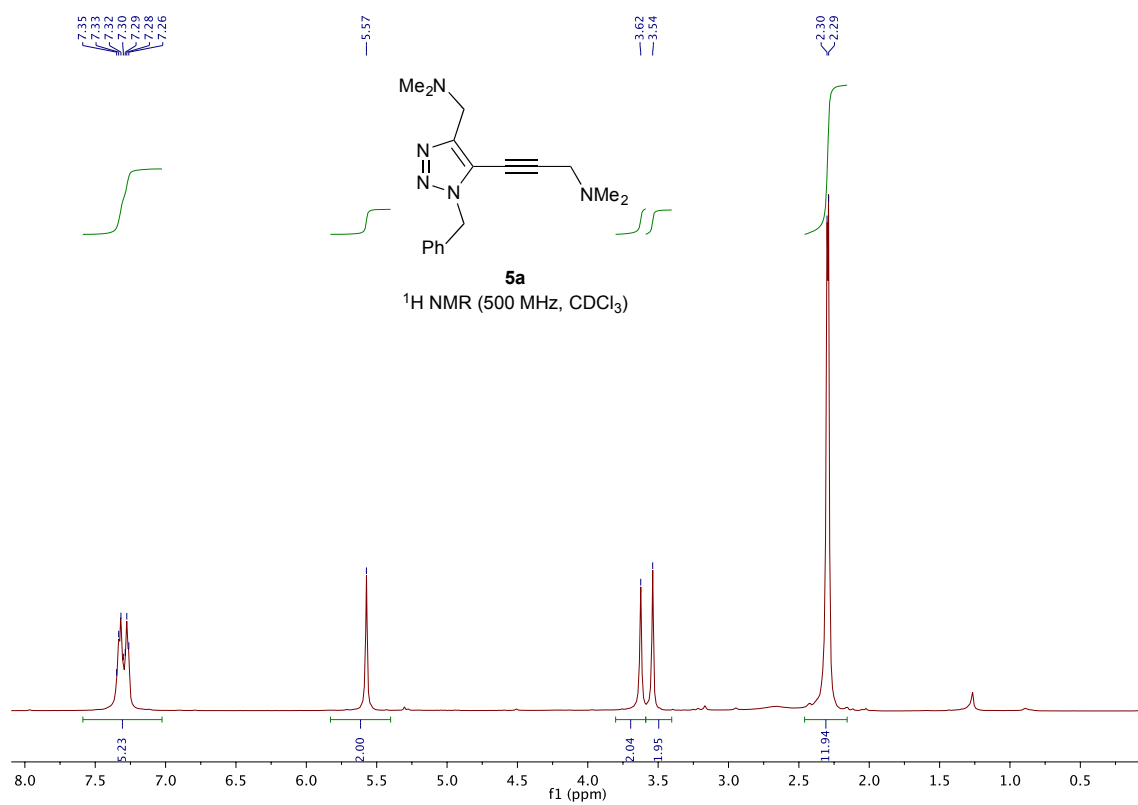
52.4 (C_q), 110.0 (CH_{Ar}), 111.8 (CH_{Ar}), 114.7 (C_{Ar}), 119.2 (CH_{Ar}), 122.4 (CH_{Ar}), 123.0 (CH_{Ar}), 124.8 (CH_{Ar}), 125.2 (CH_{Ar}), 125.8 (CH_{Ar}), 126.4 (C_{Ar}), 128.00 (C_{Ar}), 128.02 (CH_{Ar}), 128.6 (CH_{Ar}), 129.1 (CH_{Ar}), 133.6 (C_{Ar}), 136.9 (C_{Ar}), 137.8 (C_{Ar}), 142.1 (C_{Ar}), 177.1 ($C=O$); HRMS (ESI⁺): m/z $[M+Na]^+$ calcd for $C_{31}H_{21}Cl_2N_3NaO$ 544.0954, found 544.0962.

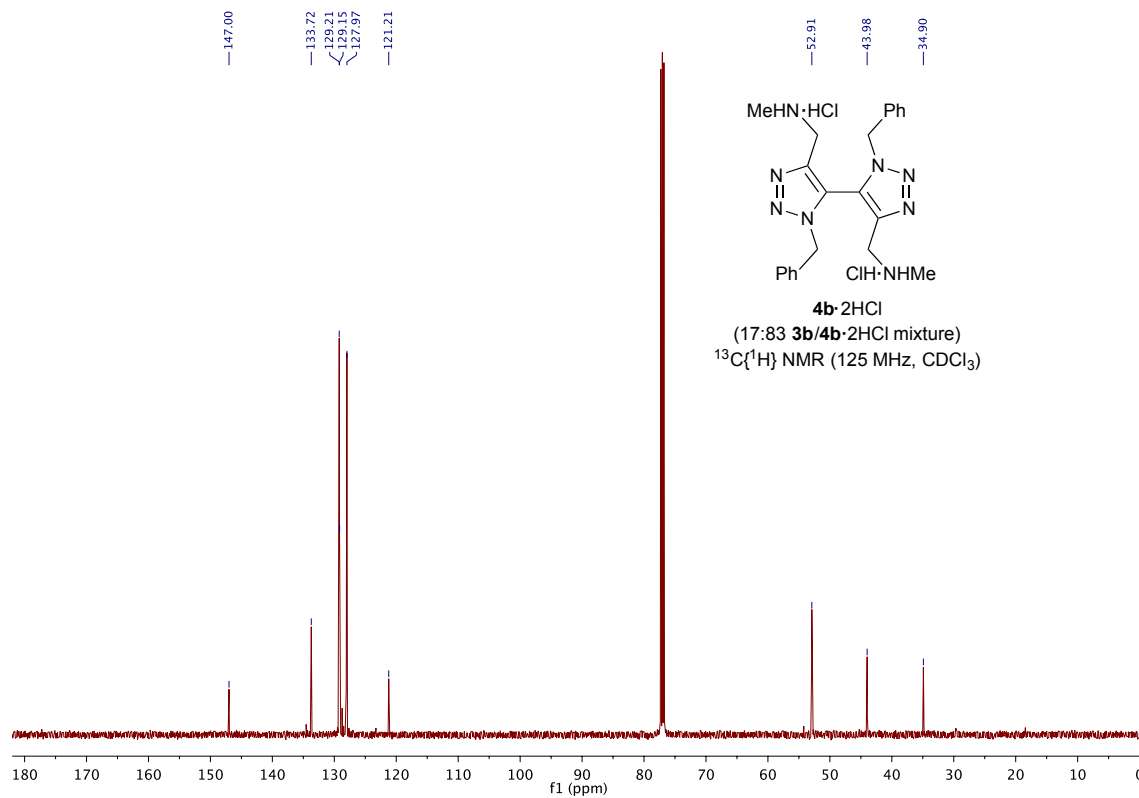
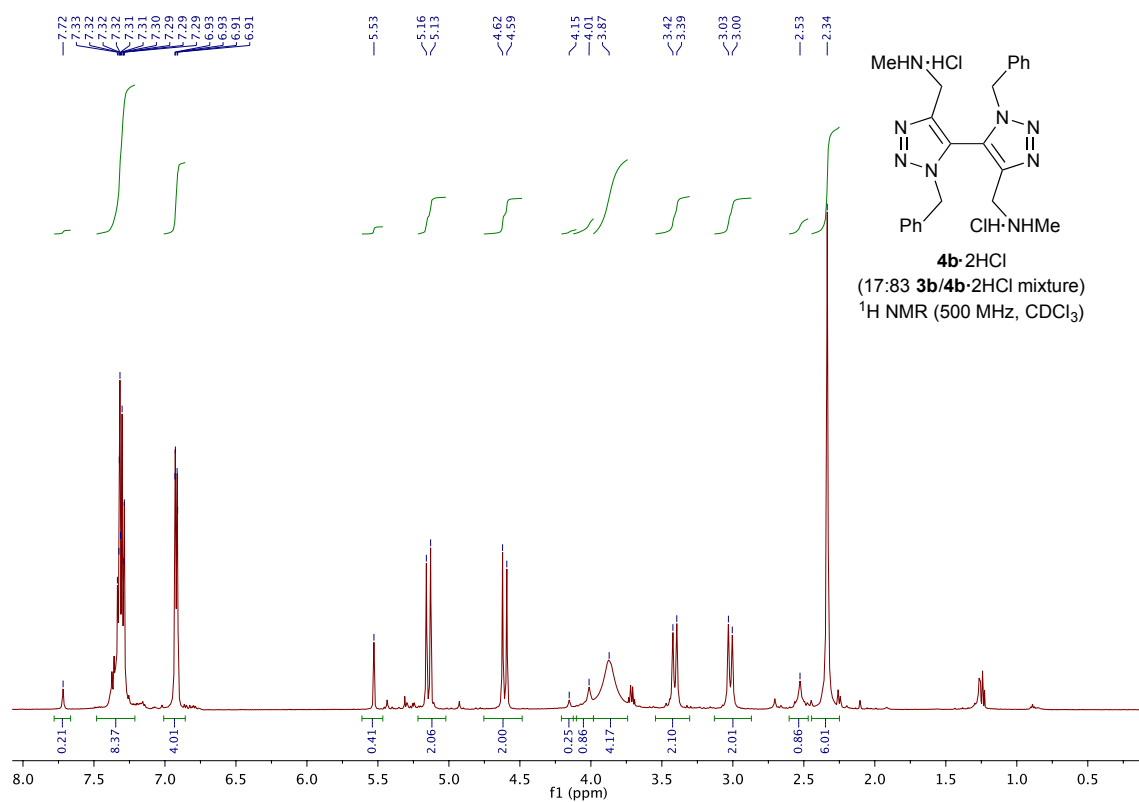
(K) NMR spectra of all compounds

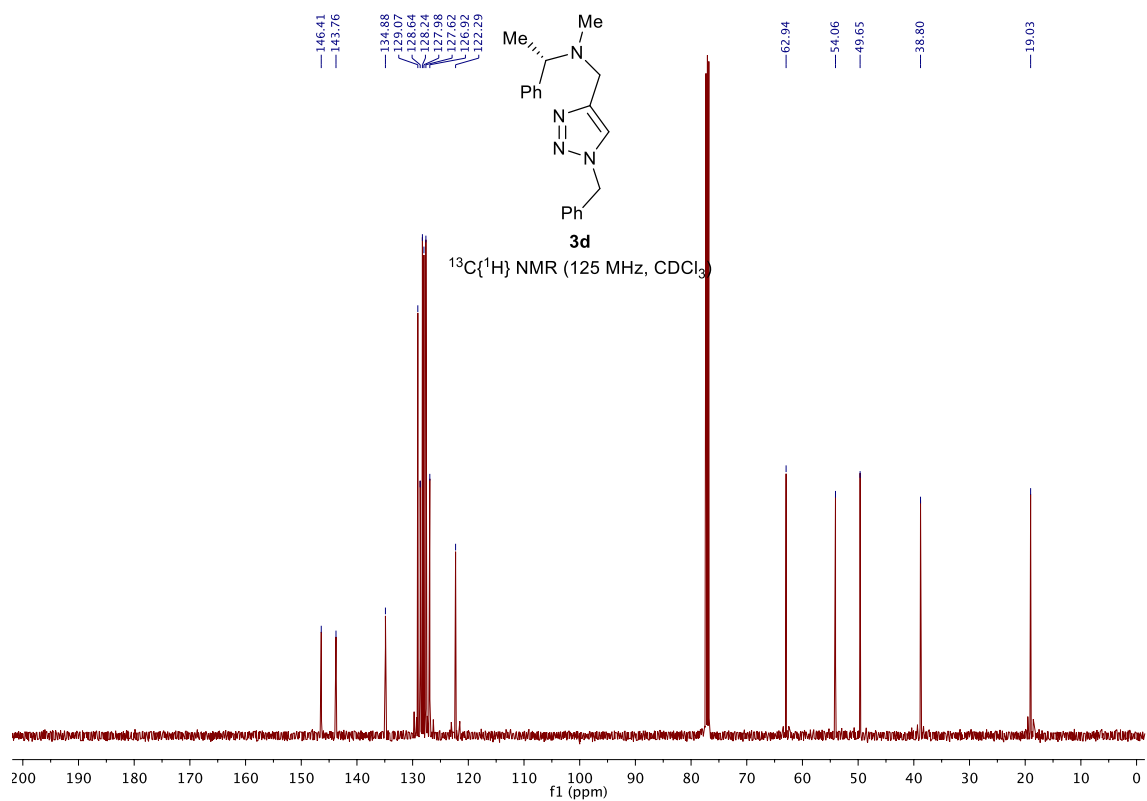
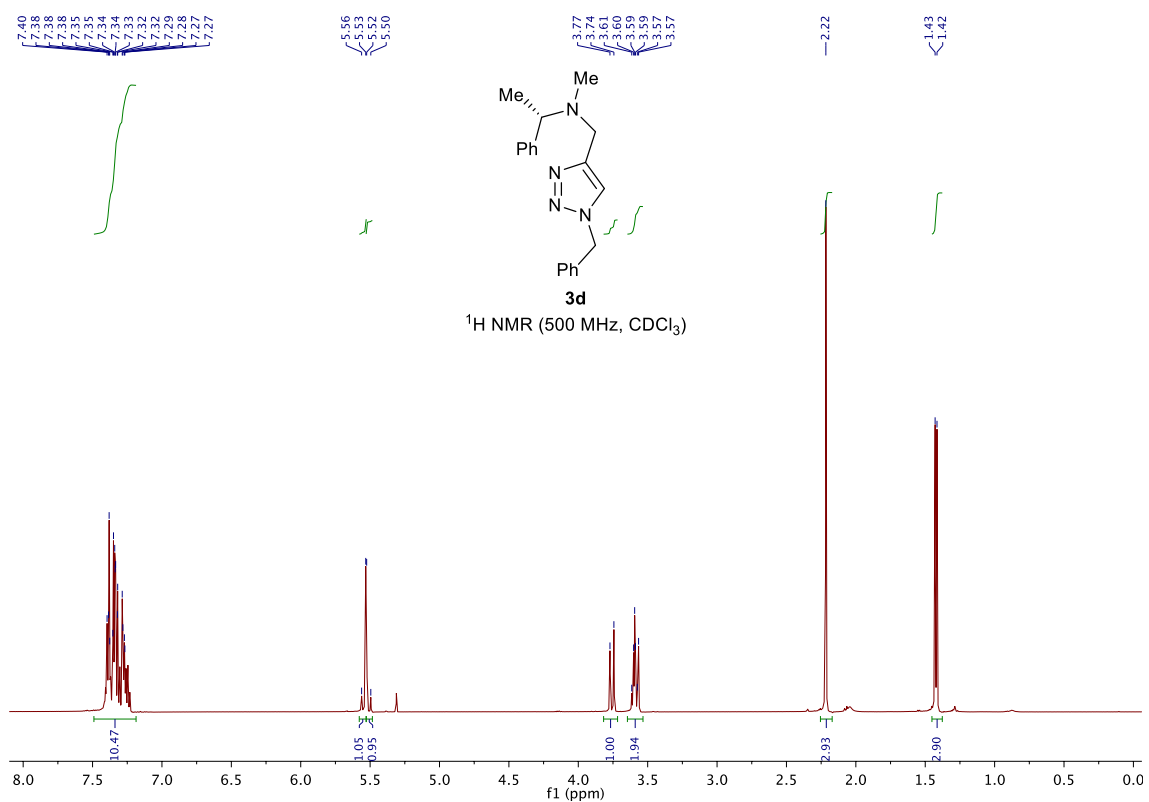


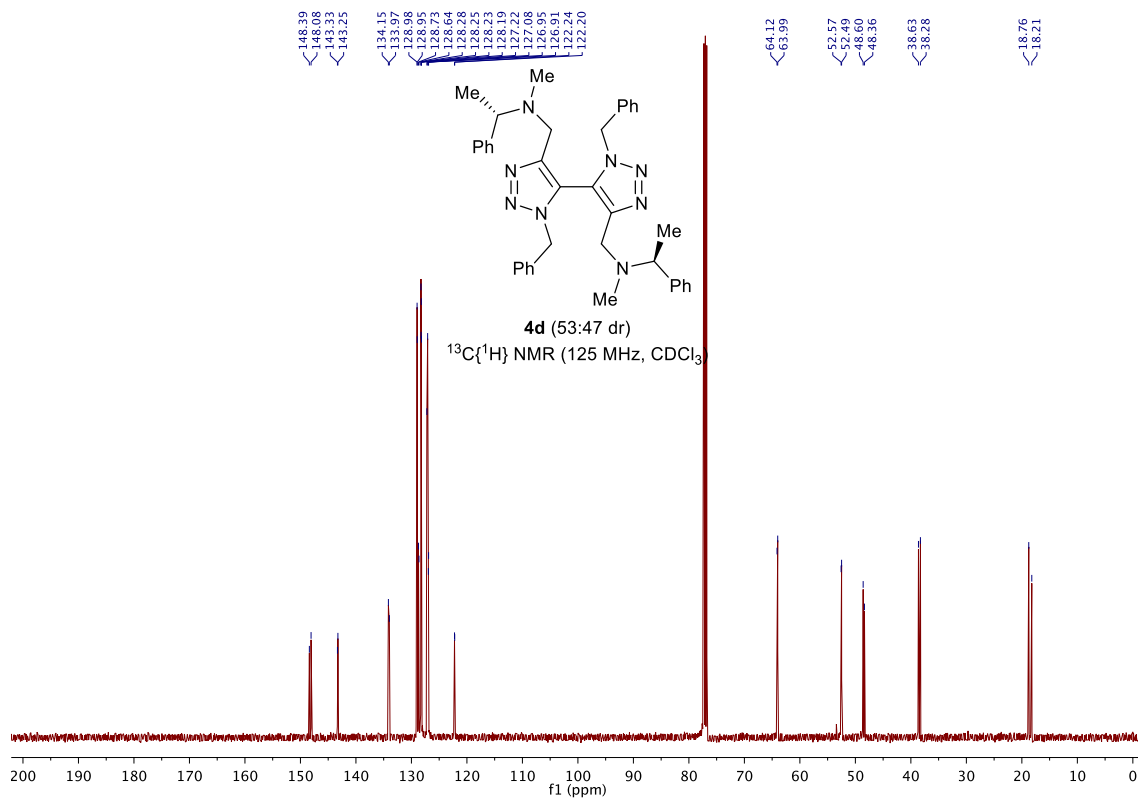
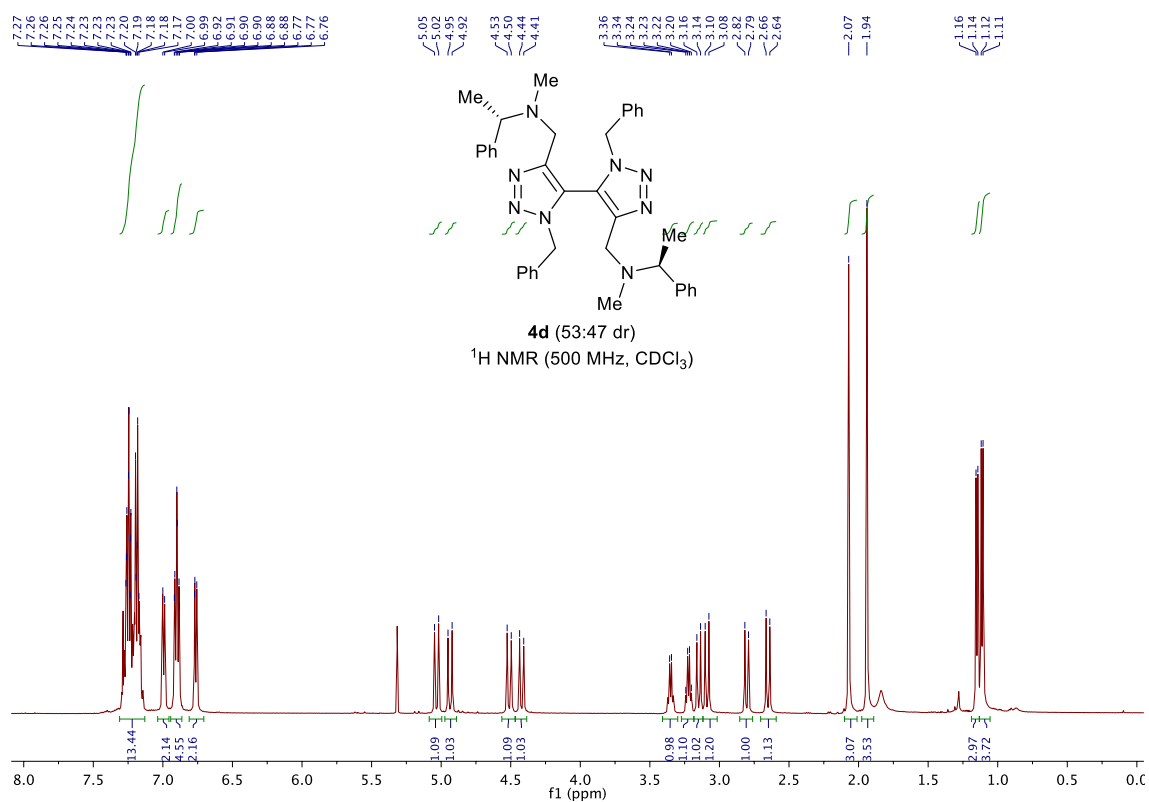


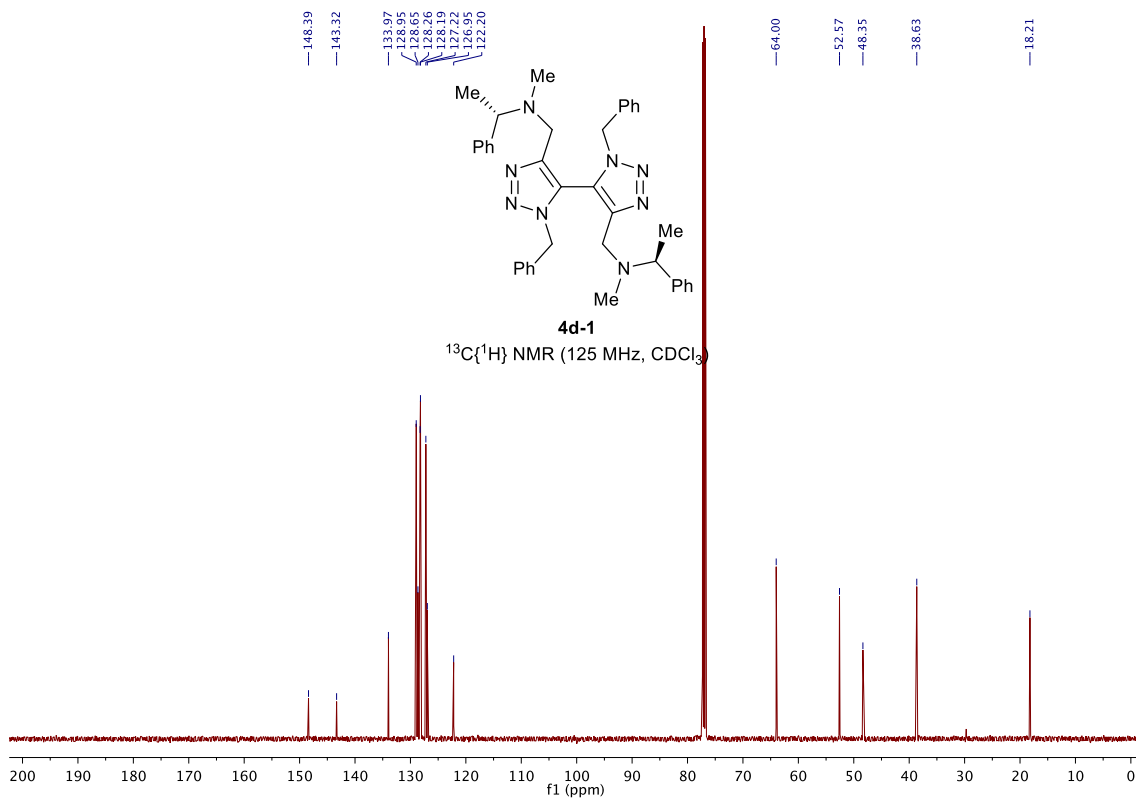
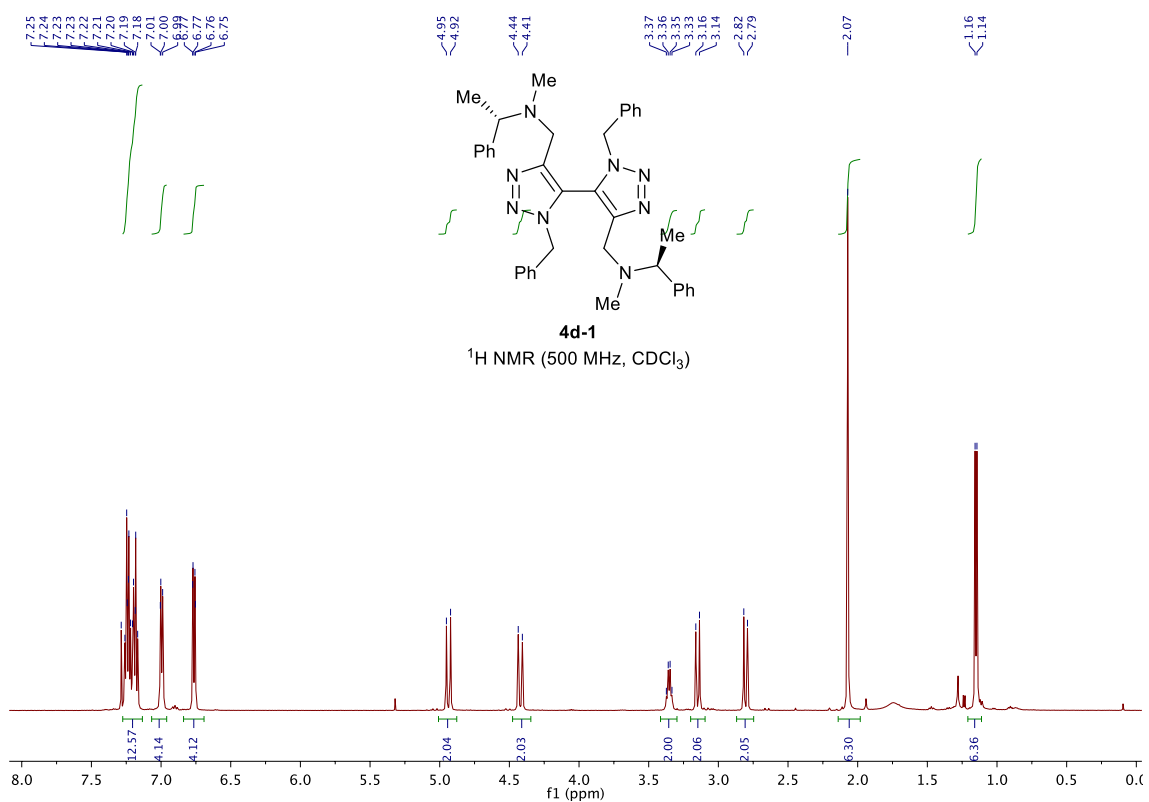


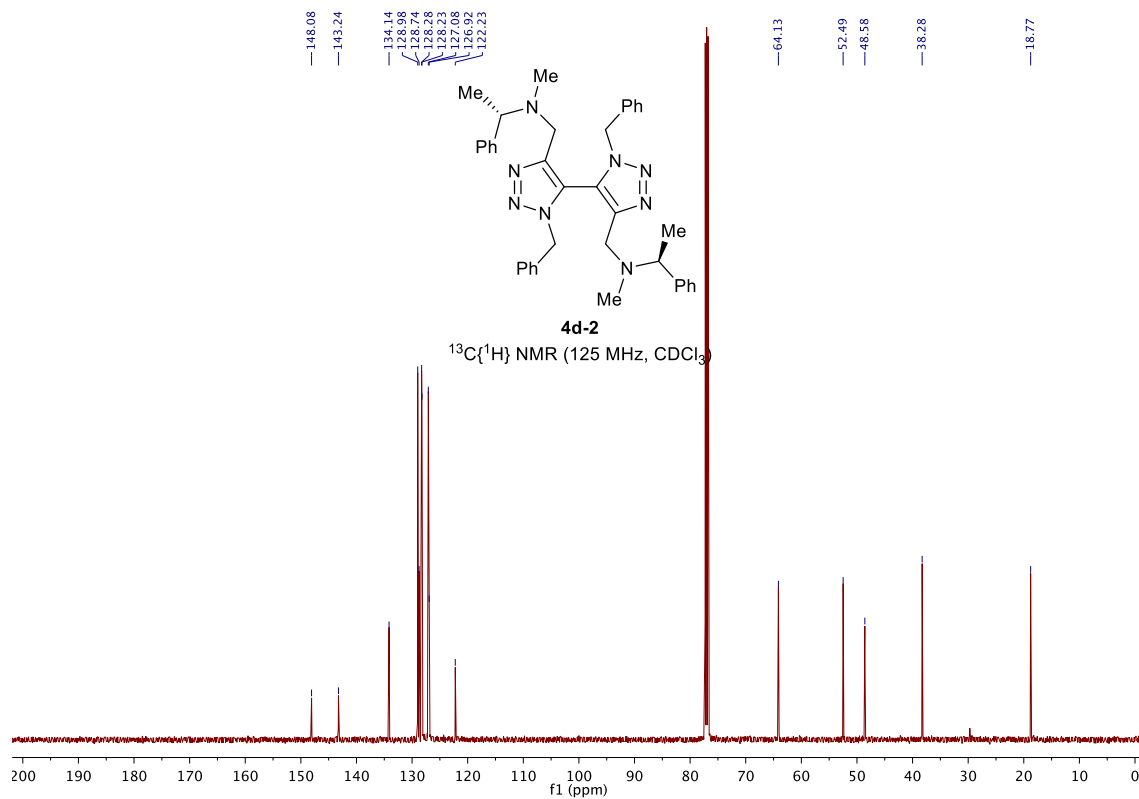
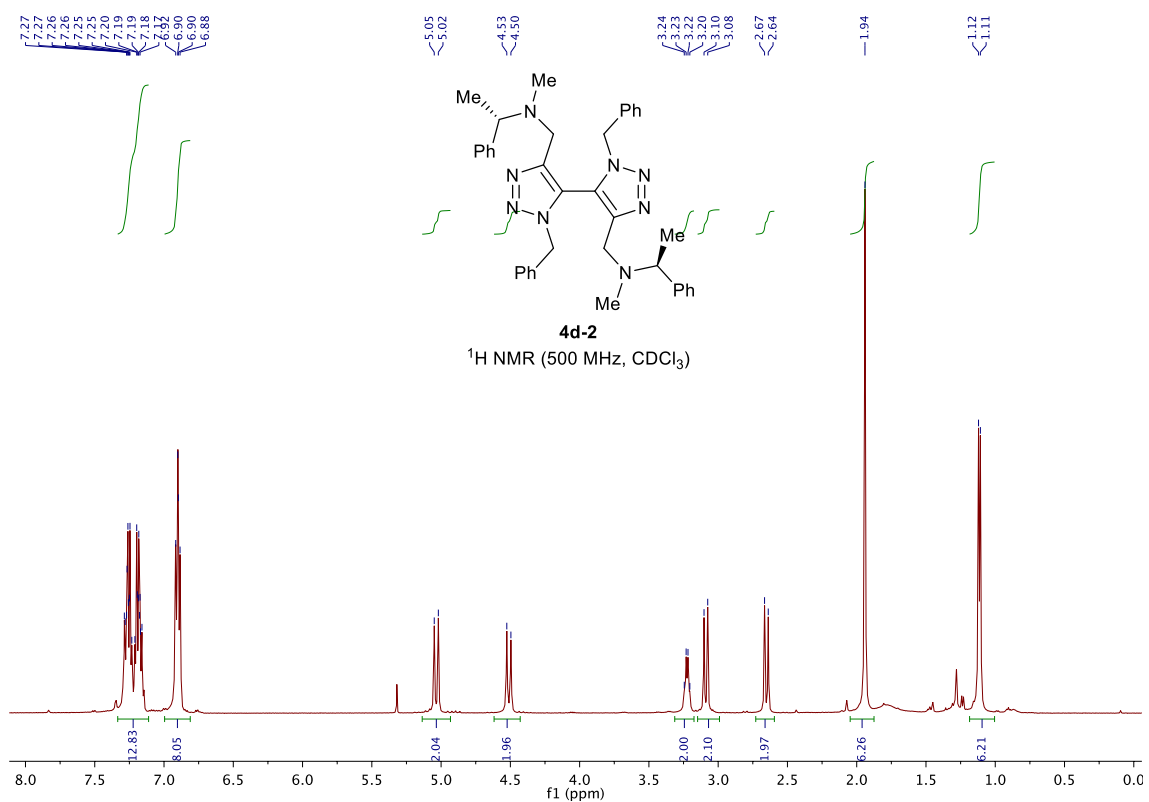


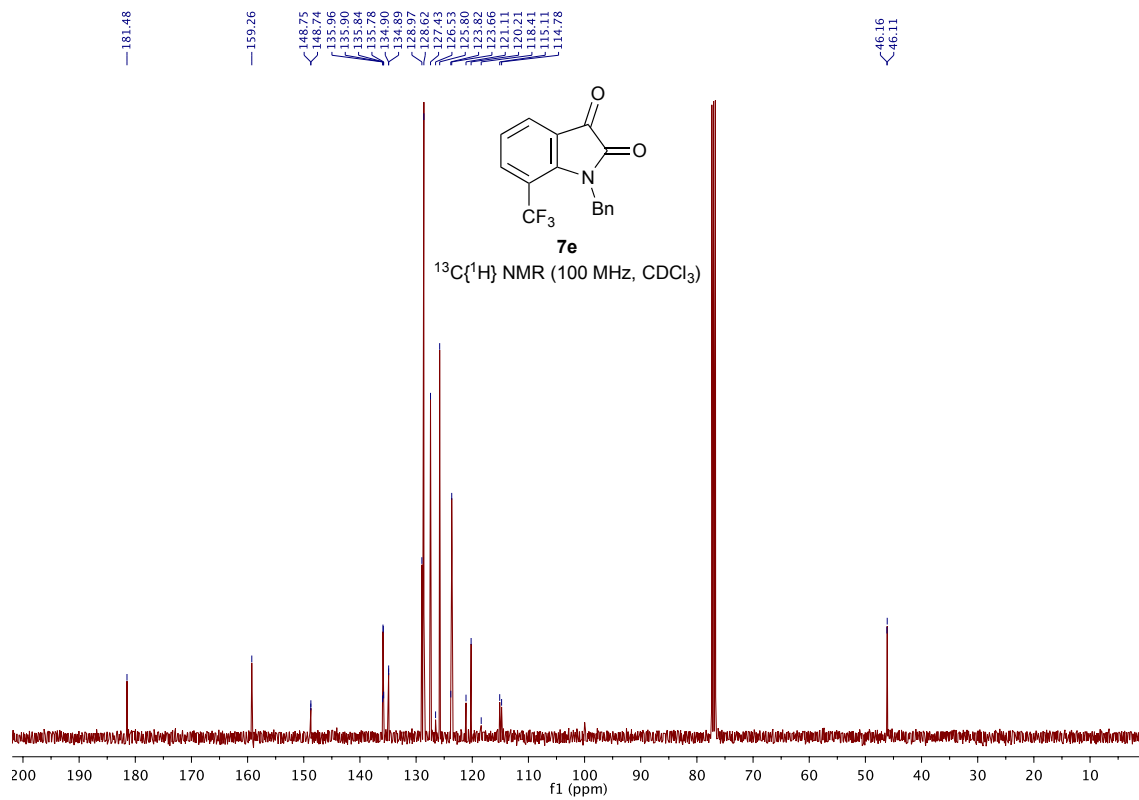
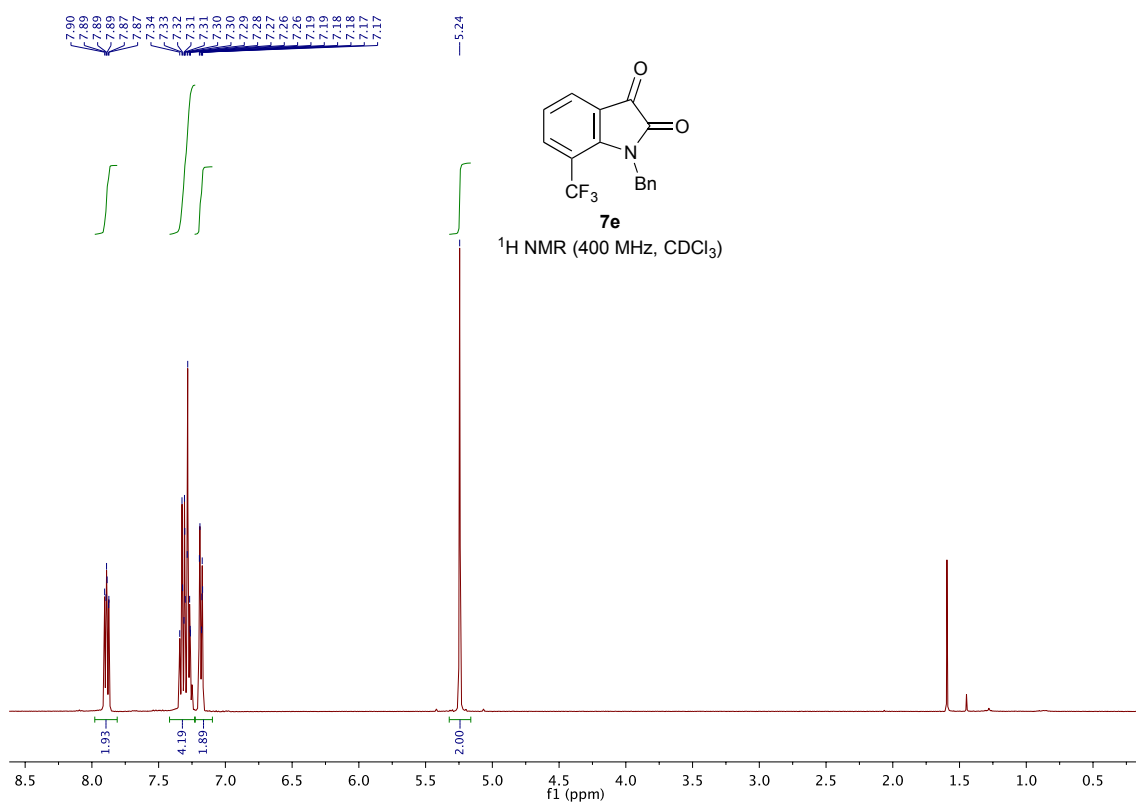


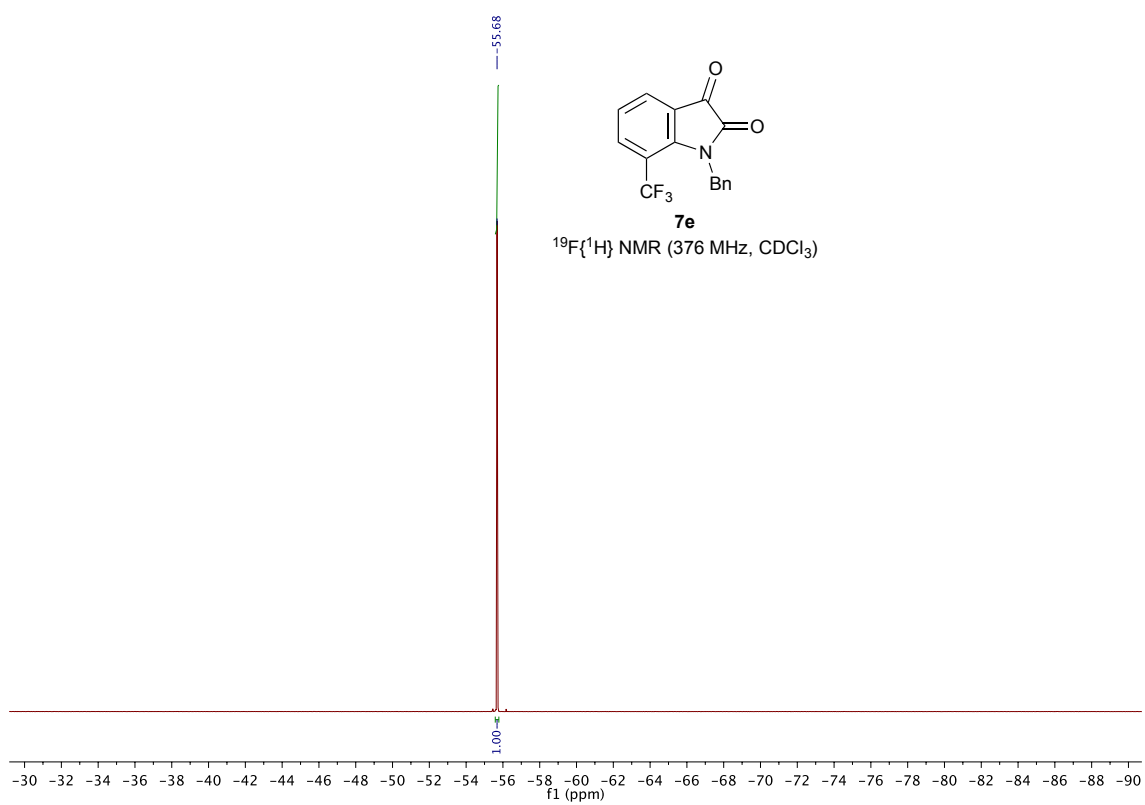


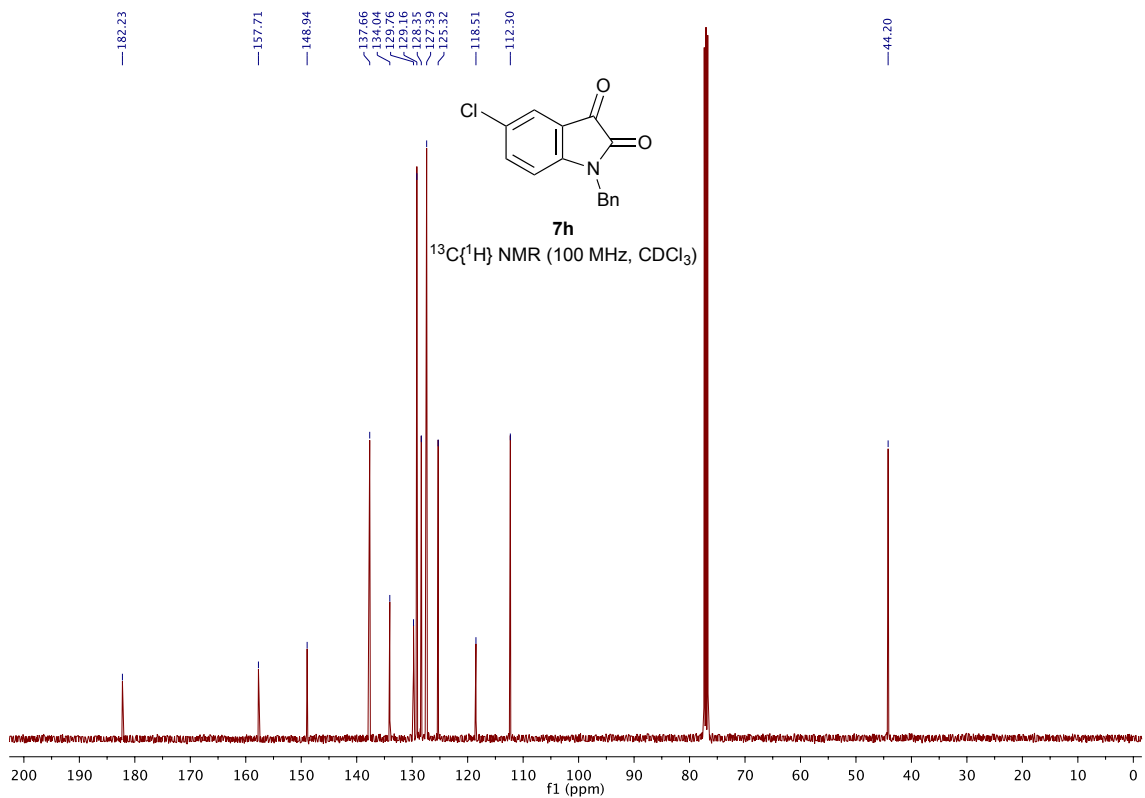
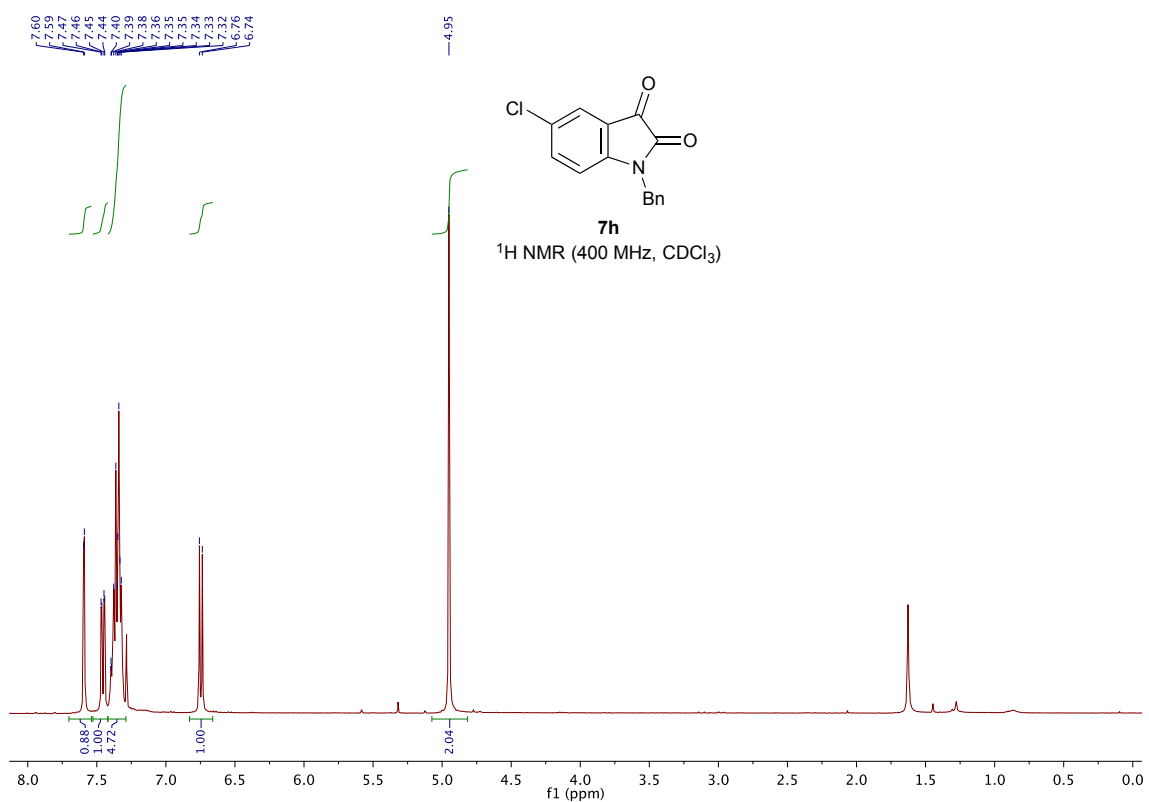


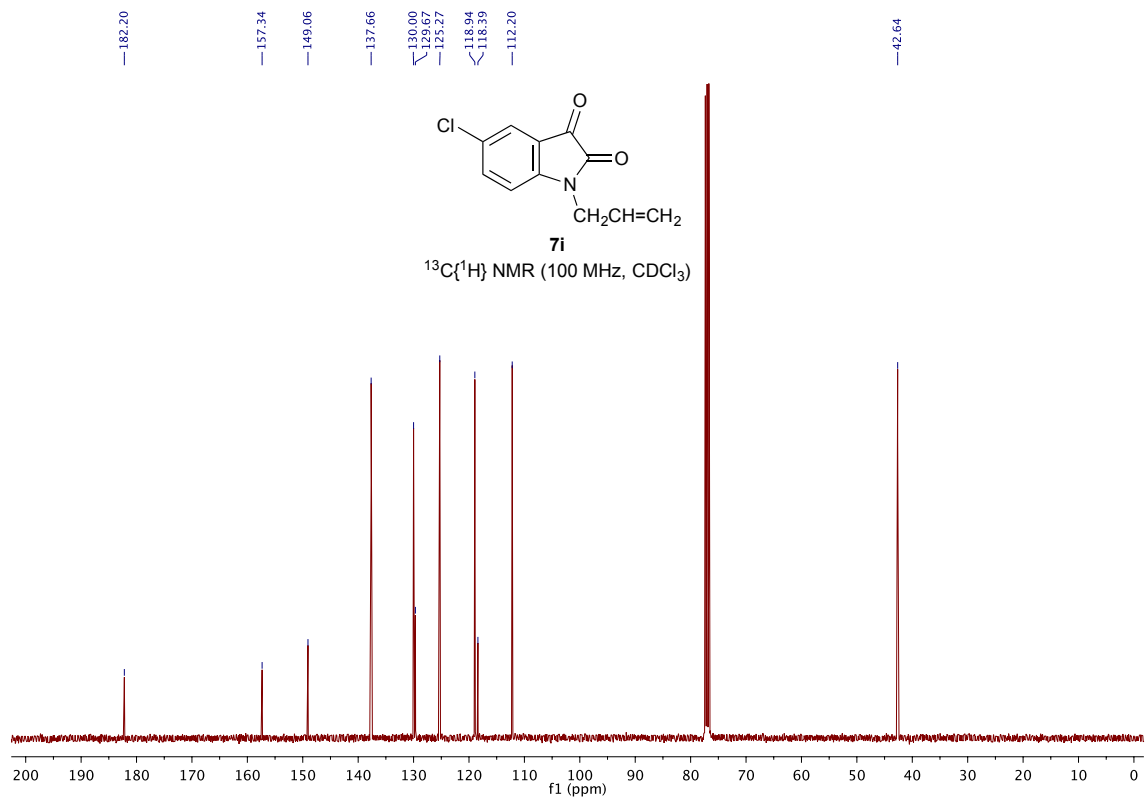
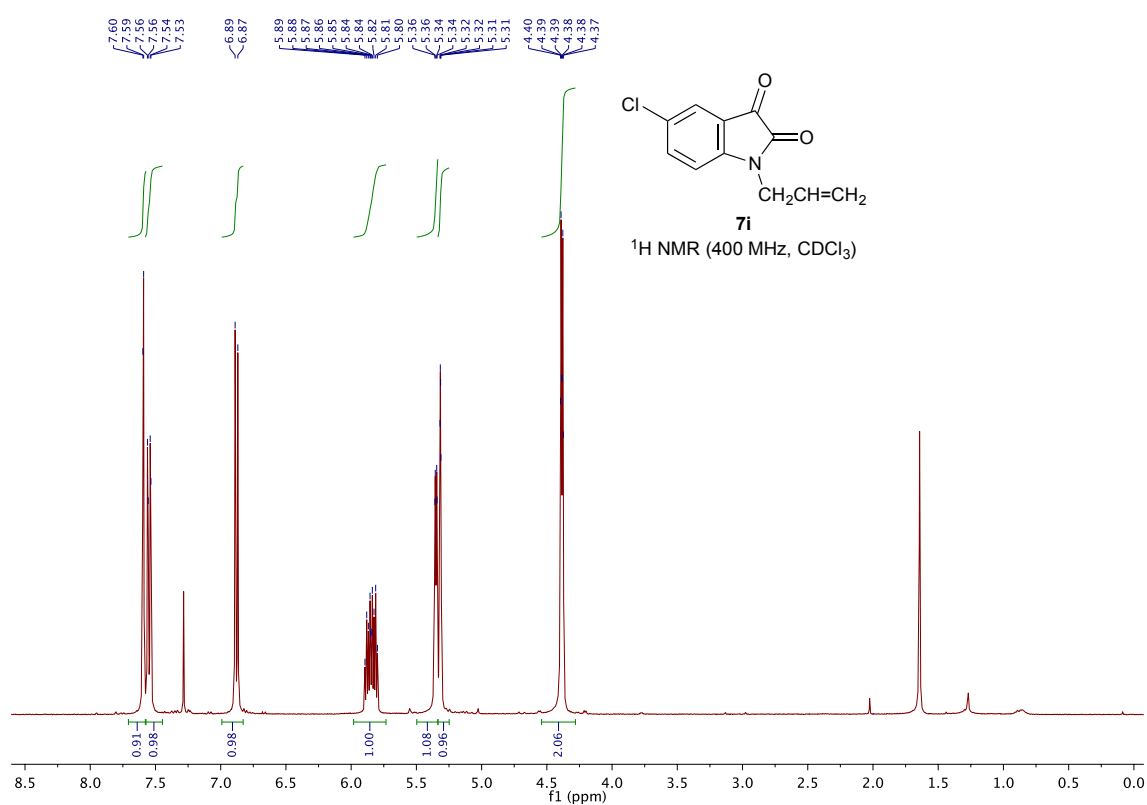


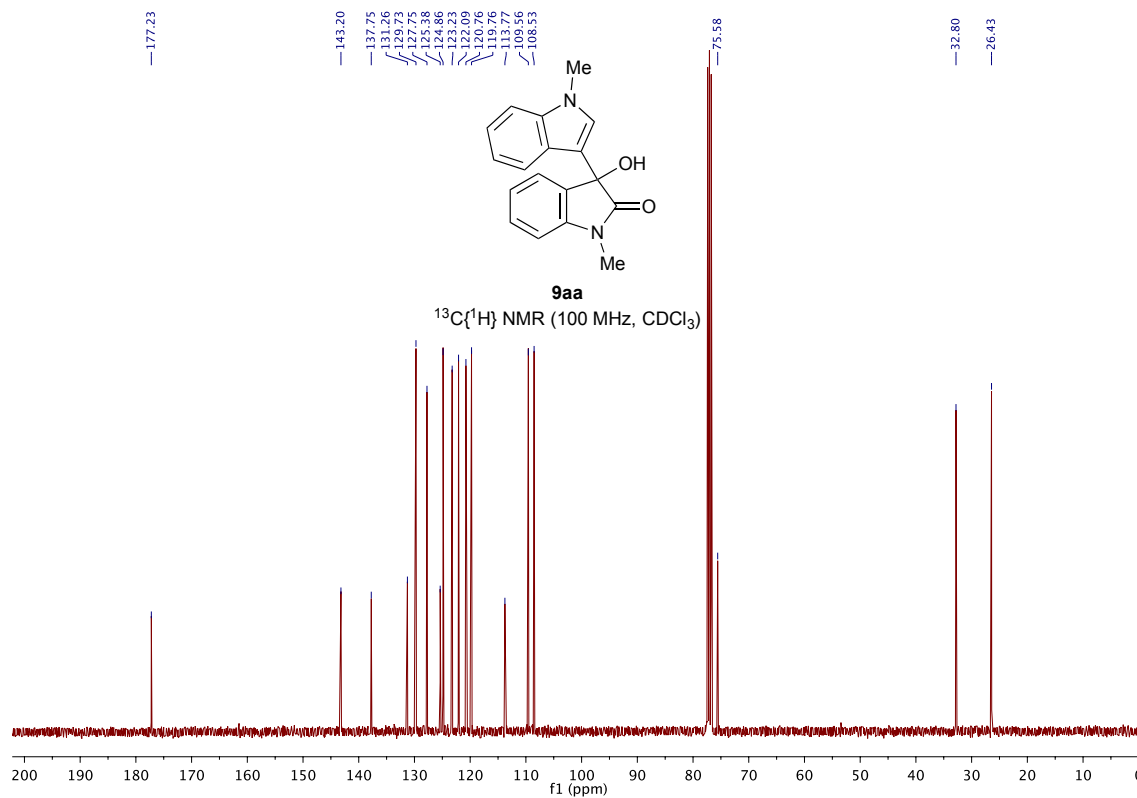
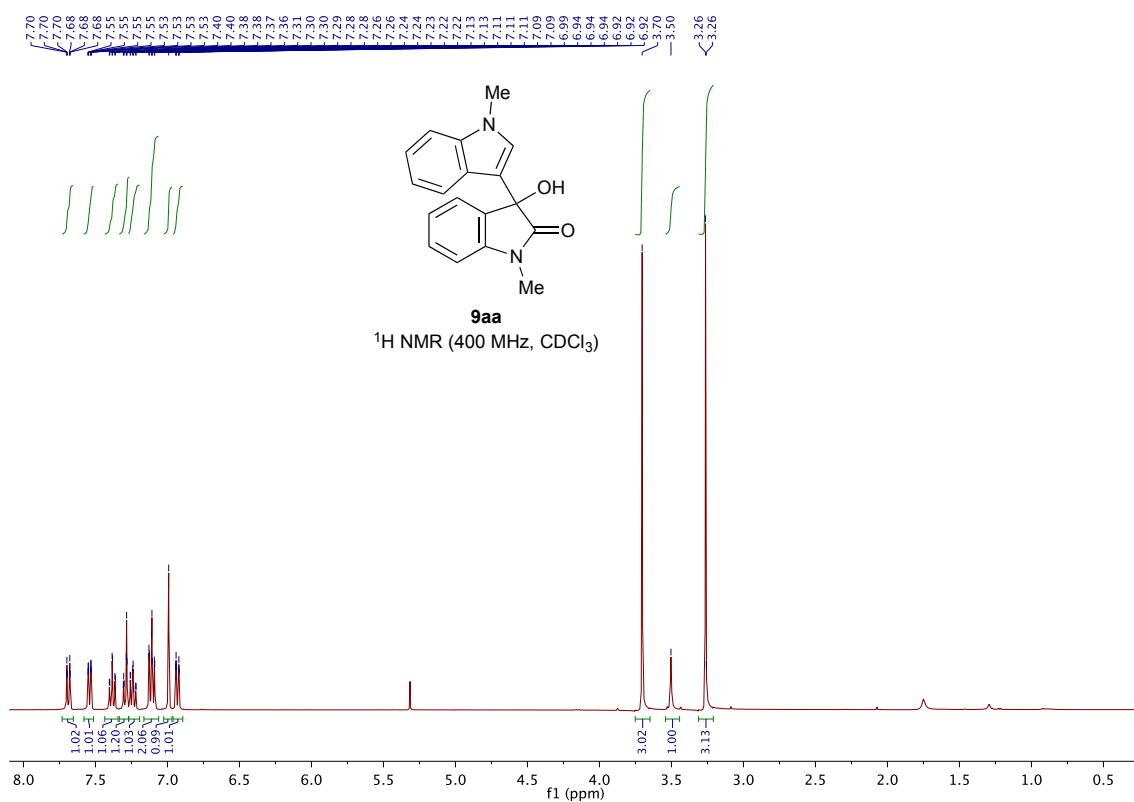


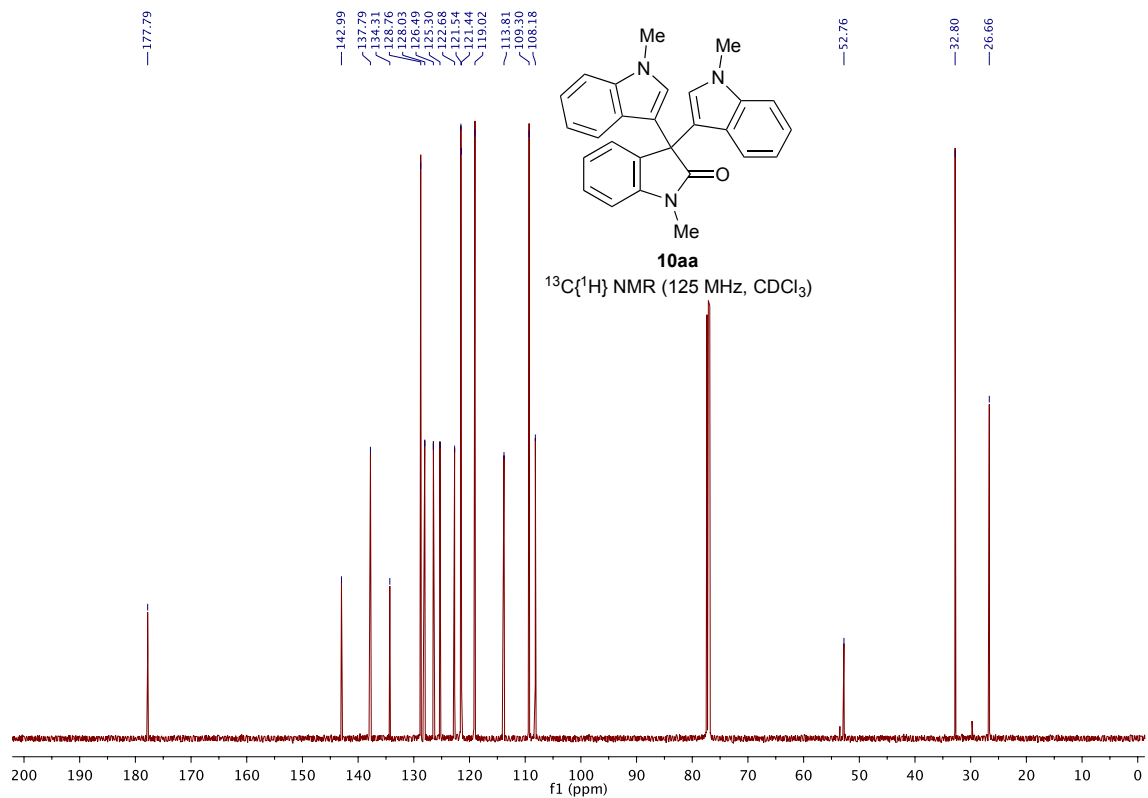
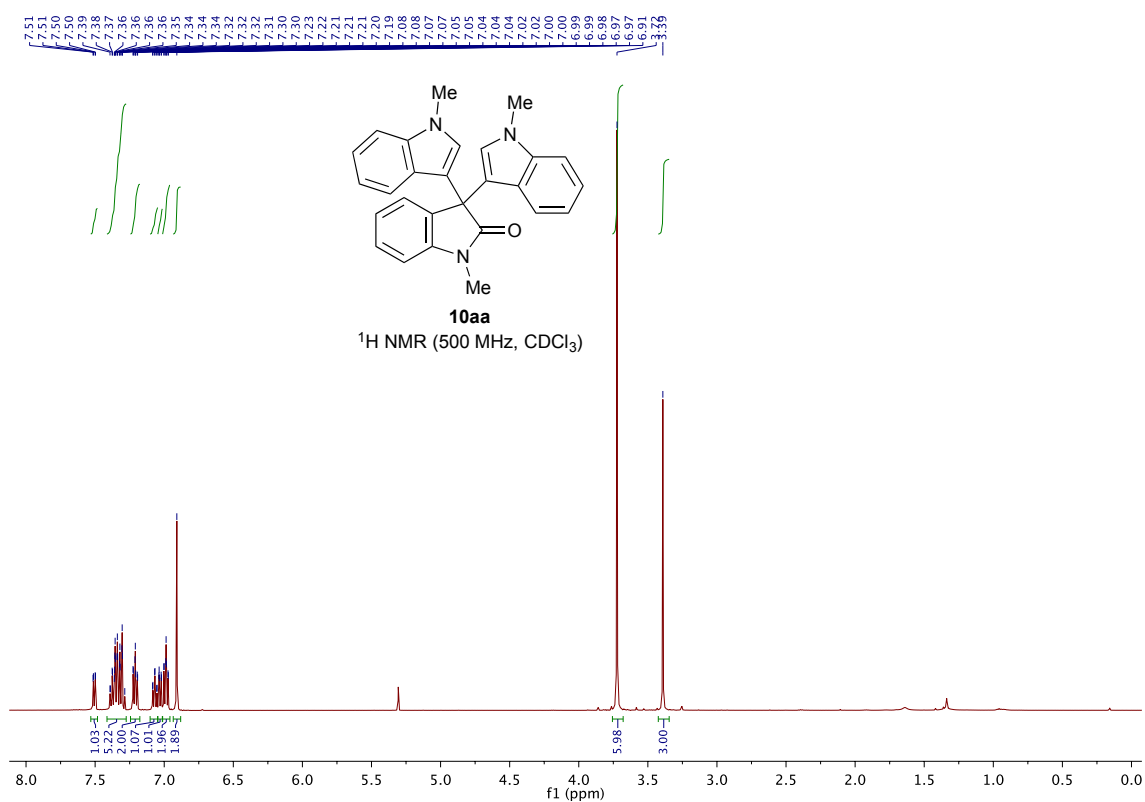


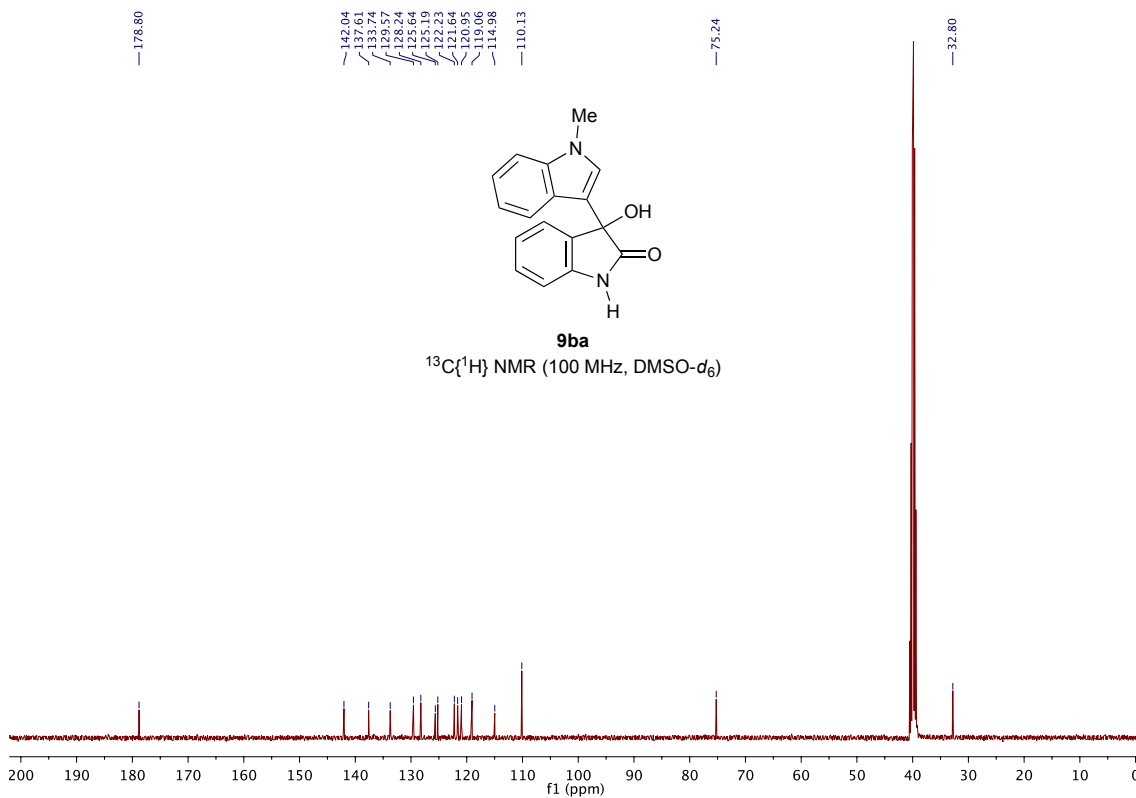
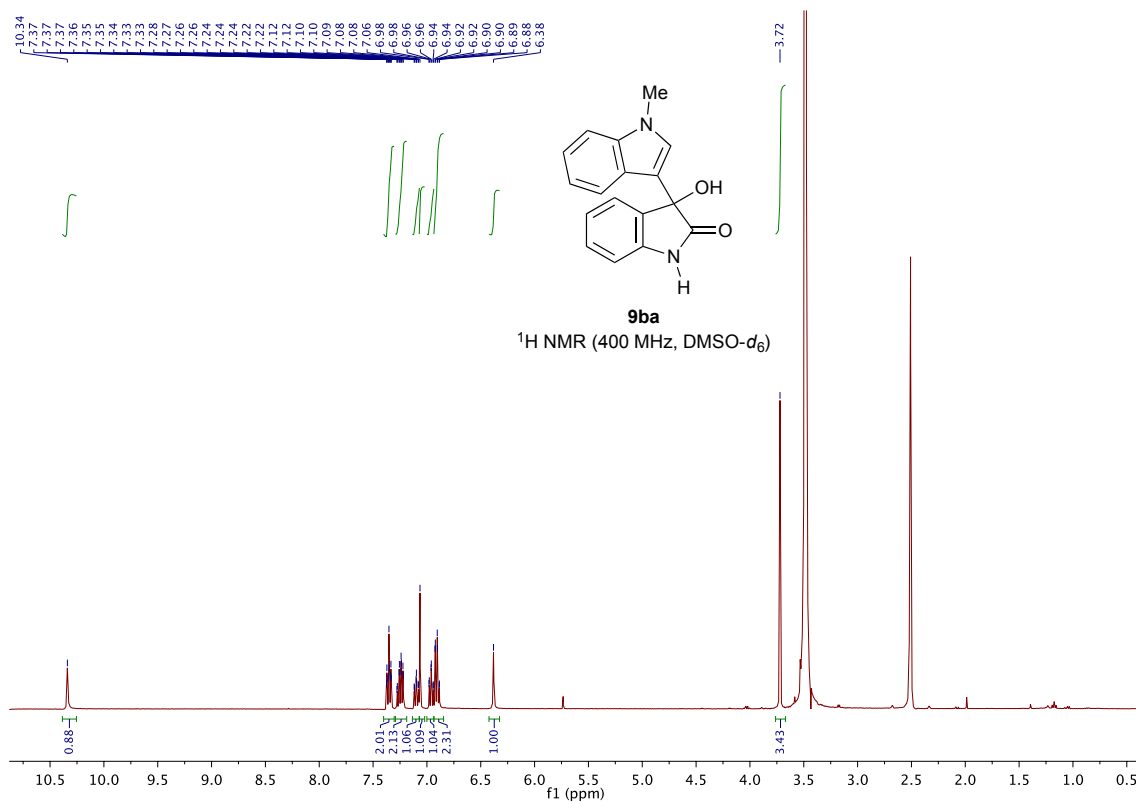


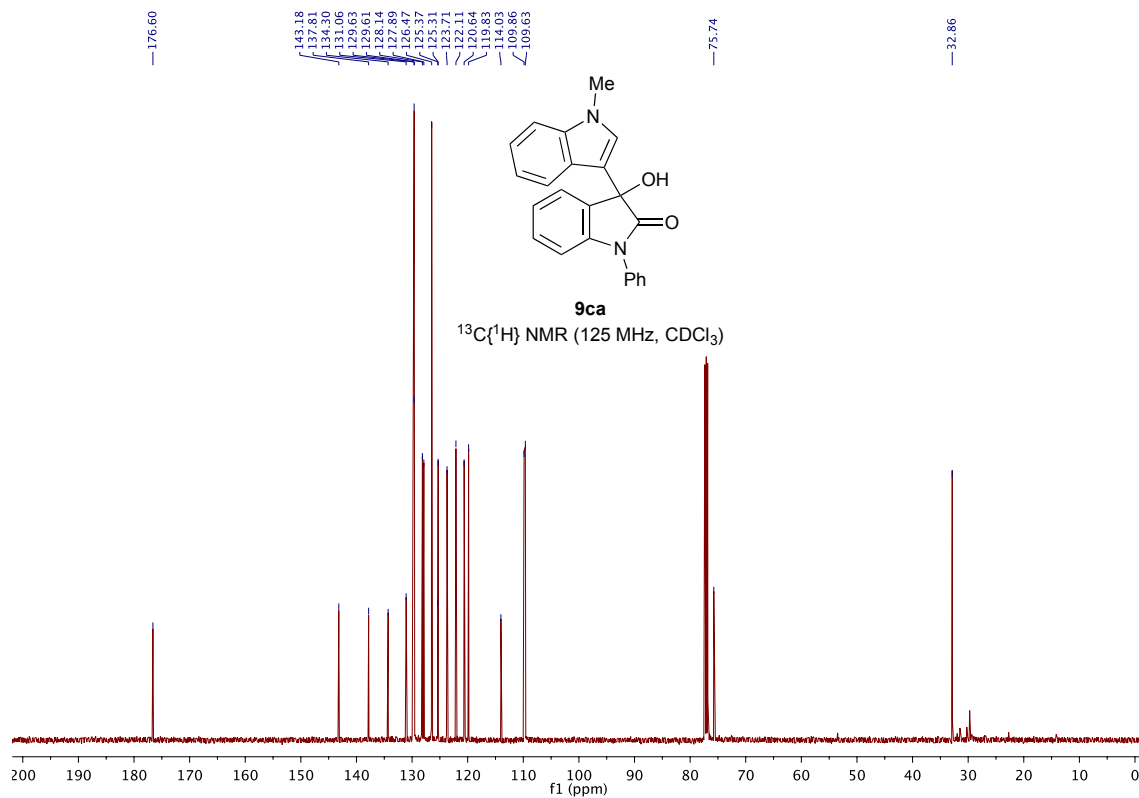
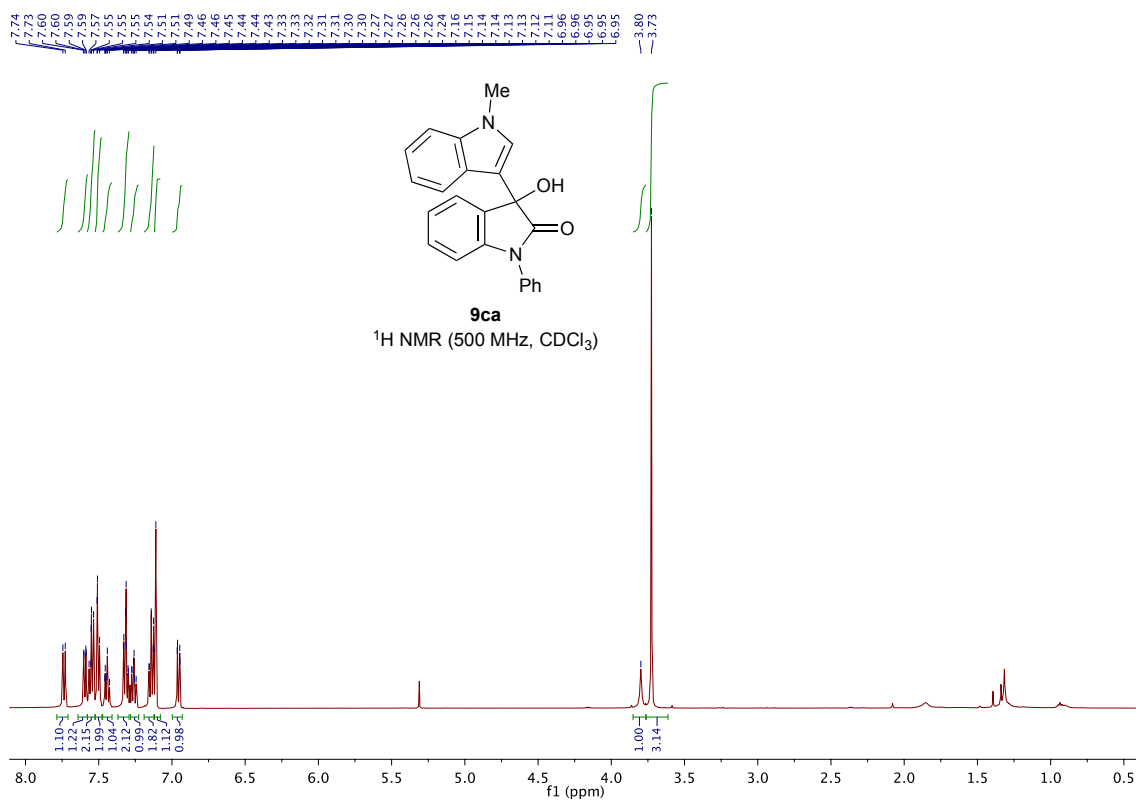


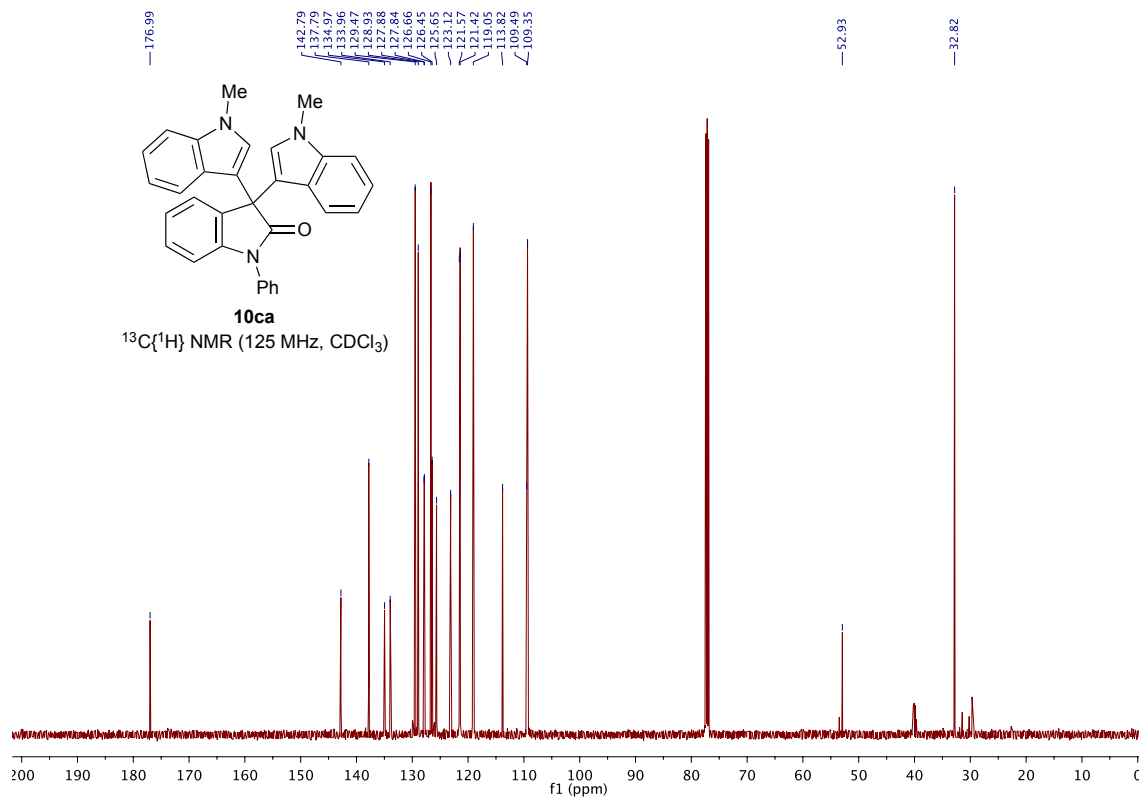
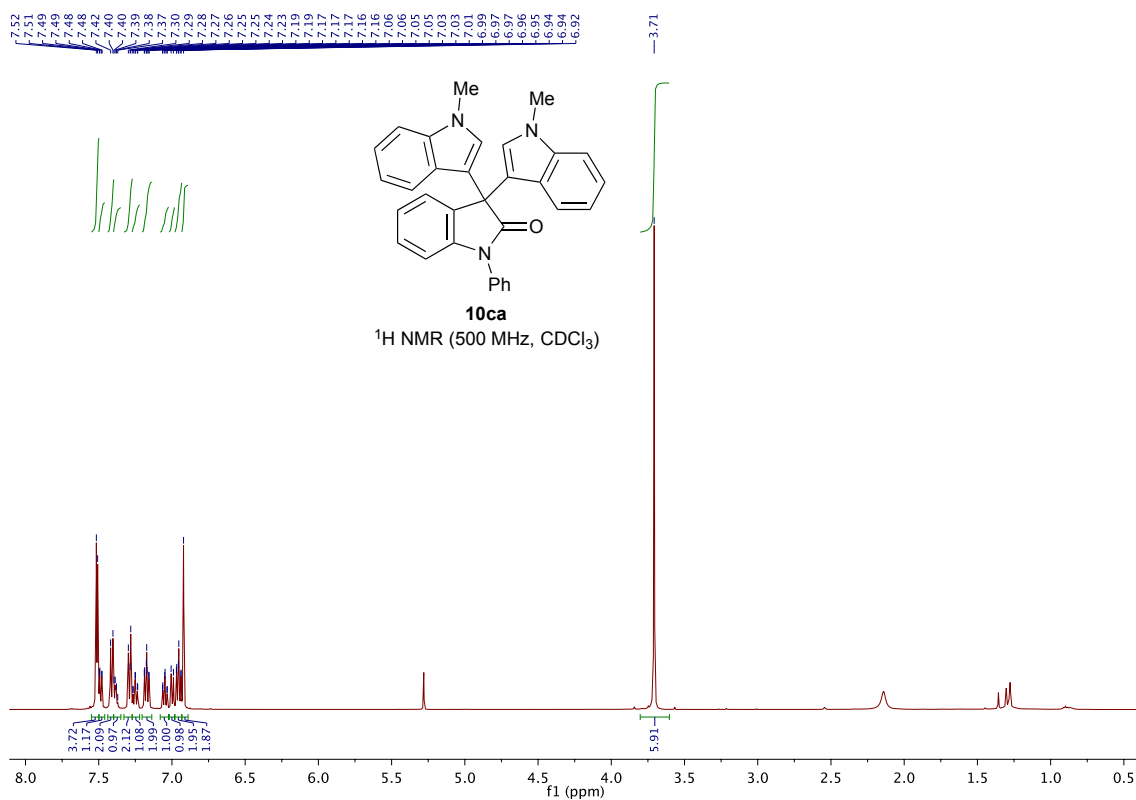


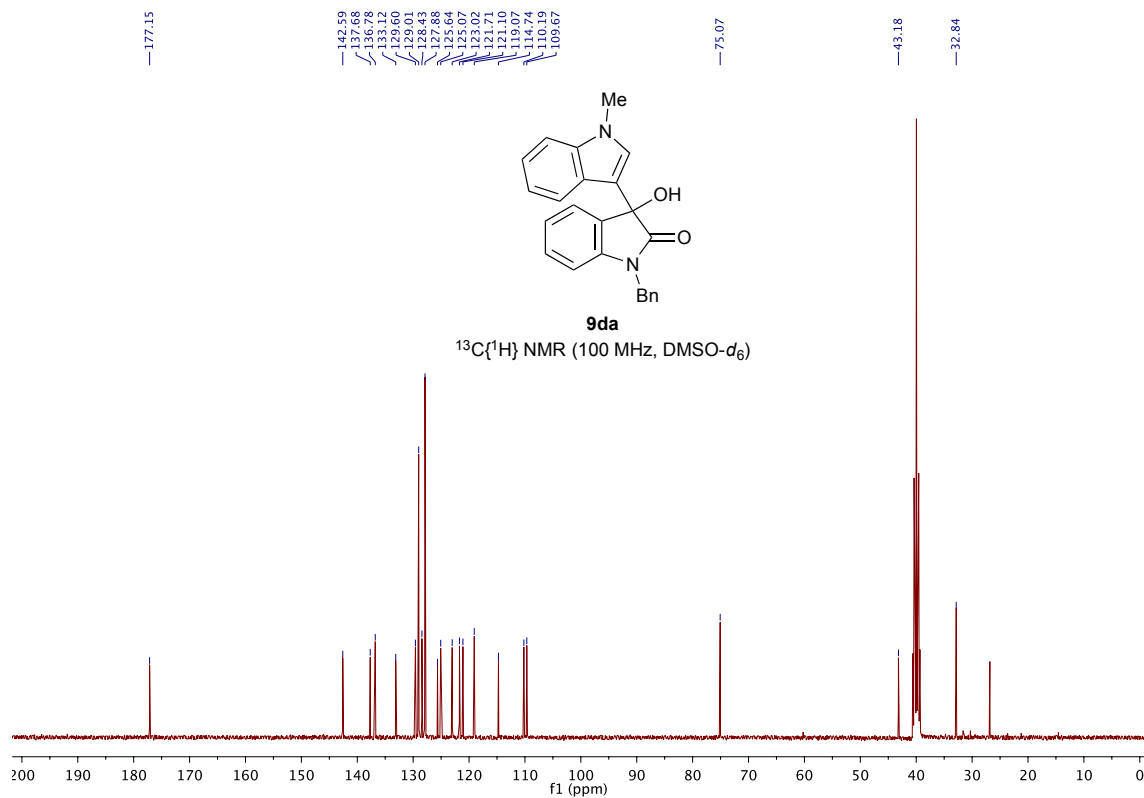
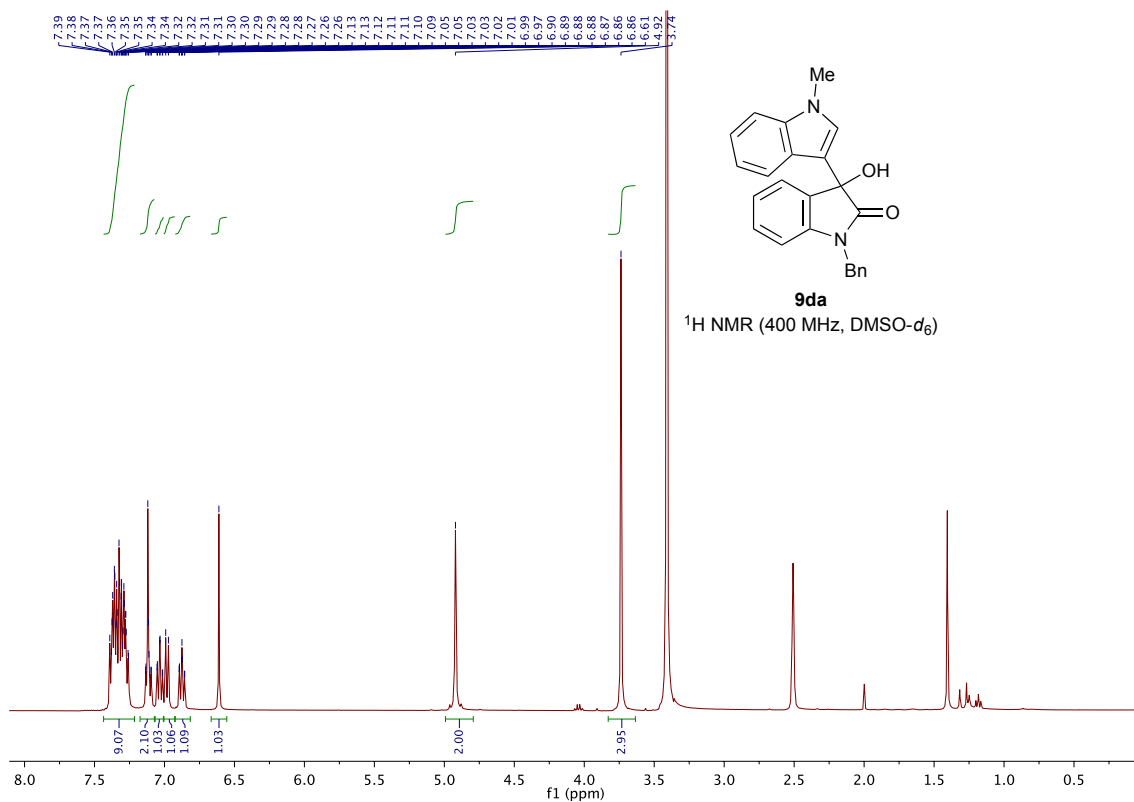


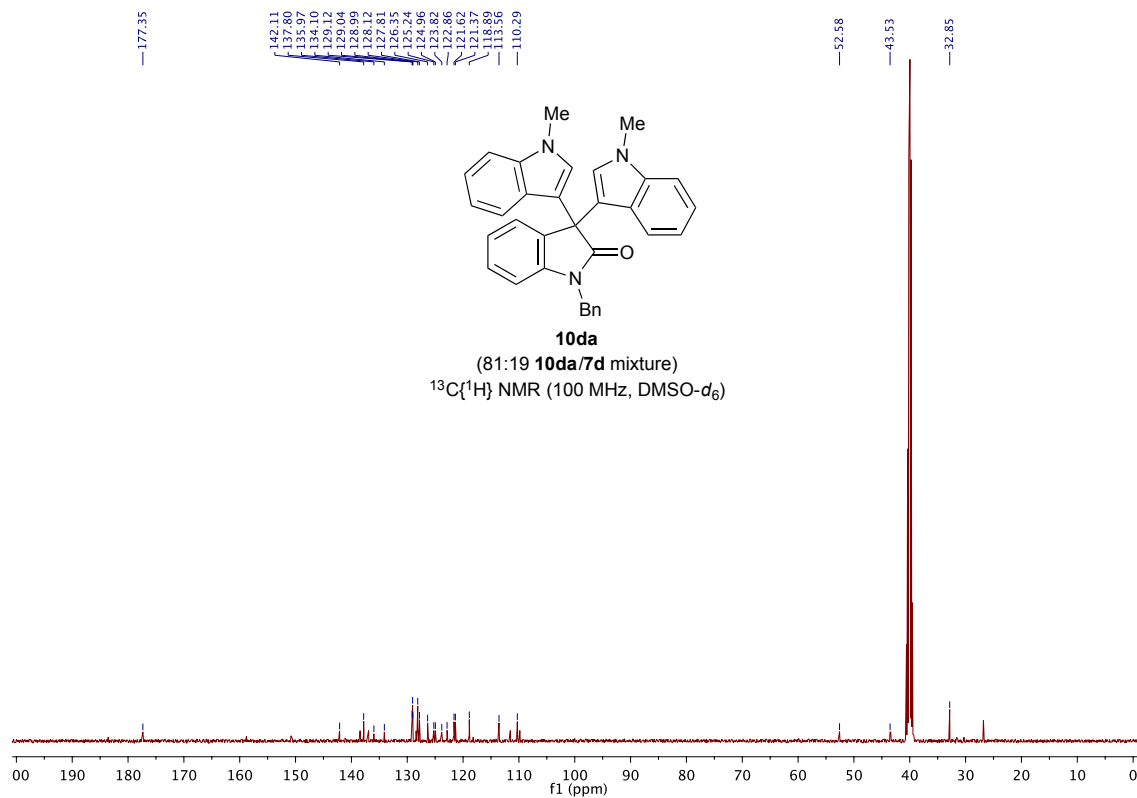
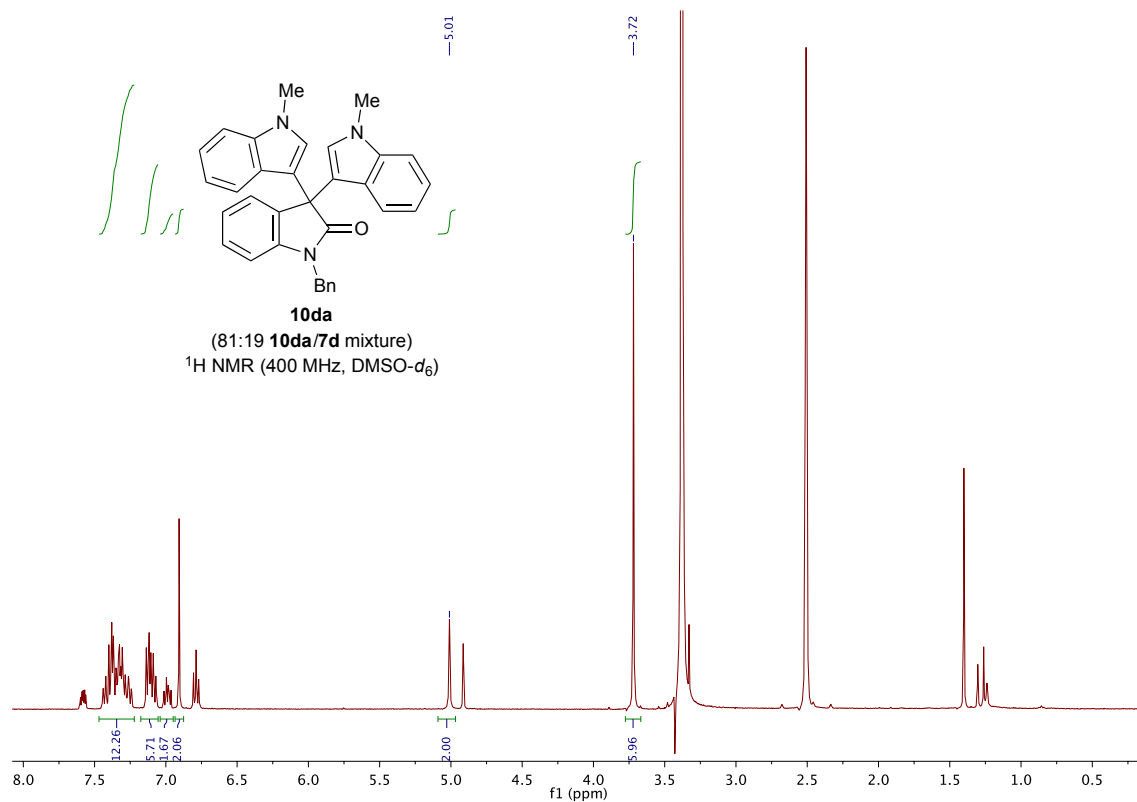


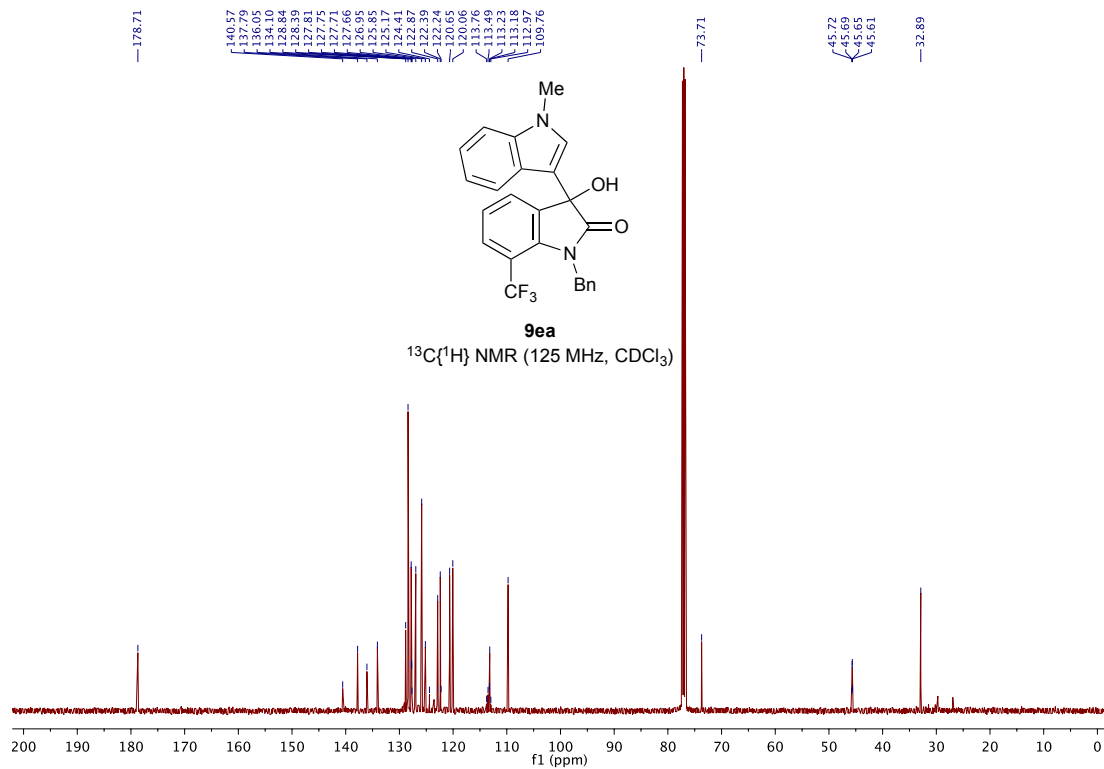
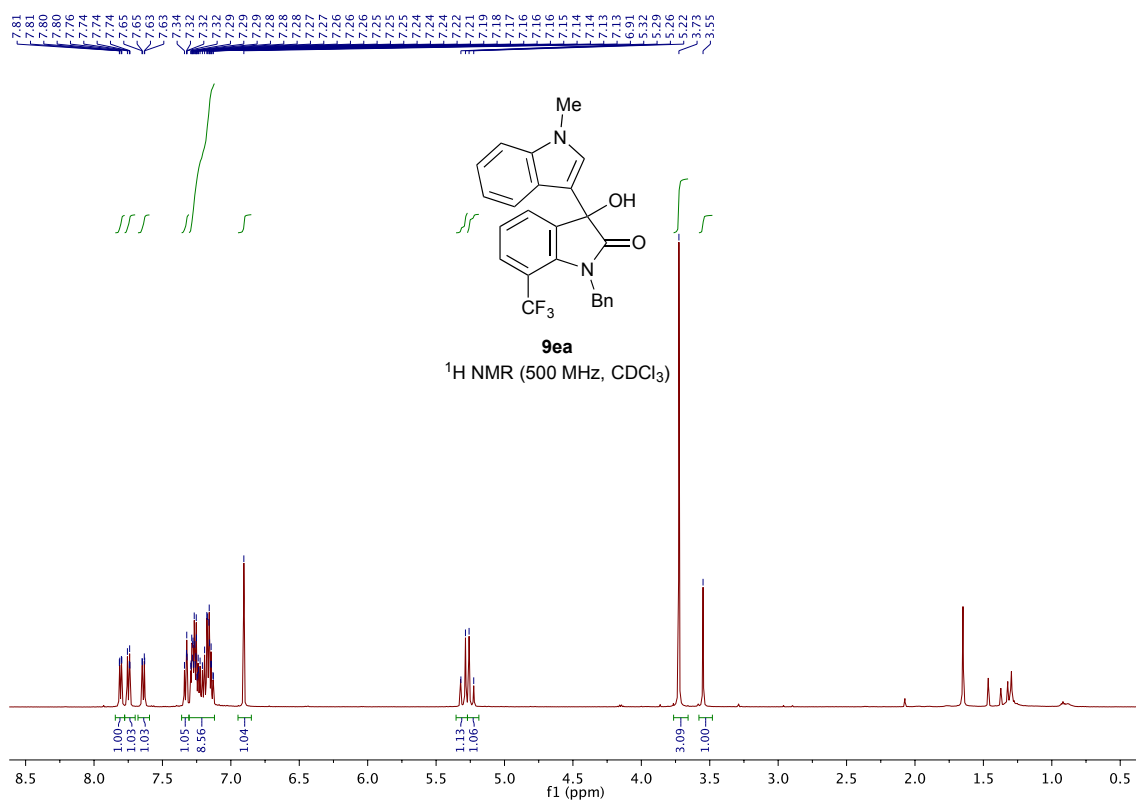


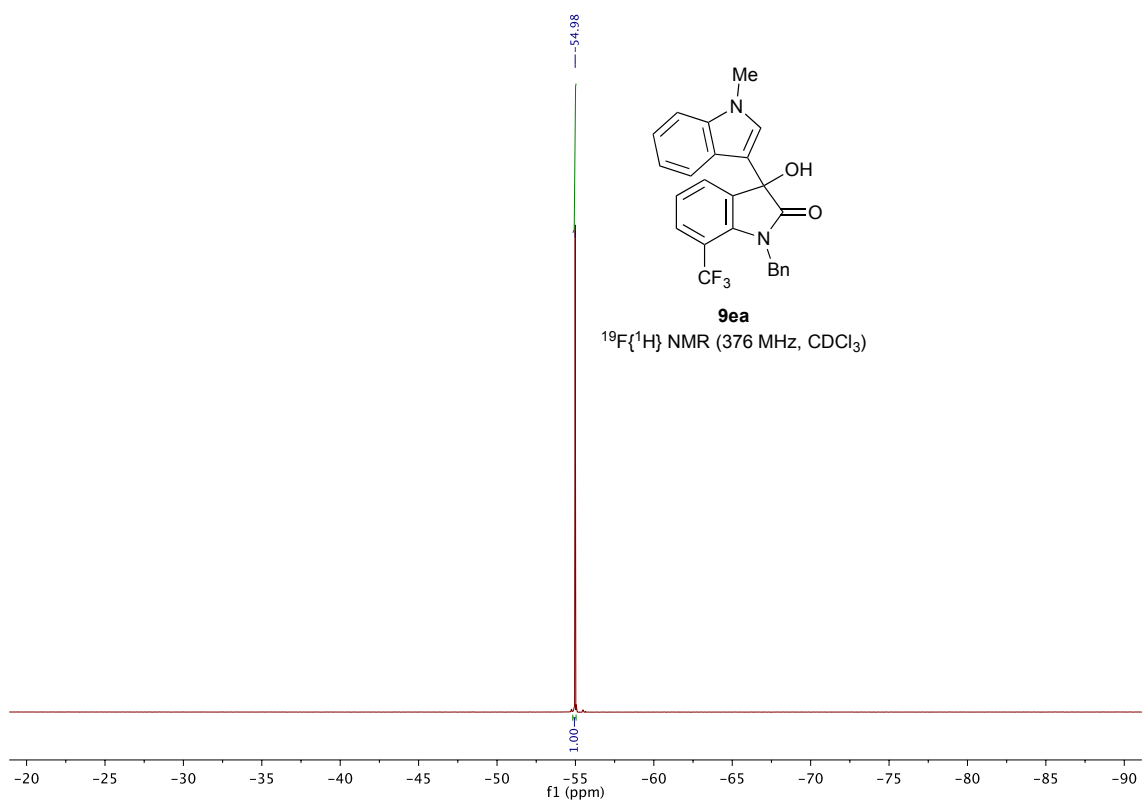


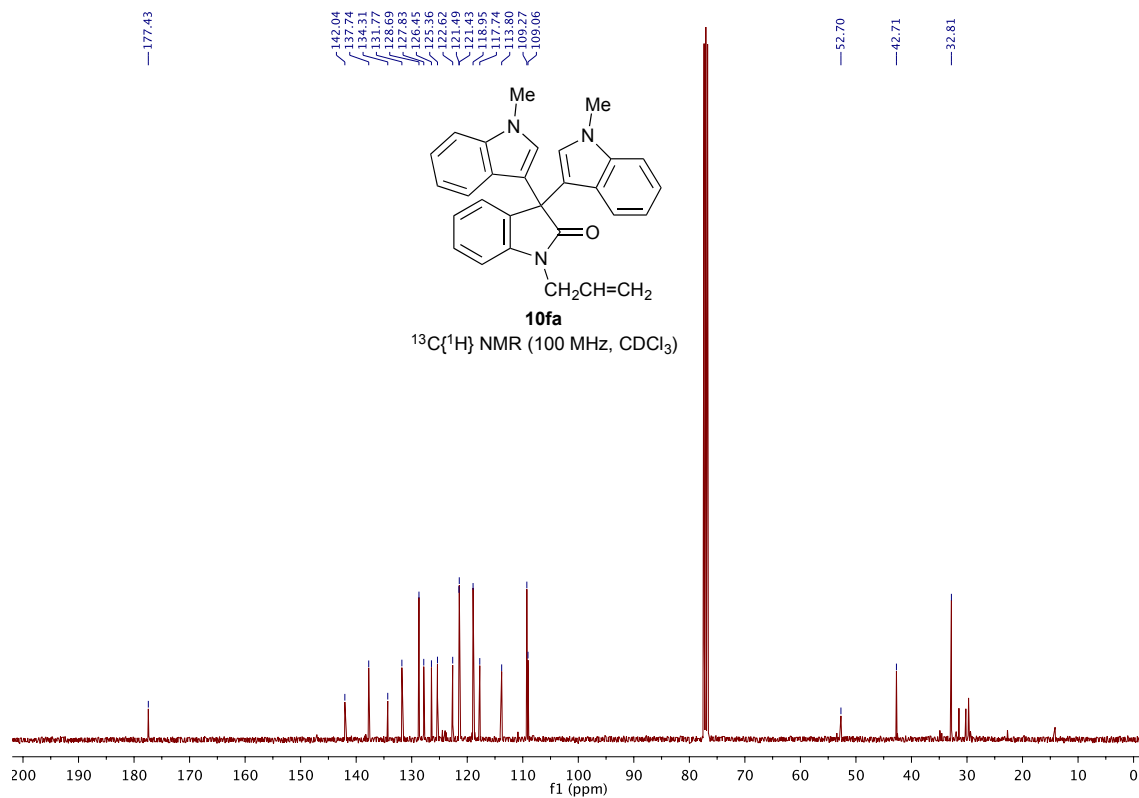
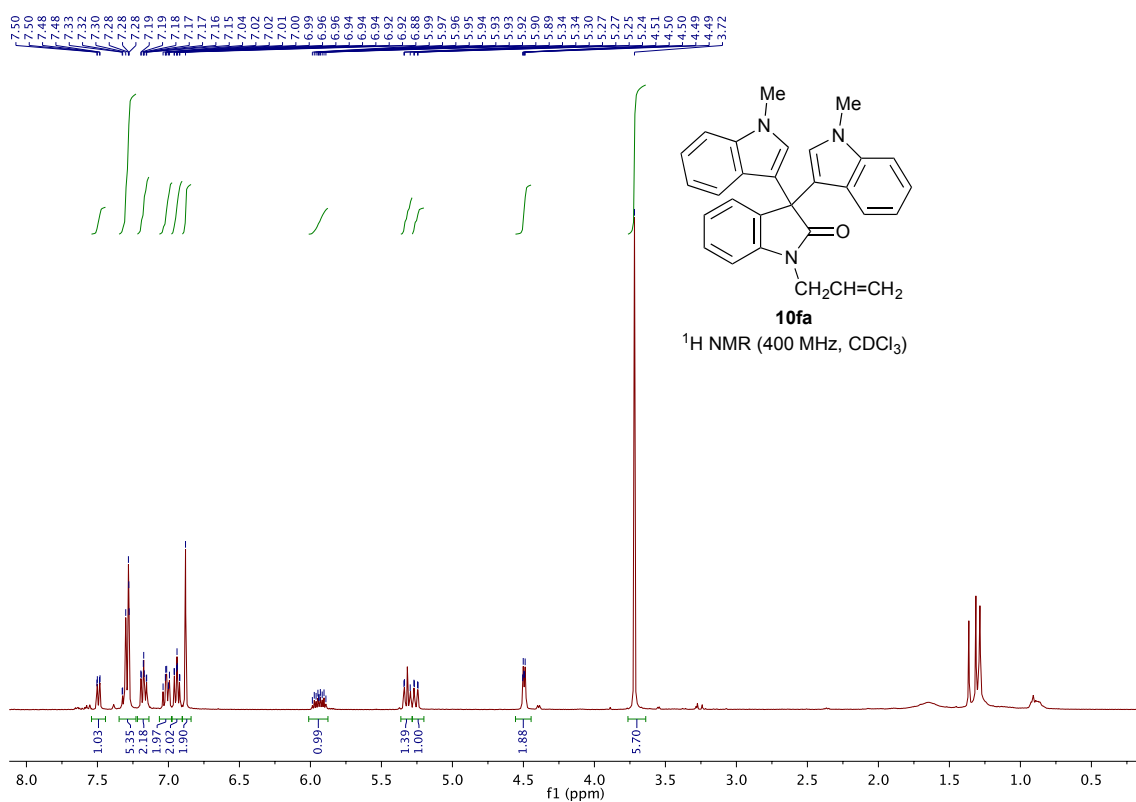


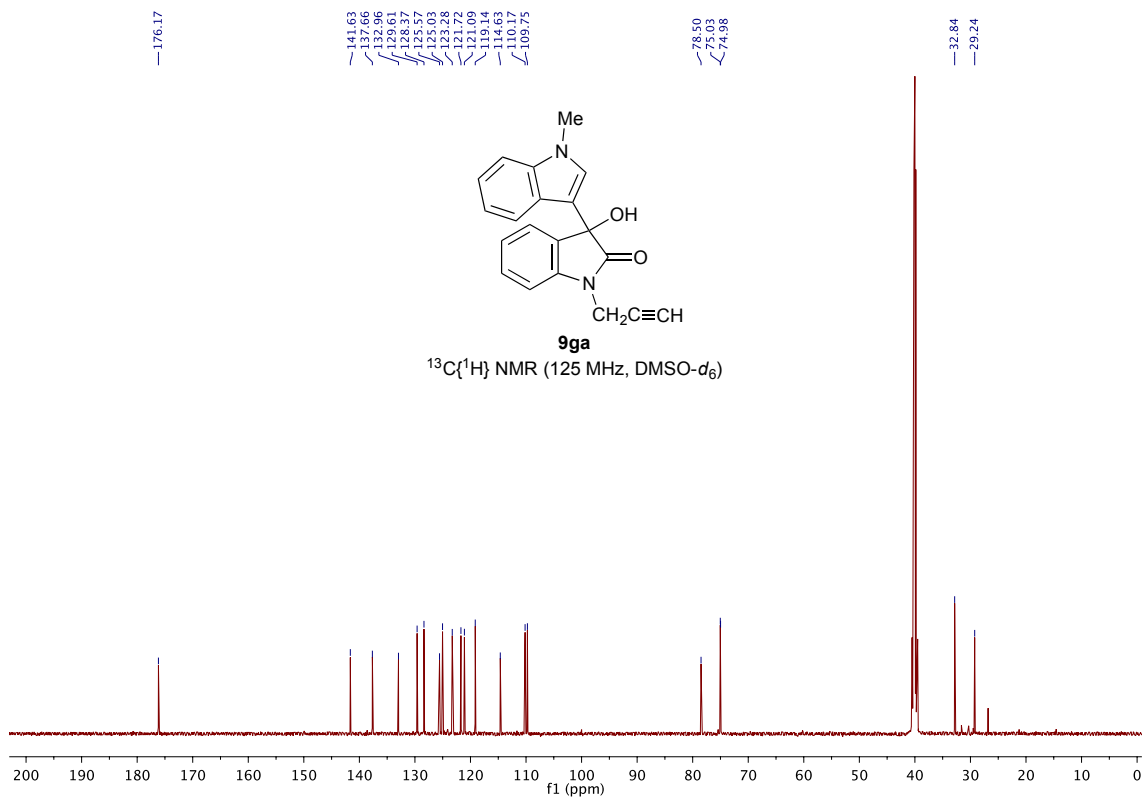
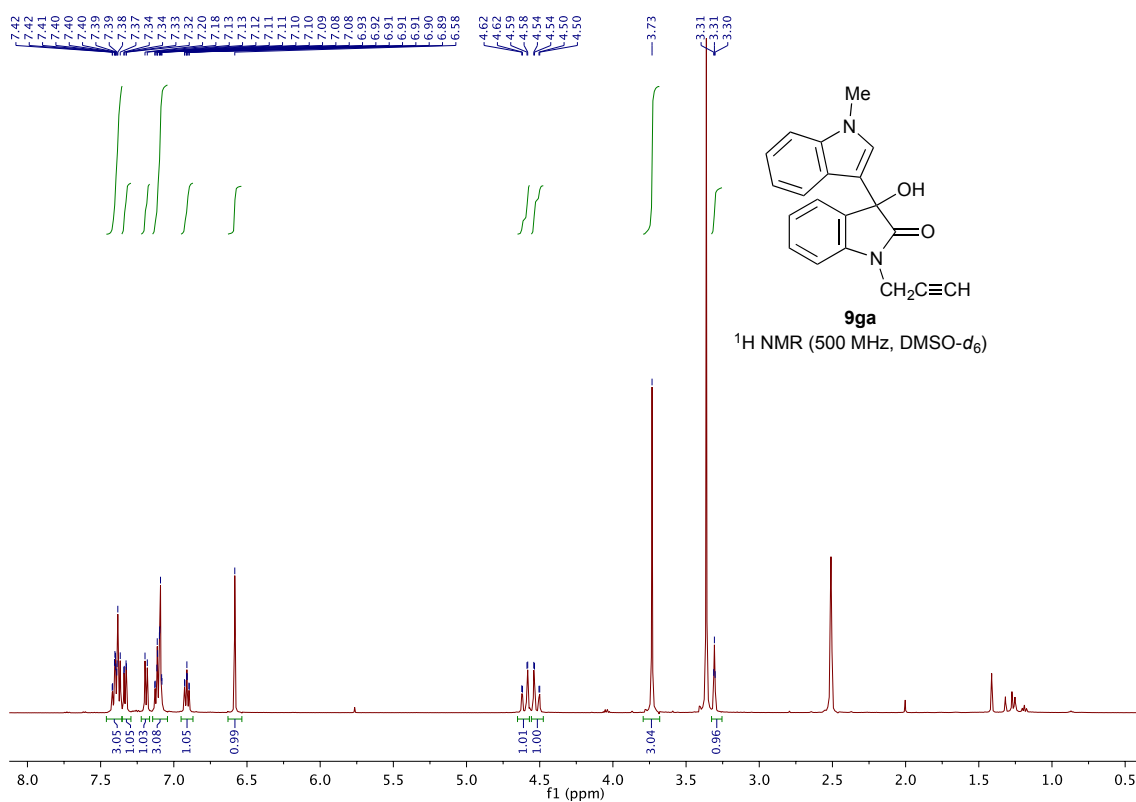


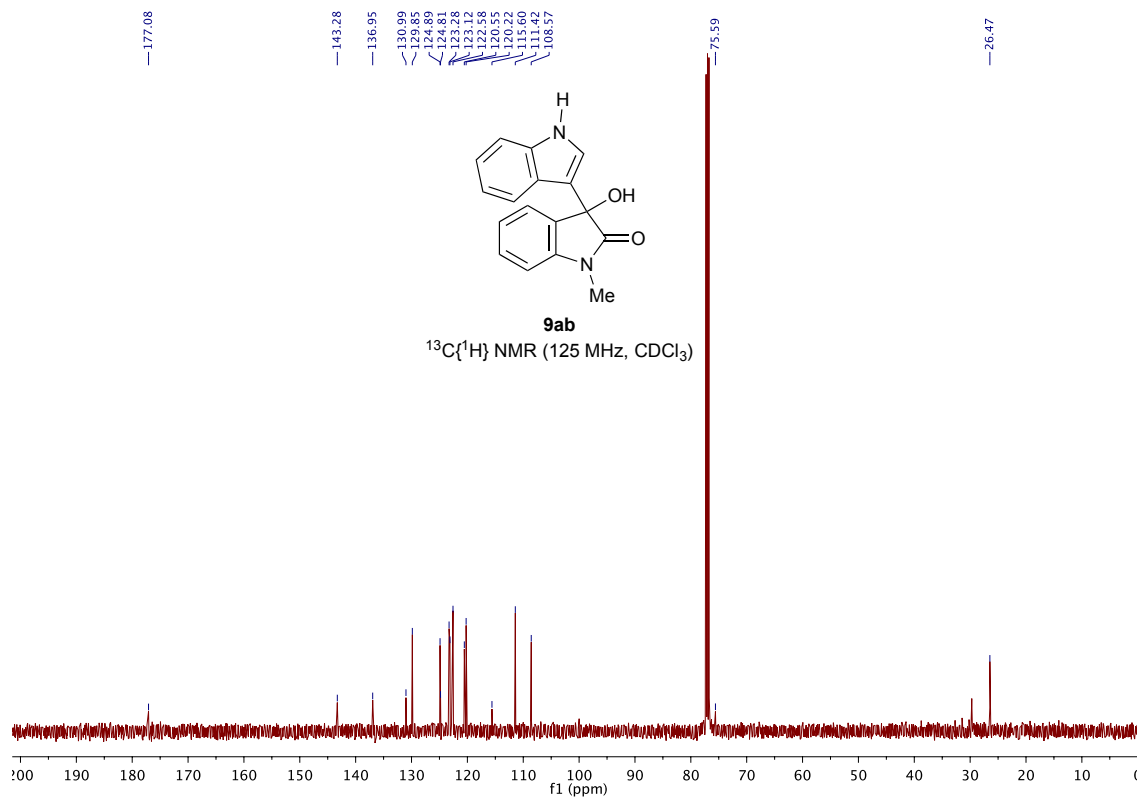
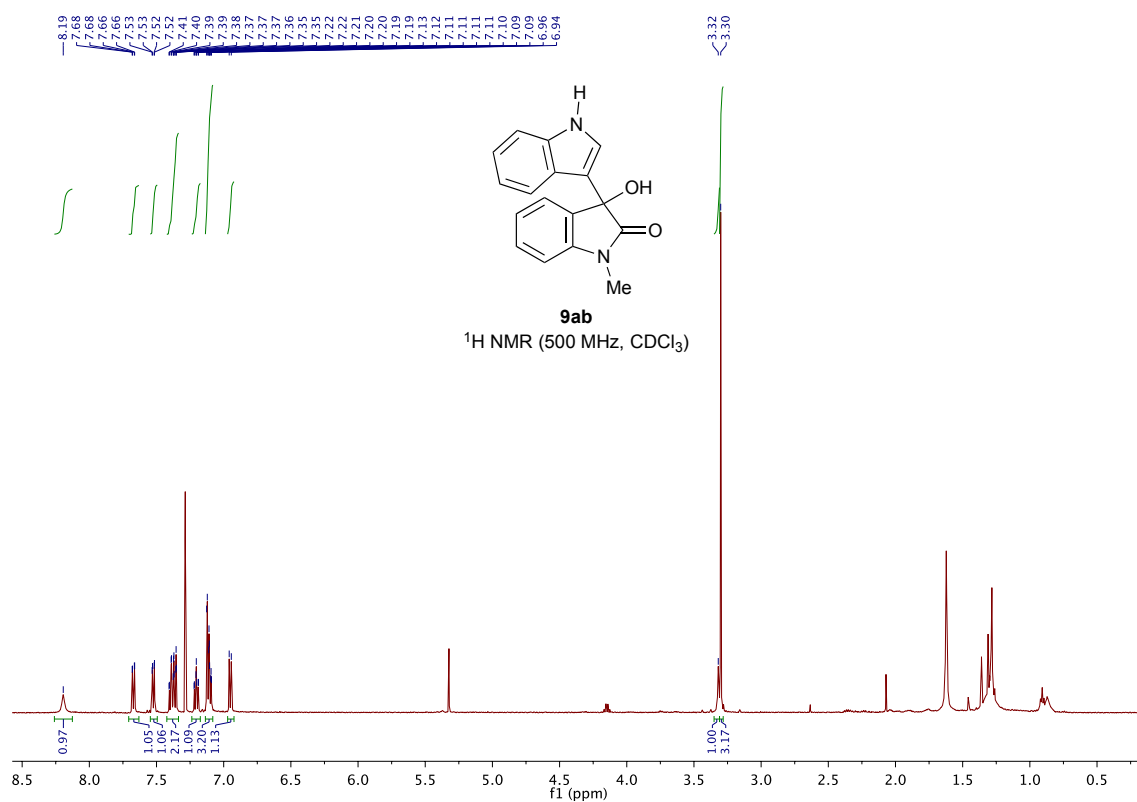


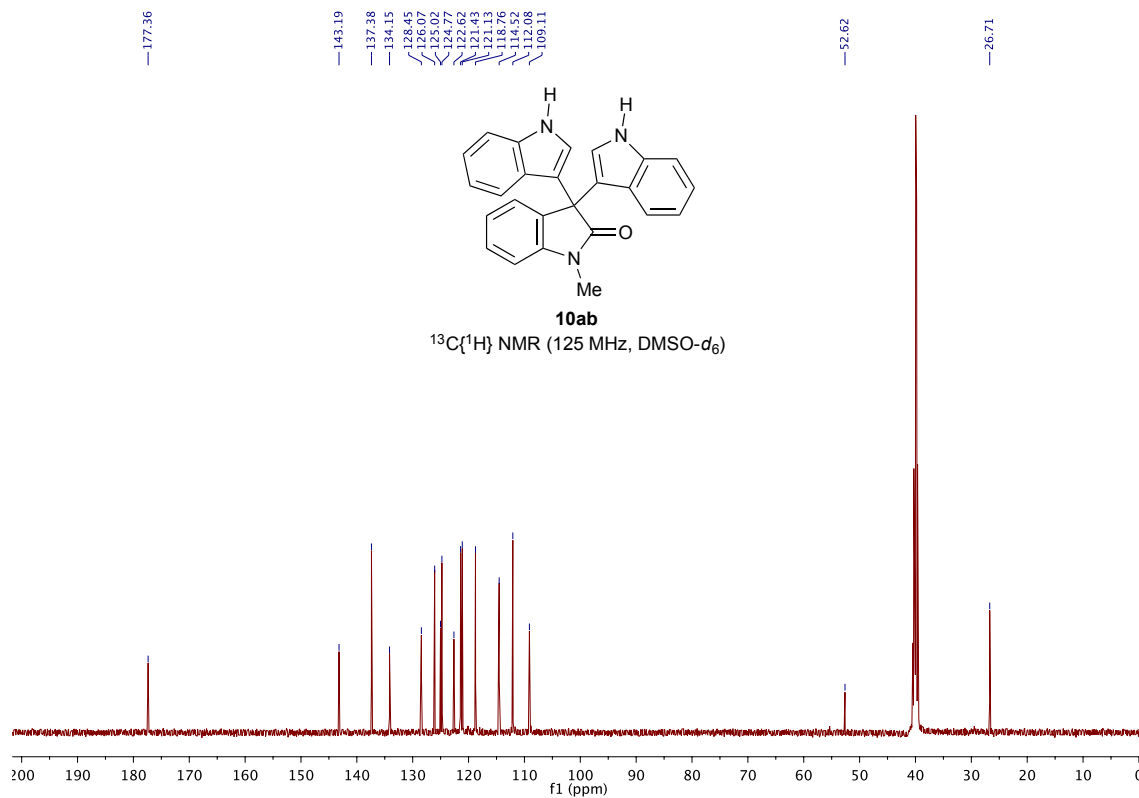
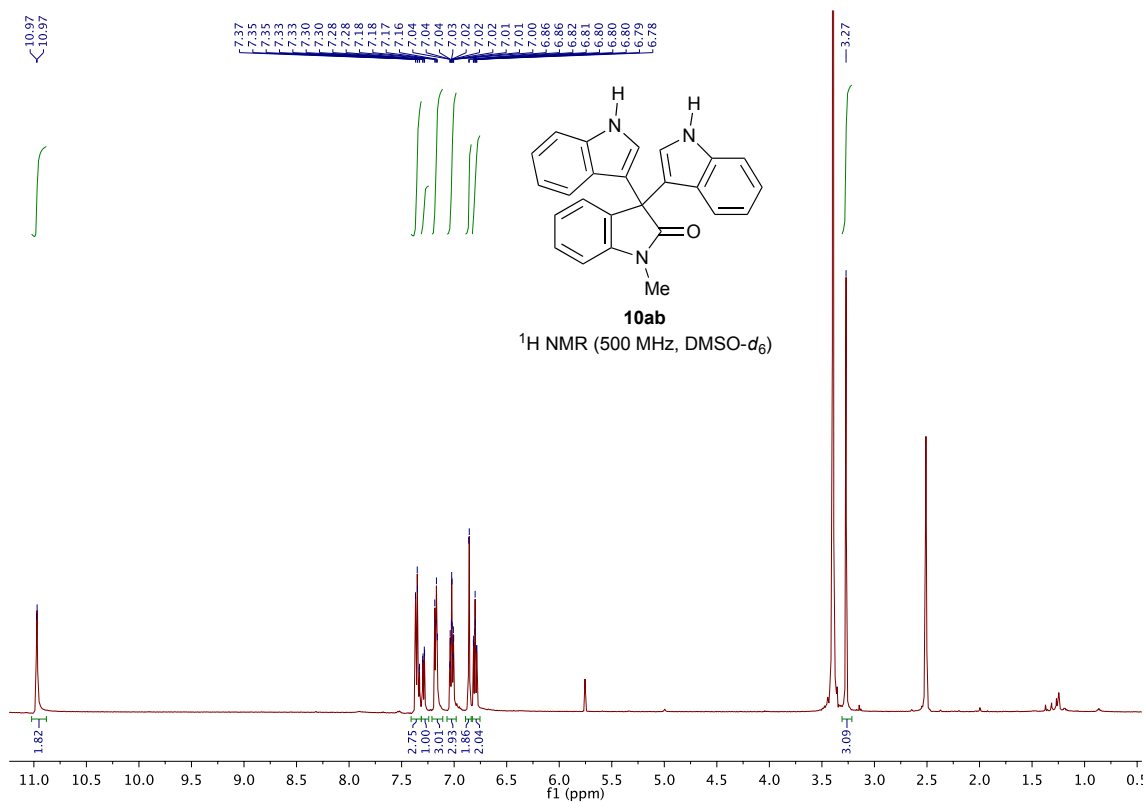


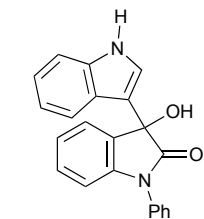




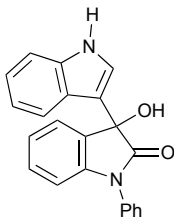




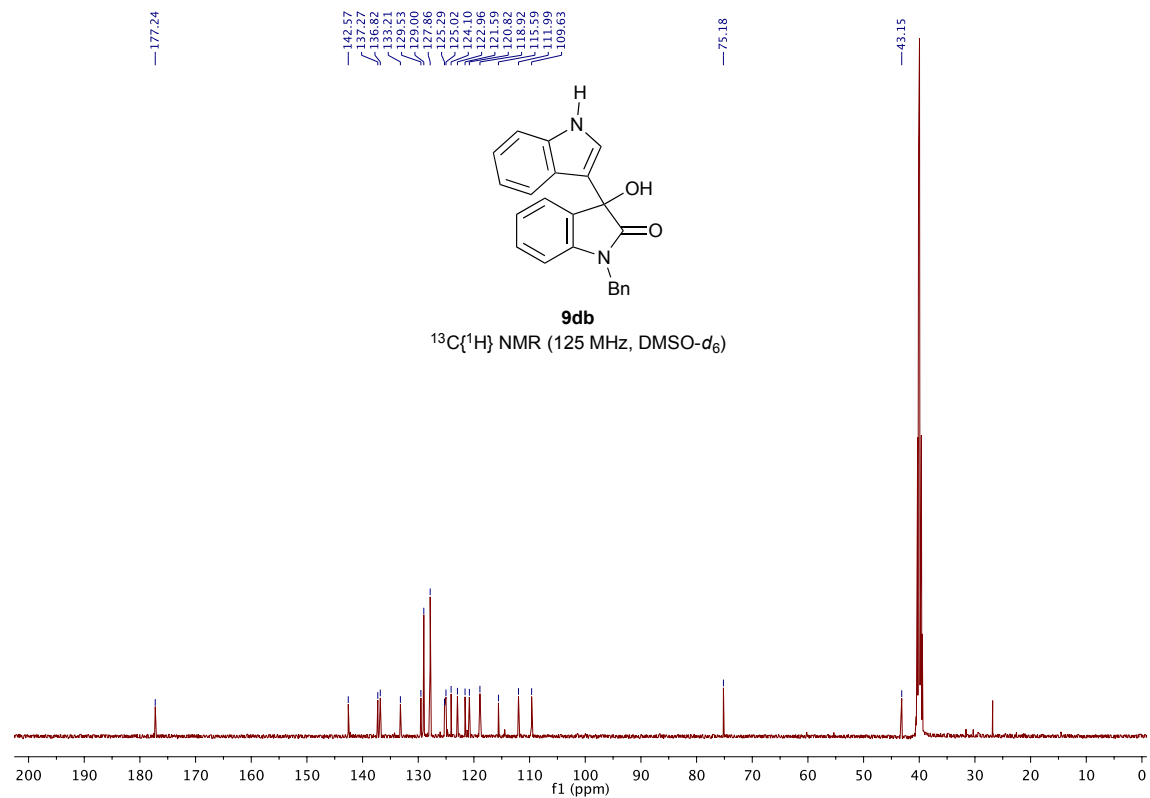
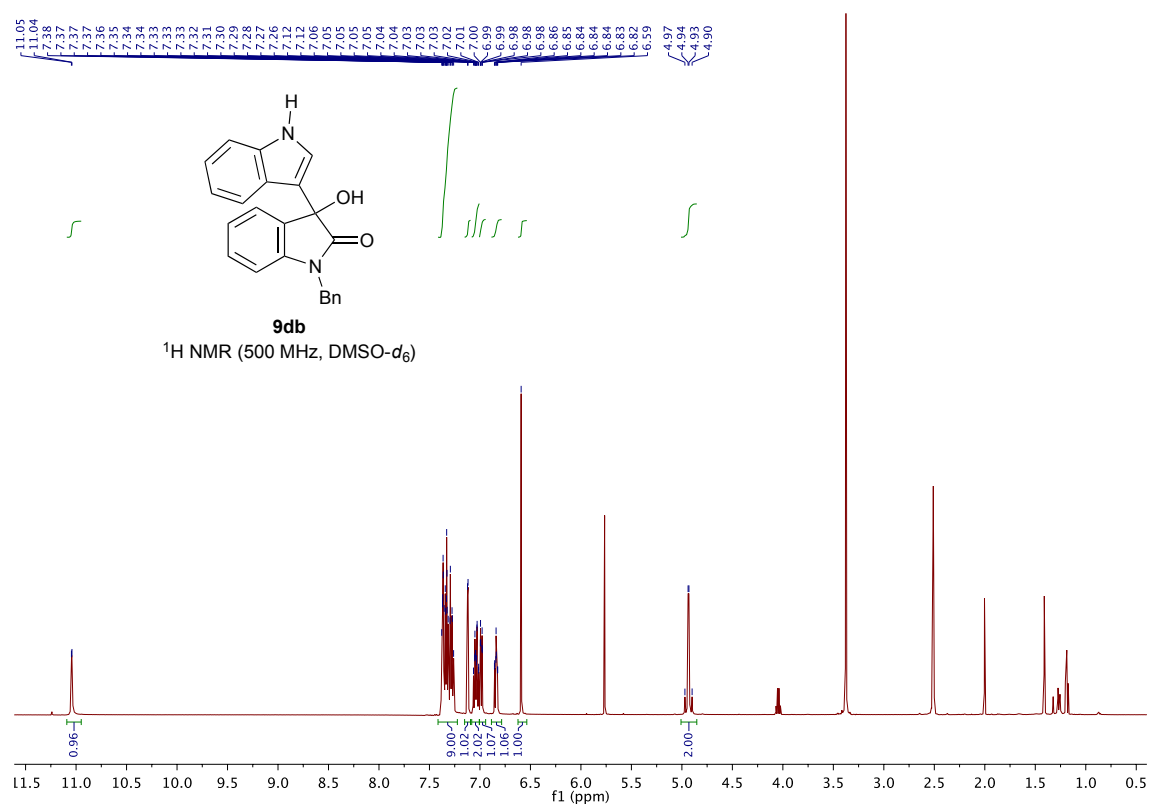


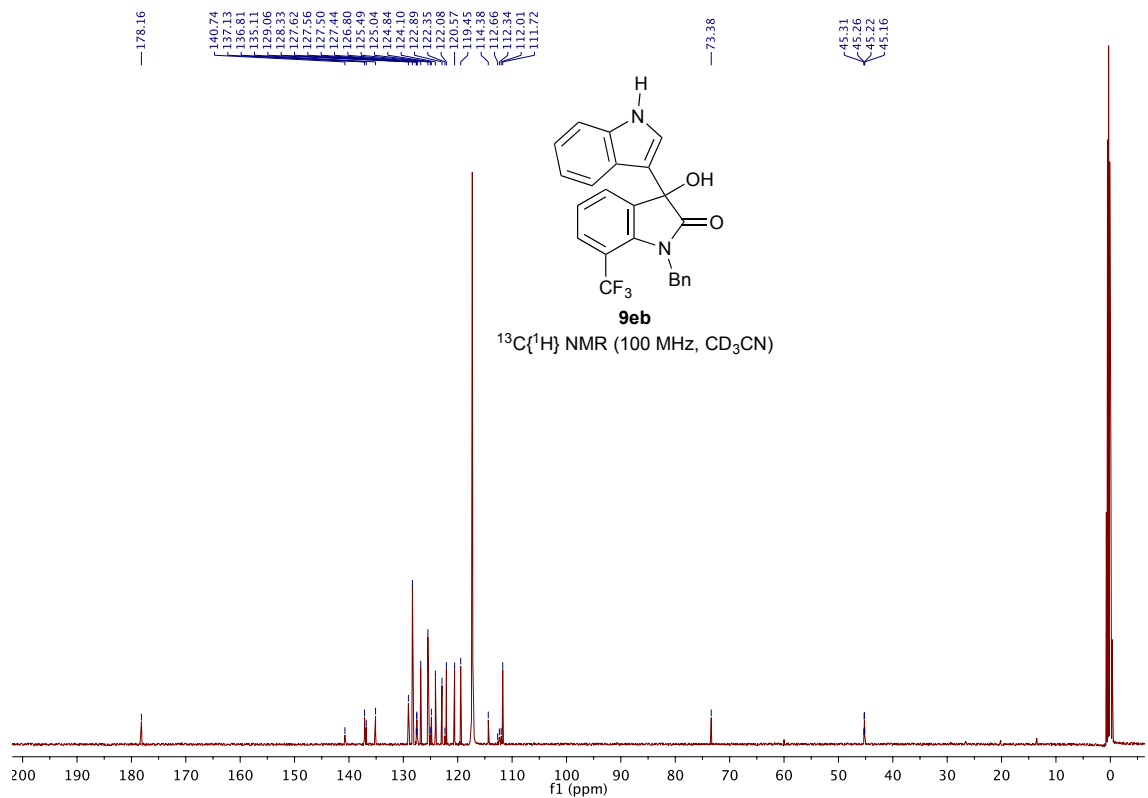
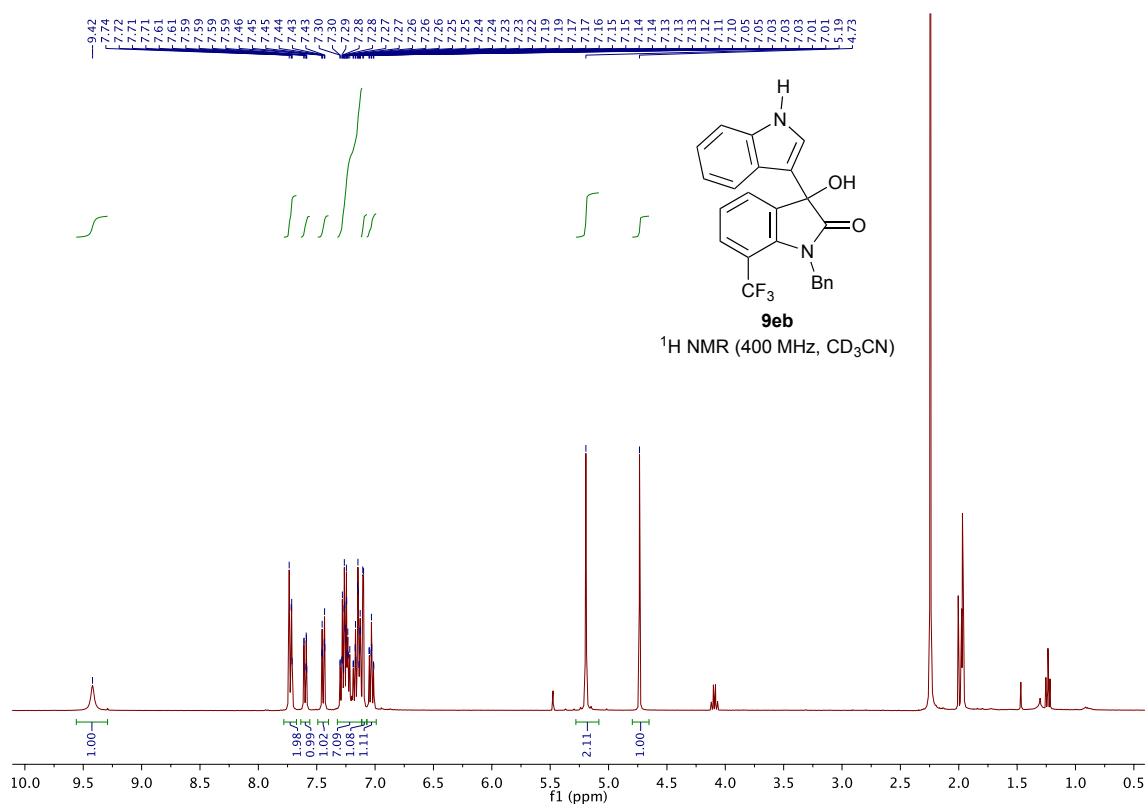


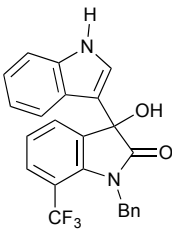
9cb
¹H NMR (500 MHz, CDCl₃)



9cb
 $^{13}\text{C}\{^1\text{H}\}$ NMR (125 MHz, CDCl_3)







9eb
 $^{19}\text{F}\{^1\text{H}\}$ NMR (376 MHz, CD_3CN)

